From Concept to Reality:

The Evolution of Laser and Optical Technologies for Gravitational-Wave Detectors

Department of astronomy

June Gyu Park

YONSEI UNIVERSITY

Gravity and general relativity

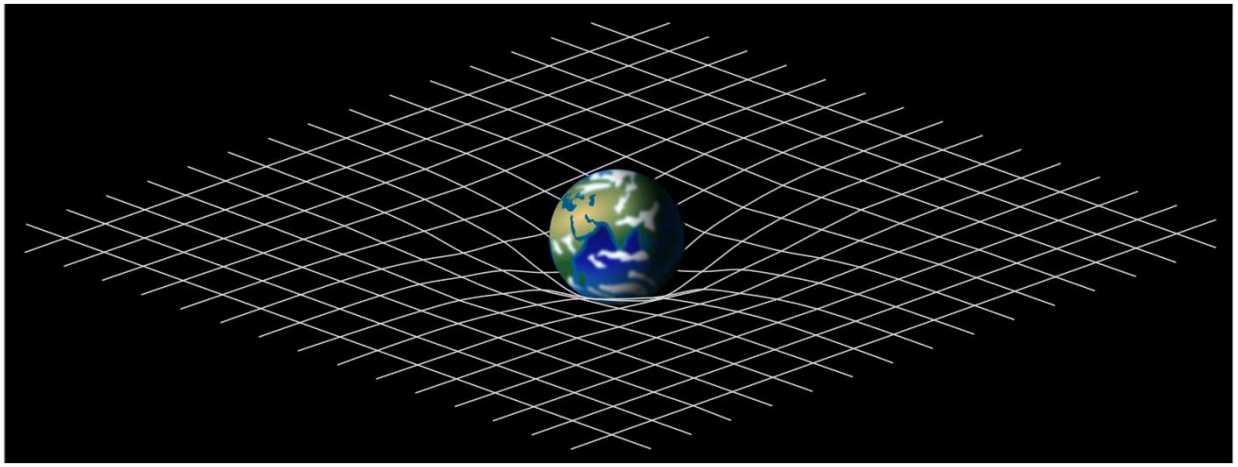

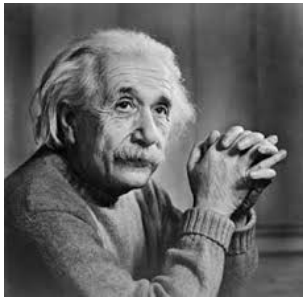

$$G_{\mu\nu} + \Lambda g_{\mu\nu} = \kappa T_{\mu\nu}$$

Local space time curvature Local energy, momentum stress

Mass of object

Gravitational wave detector

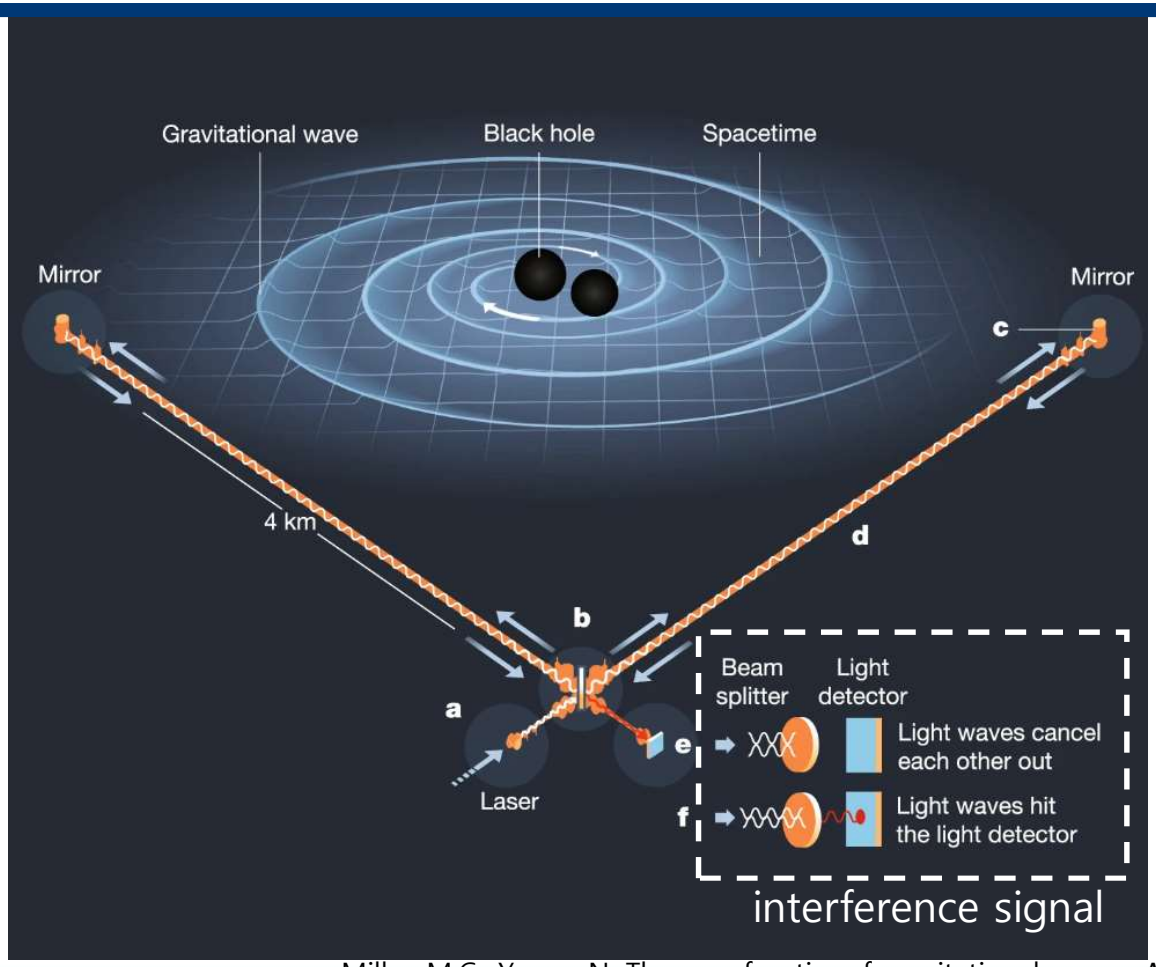

- Ground scale Michelson interferometer
- 4 km vacuum tunnel arm
- Over 1000 km interaction length

Miller, M.C., Yunes, N. The new frontier of gravitational waves. *Nature* **568**, 469–476 (2019)

Light(Electromagnetic wave)

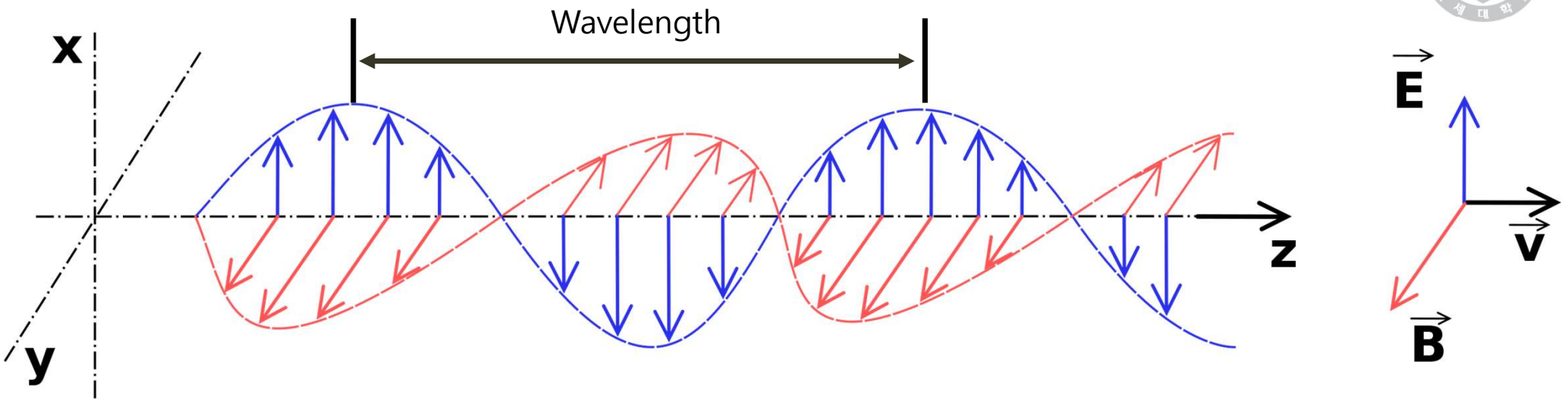

$$\left|\vec{E}\right| \propto Intensity\ of\ Light$$

Interference

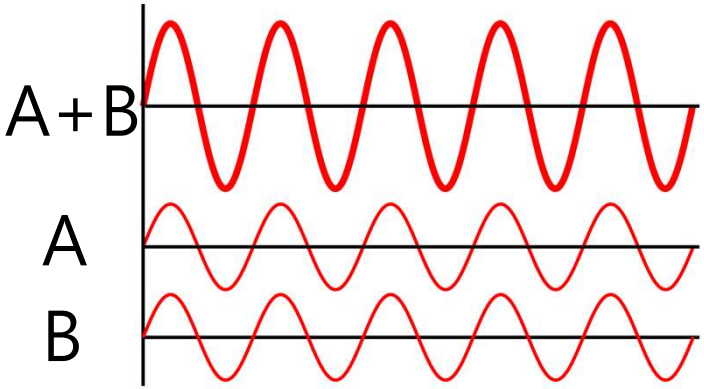

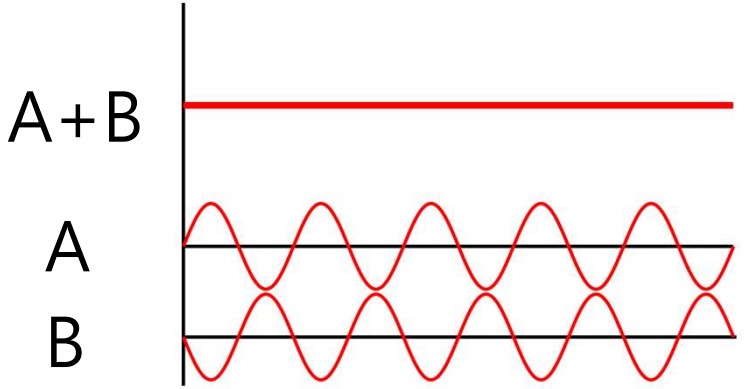

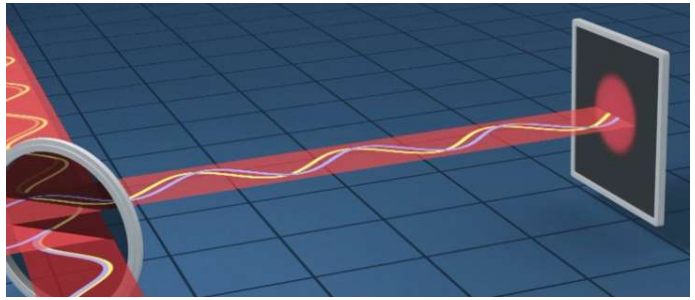

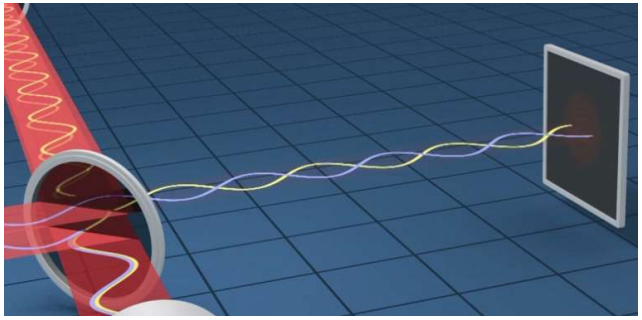

Constructive

Destructive

Interference signal

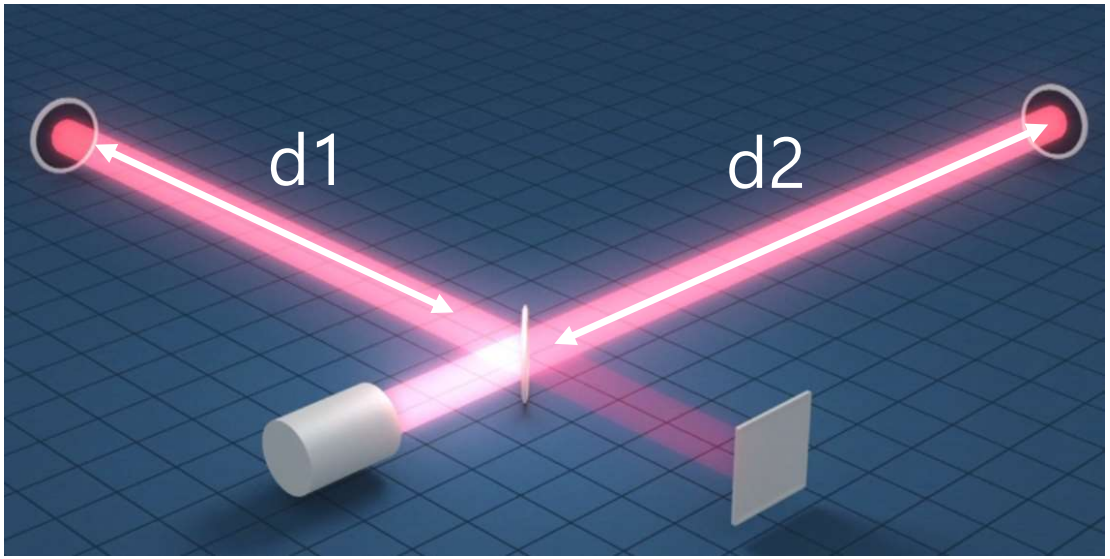

$$\vec{\mathrm{E}} = E_0 \cos(kx - \omega t + \varphi)$$

$$\varphi \propto d1 - d2 \text{ (in some condition)}$$

$$k = \frac{2\pi}{\lambda} \qquad \lambda : \text{wavelength}$$

Gravitational wave detector

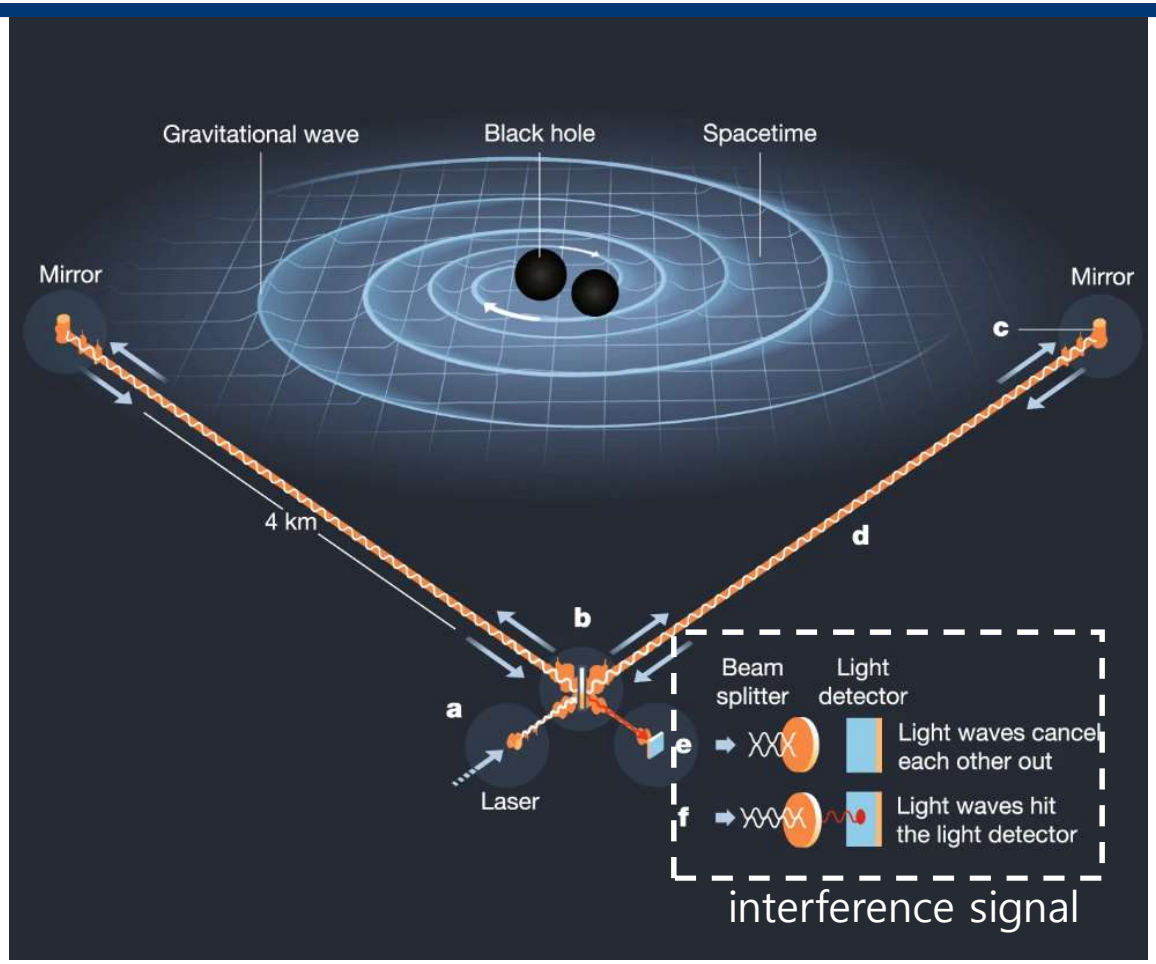

- Ground scale Michelson interferometer
- 4 km vacuum tunnel arm
- Over 1000 km interaction length

Build most sensitive system using most simple arrangement

Gravitational wave and GW detector

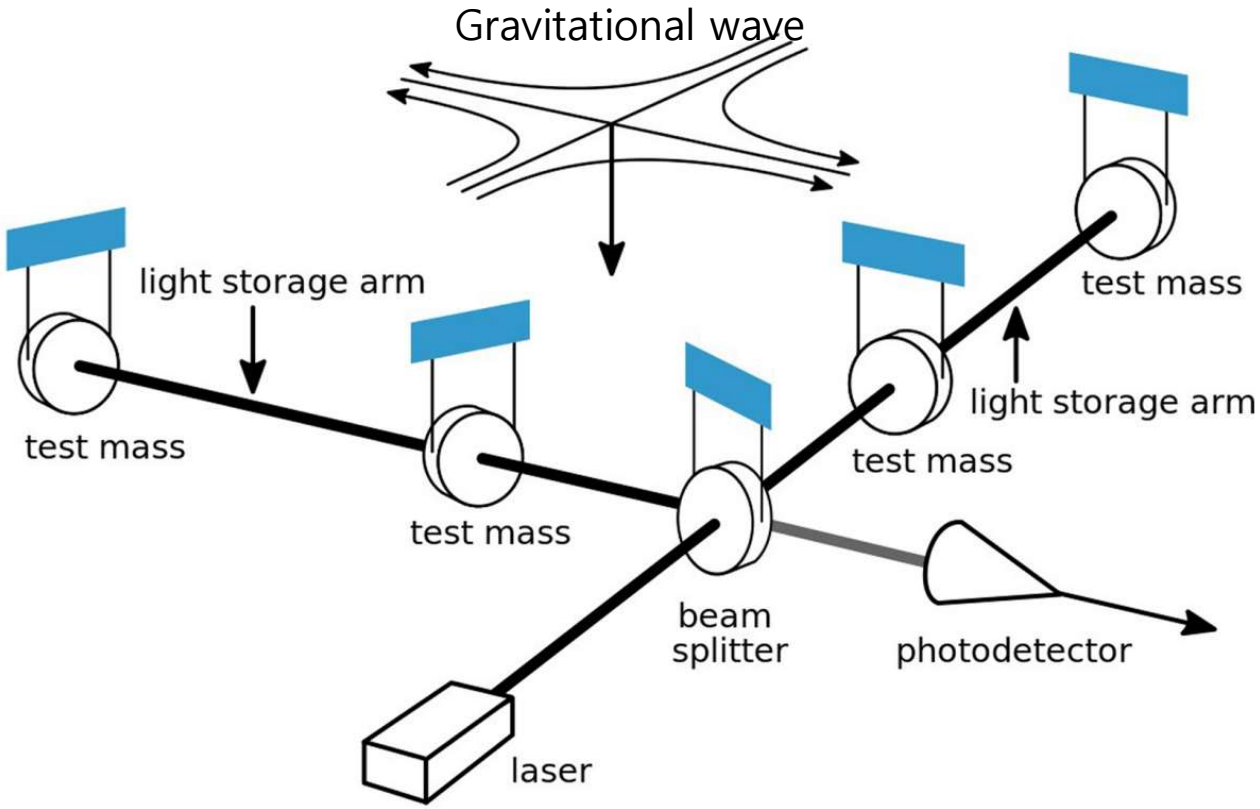

https://www.ligo.caltech.edu/

Gravitational wave and GW detector

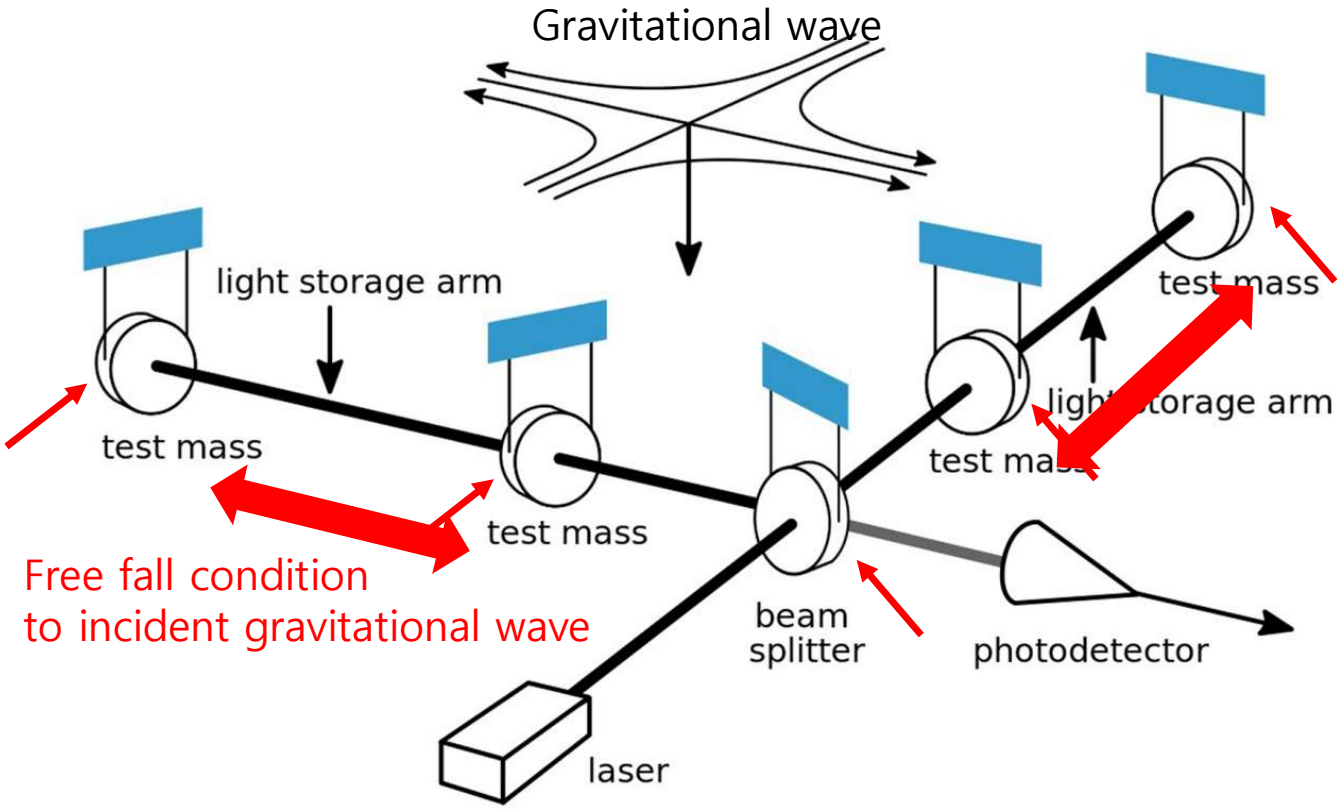

Strain sensitivity

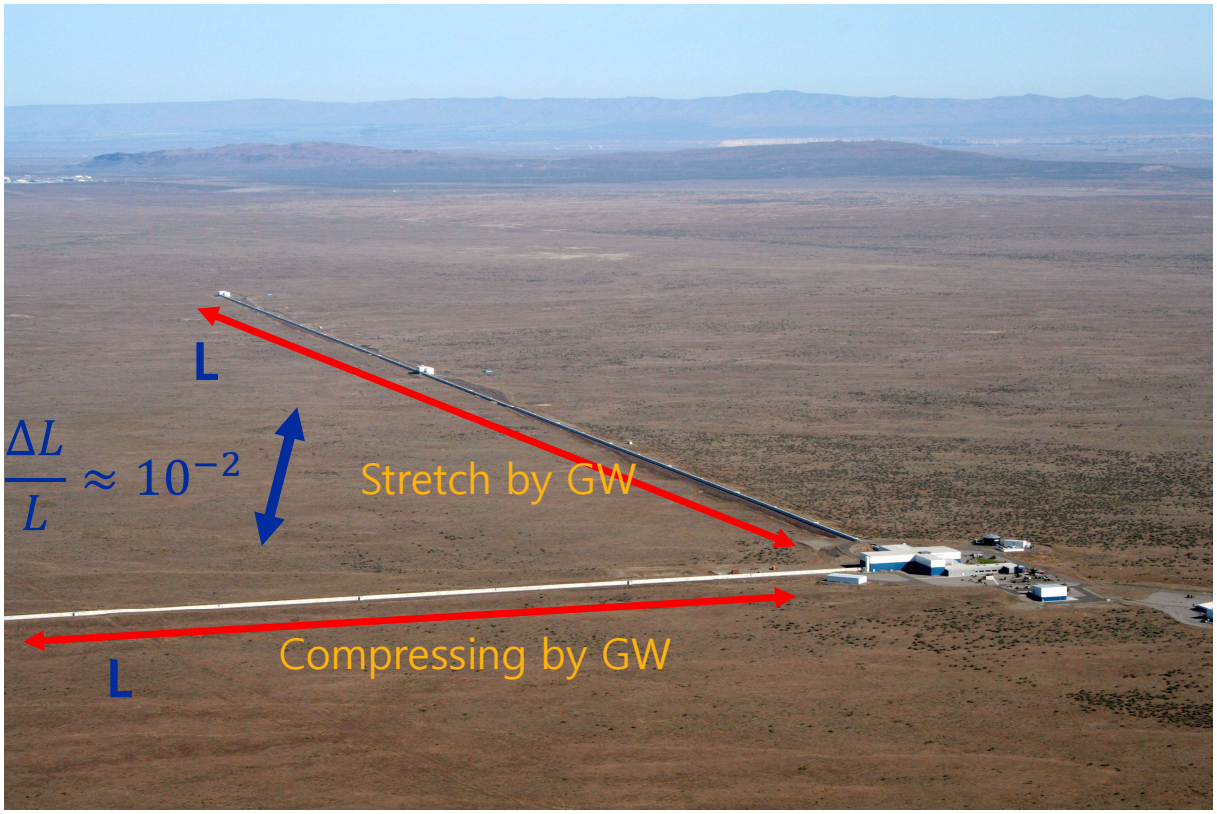

Minimum sensitivity

$$\frac{\Delta L}{L} \approx 10^{-21}$$

Strain due to gravitational wave

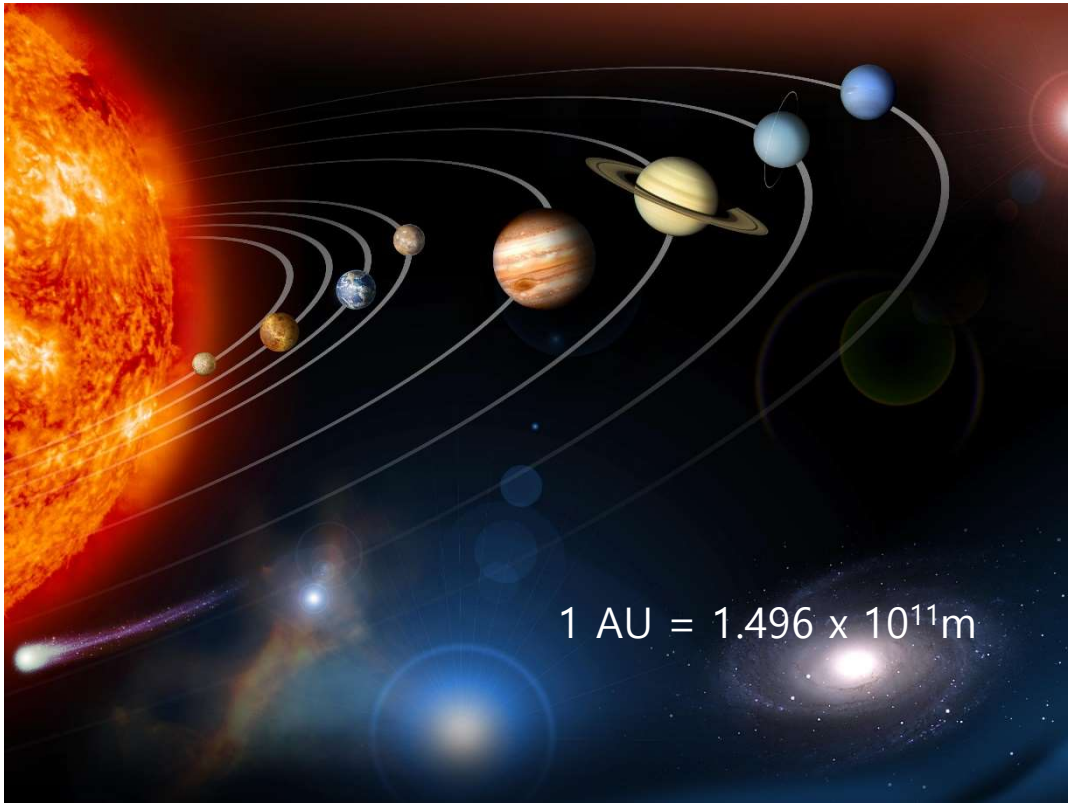

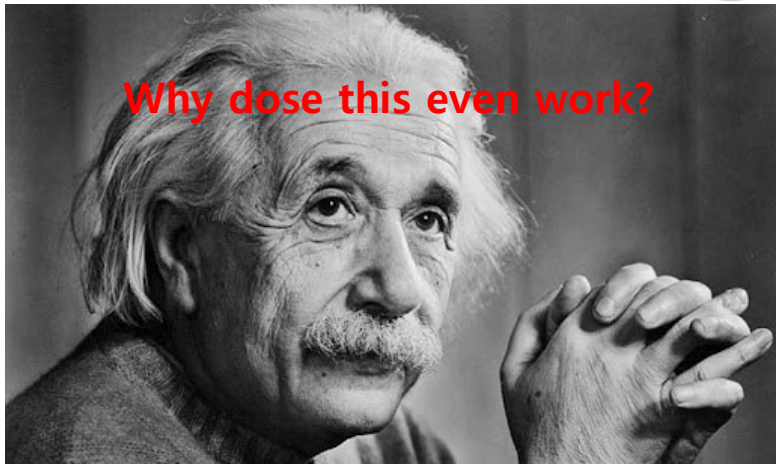

$$\frac{\Delta L}{L} \approx 10^{-21}$$

Detect existence of a single atom

Sensitivity of michelson interferometer

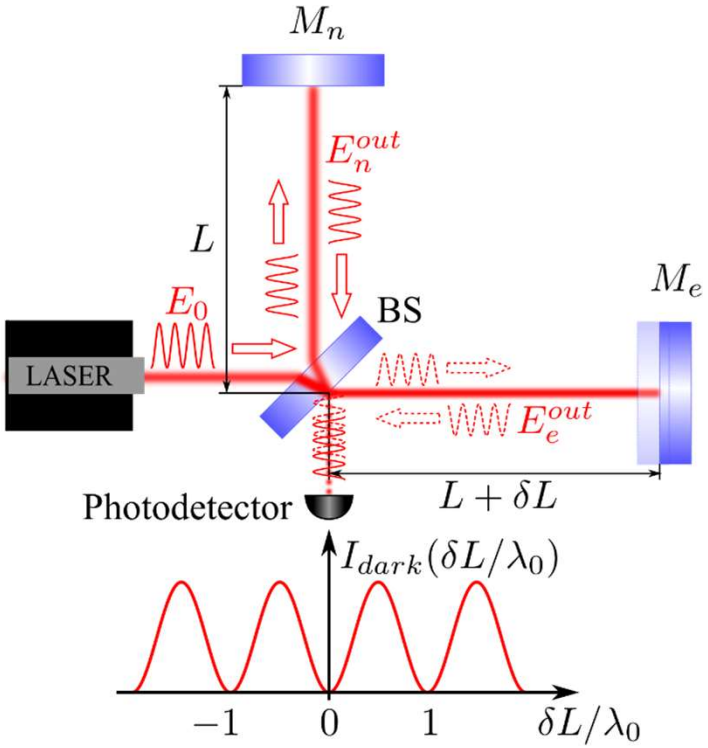

Danilishin, Stefan L. et al. Living Rev.Rel. 15 (2012) 5
arXiv:1203.1706

When L = 1 m

$$\frac{\Delta L}{L} \approx 10^{-16}$$

IF L = 1000 km

$$\frac{\Delta L}{L} \approx 10^{-2}$$

1000 km interferometer

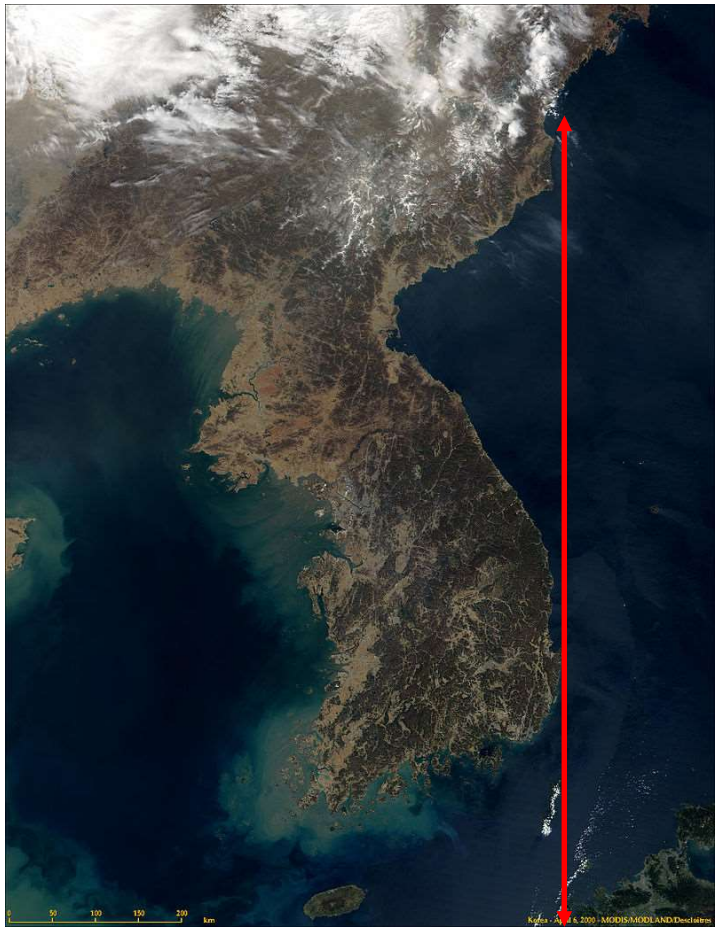

~1100km

LIGO interferometer

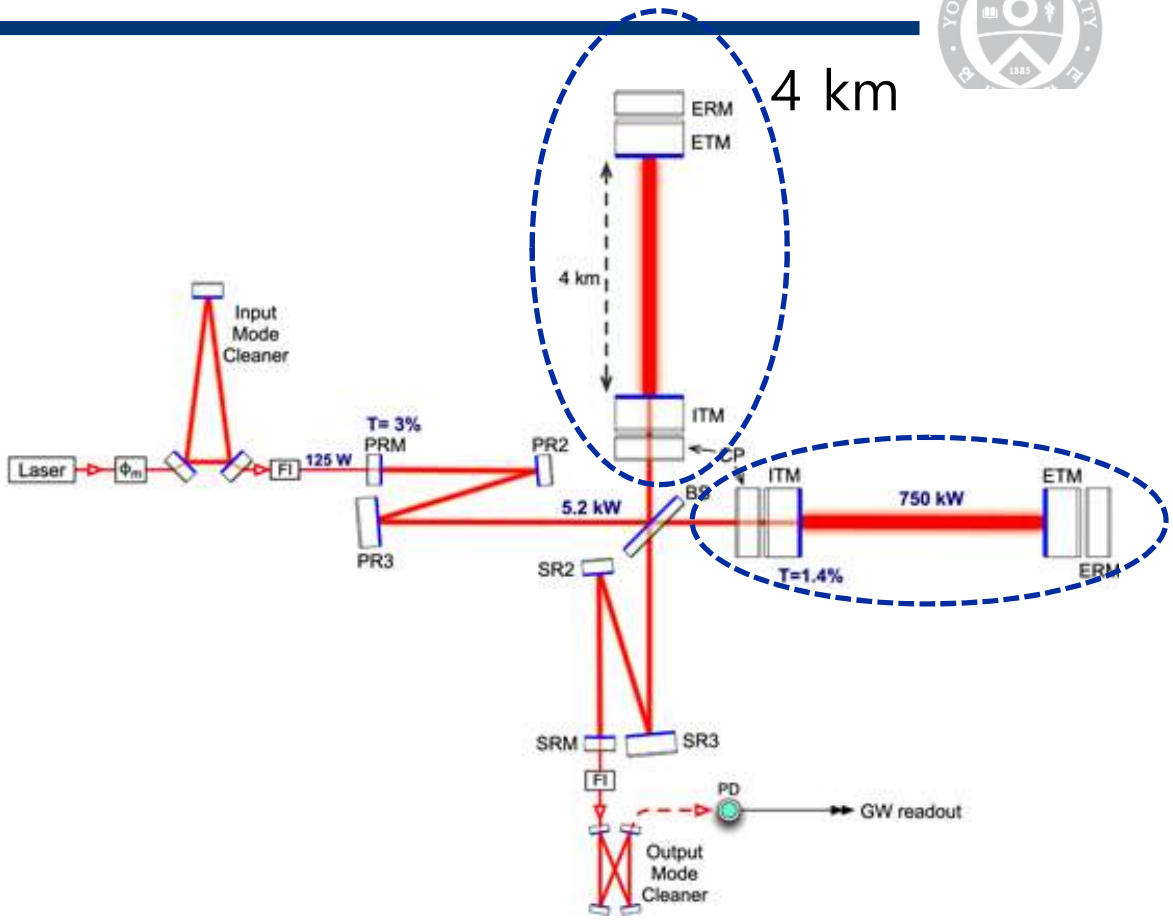

LIGO interferometer / Livingston

Fabry-perot cavity

Number of round trip > 250

4 km x 250 ~ 1000 km

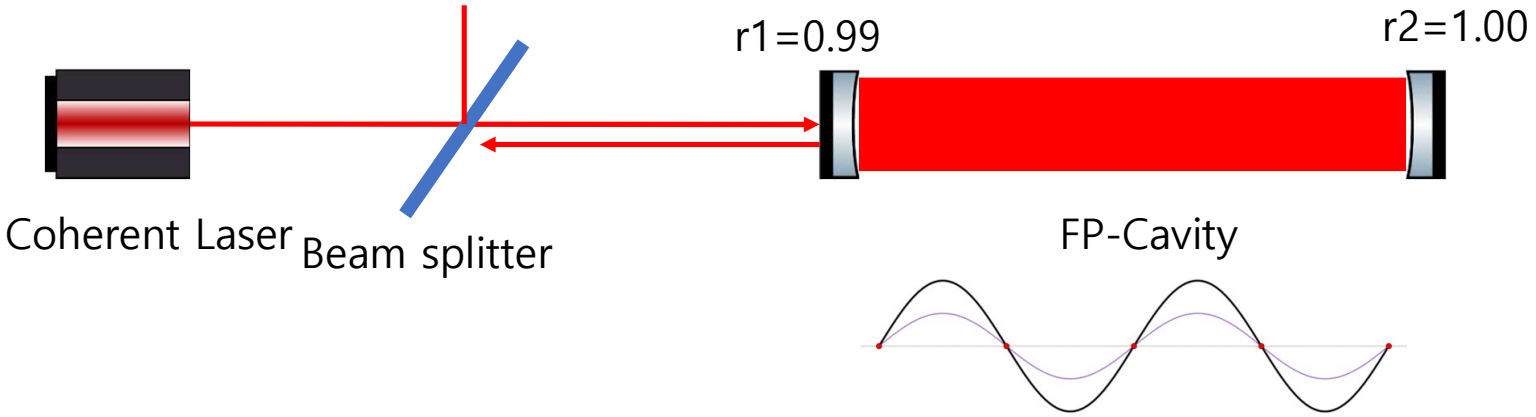

LIGO interferometer

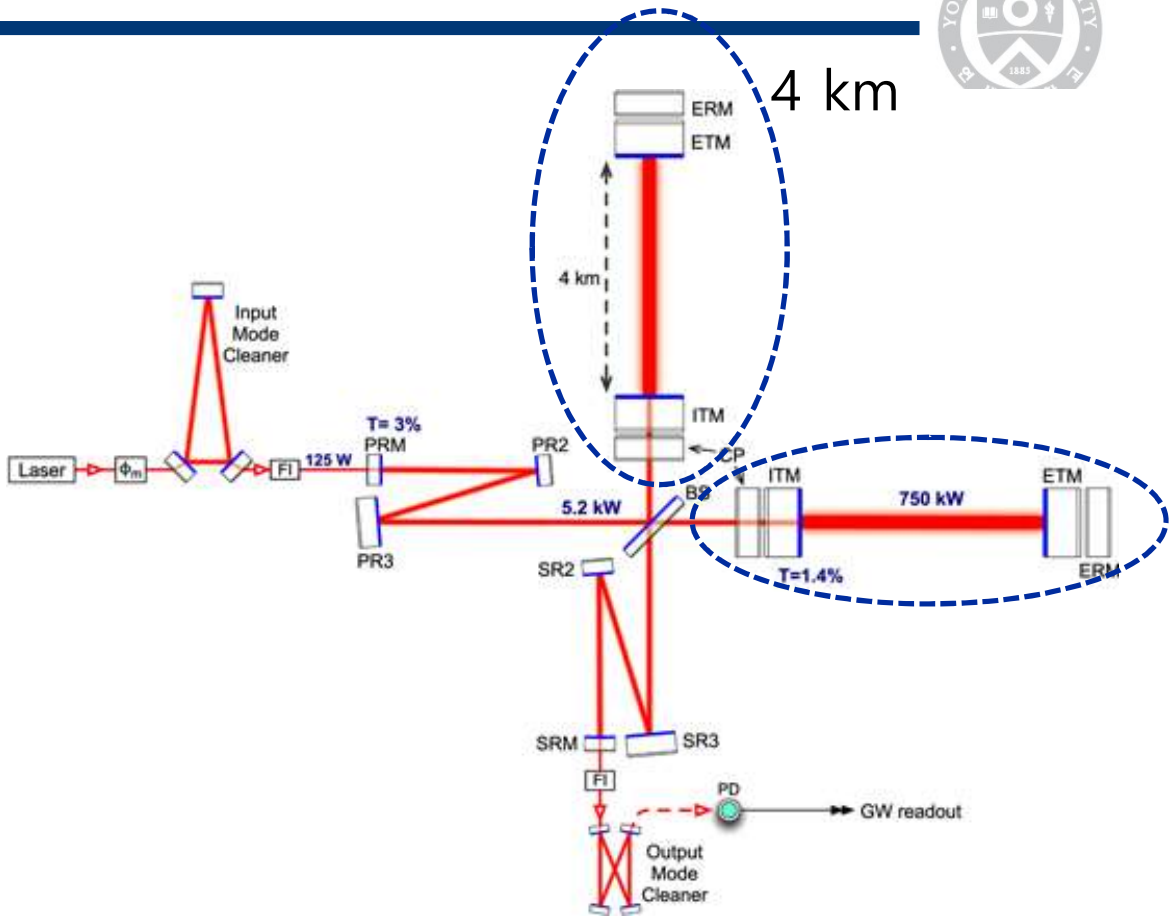

LIGO interferometer / Livingston

First detection of gravitational wave

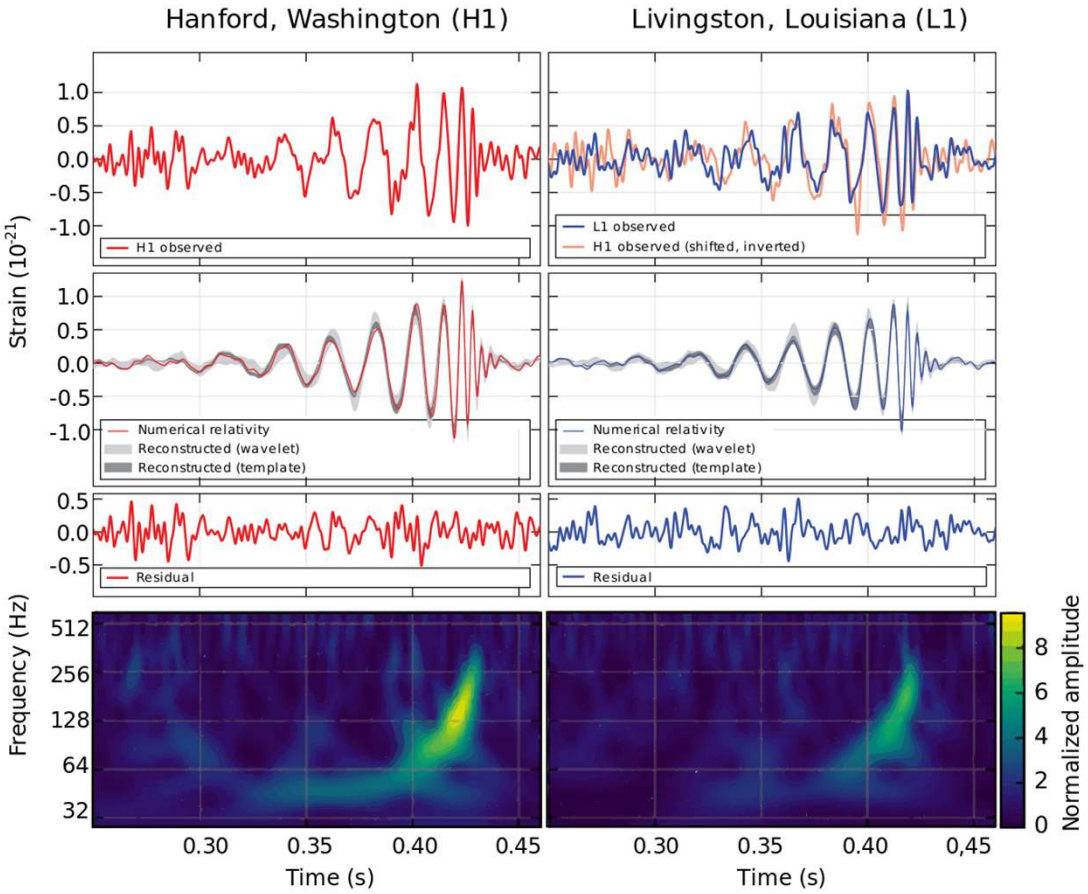

LVK Observation plan

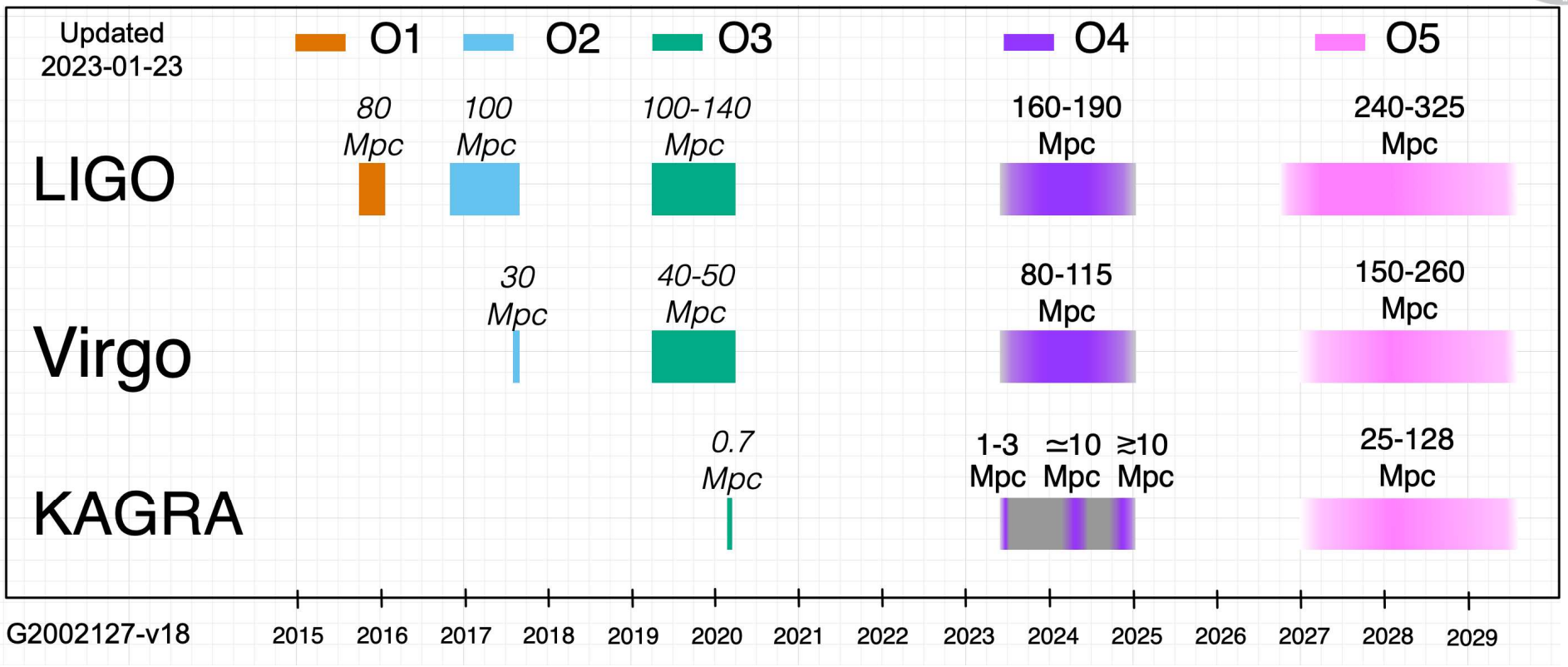

BNS range

- Binary-neutron-star range
- Common benchmark of sensitivity
- Made up of two 1.4 solar mass neutron stars
- Signal-to-noise ratio of 8

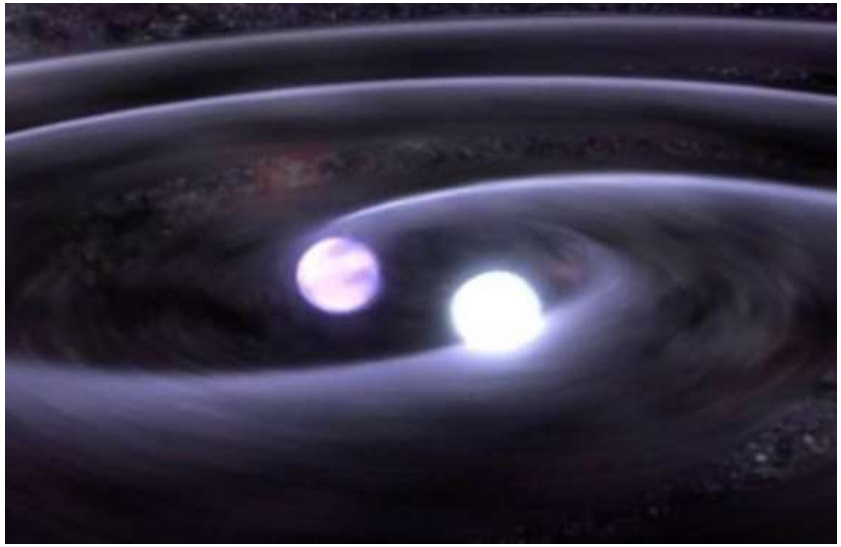

https://svs.gsfc.nasa.gov/10543

Maximum distance at which an event can be detected

Sensitivity during science run

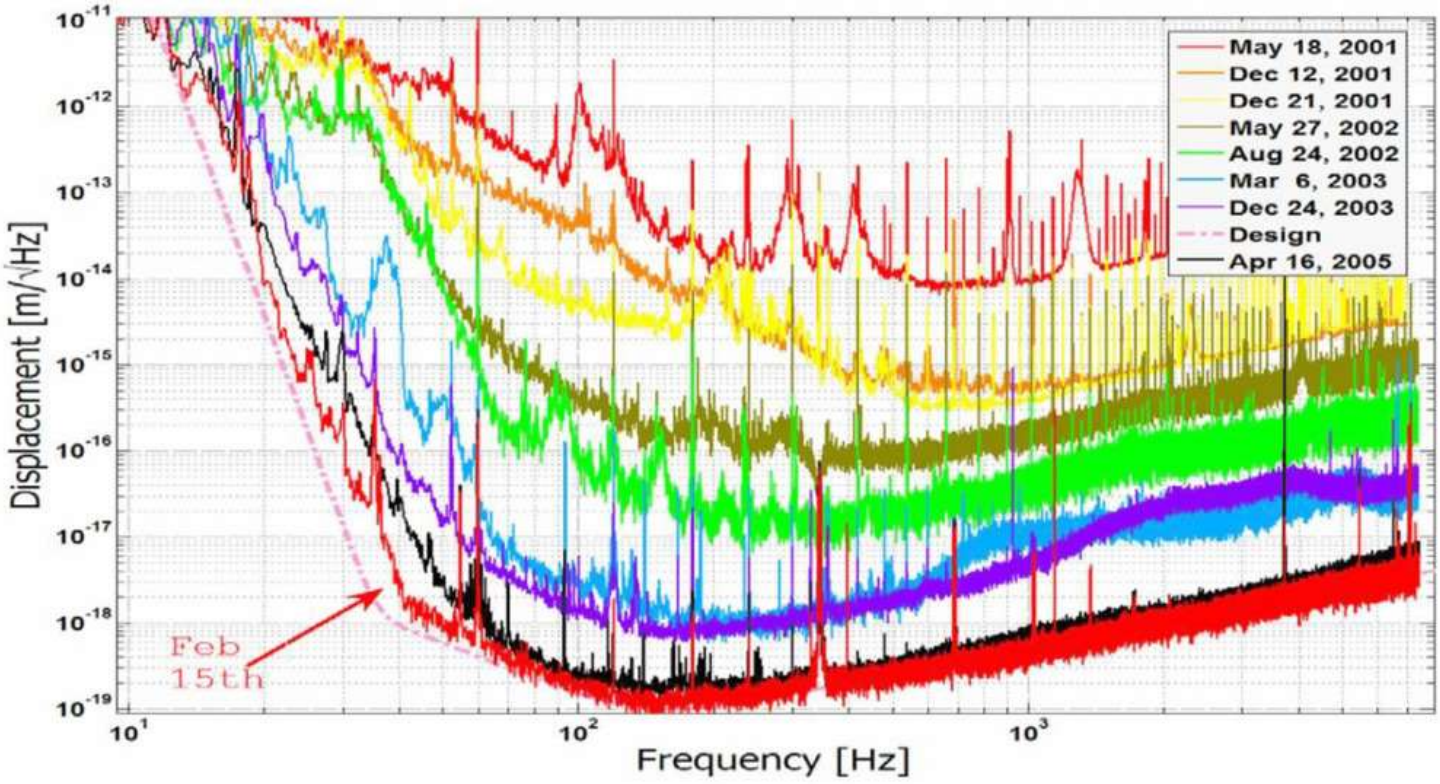

O4 sensitivity of LIGO

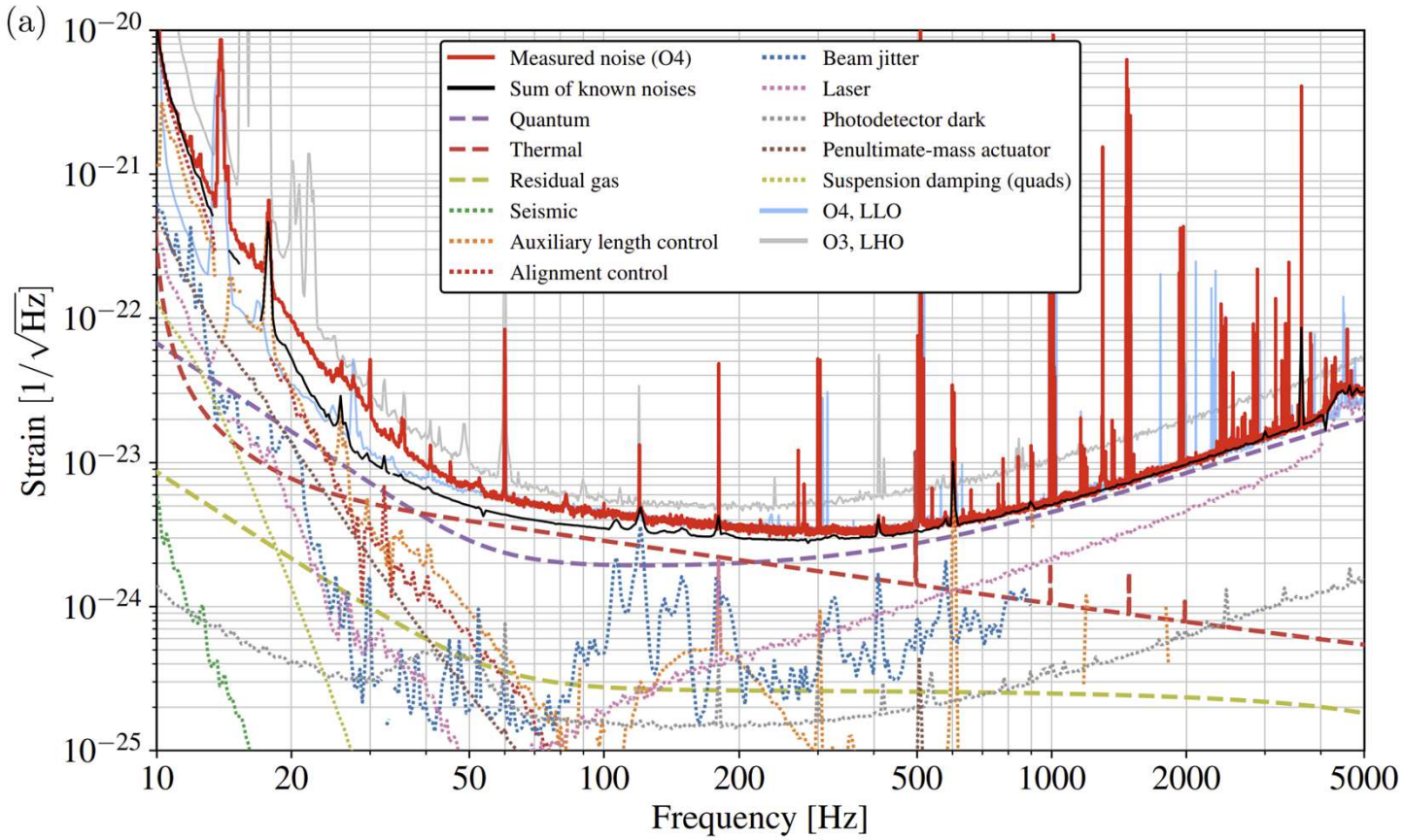

Phys. Rev. D **111**, 062002 – **Published 3 March, 2025**

LIGO interferometer

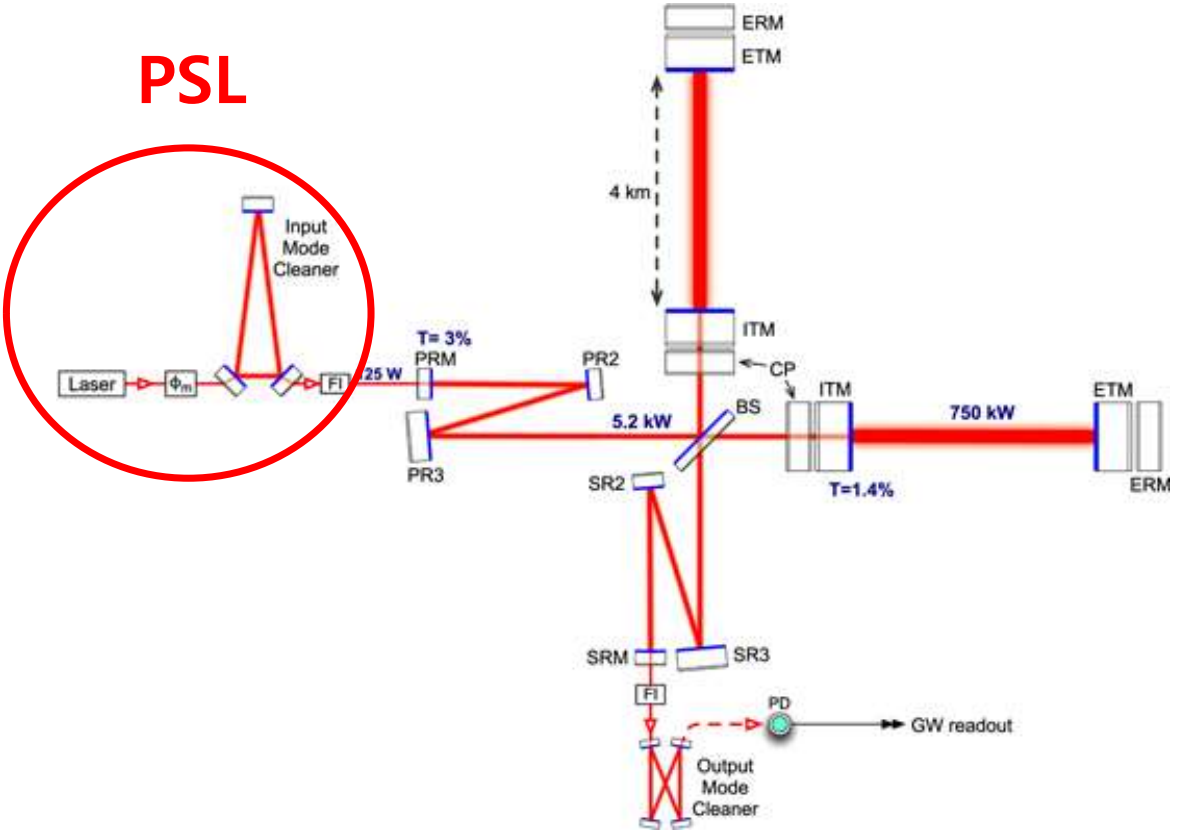

Key component of LIGO

- Stabilized laser
- Michelson interferometer
- Fabry-perot cavity
- Test mass
- Suspended system
- Dual recycling system

Pre-stabilized Laser

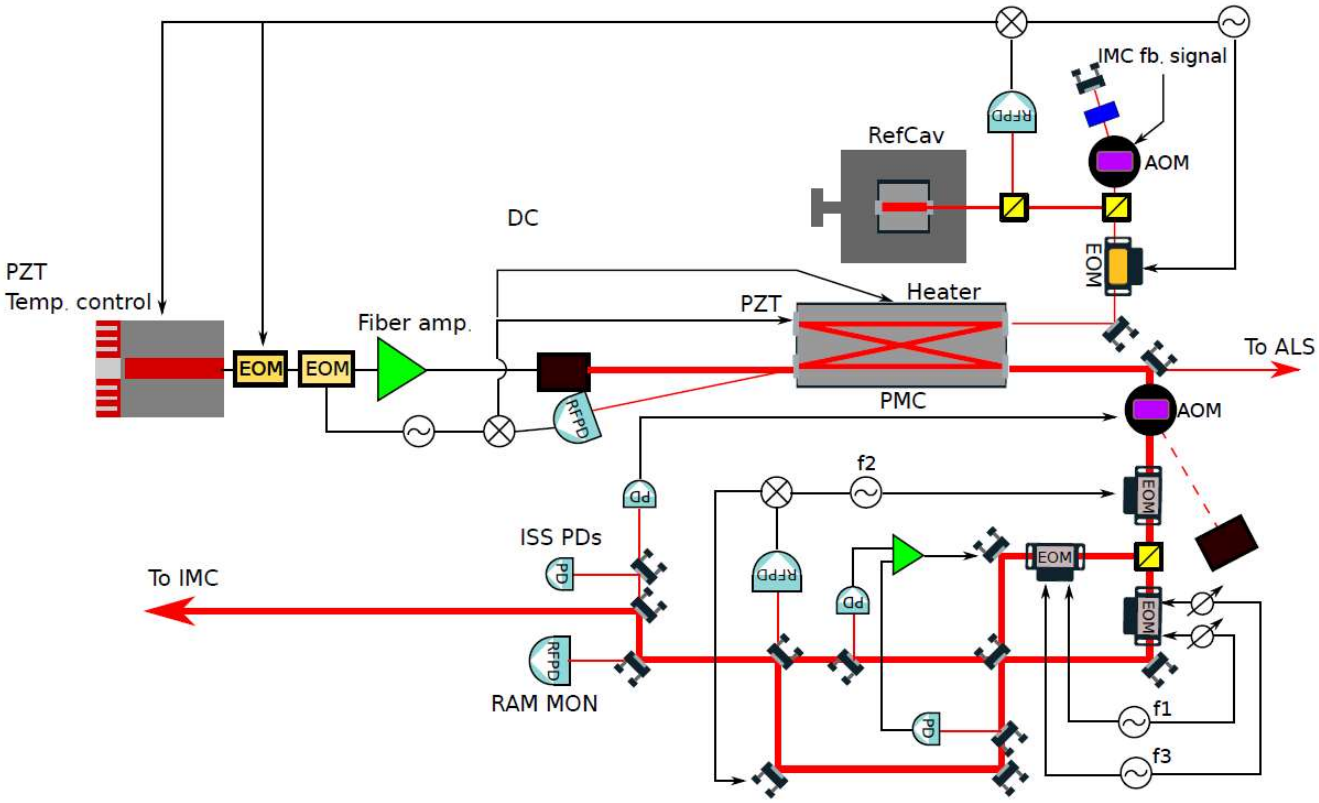

- **Frequency**
- **Linewidth**
- **Power**
- **Pointing**

(beam jitter)

High Power

Long operation

Reference cavity

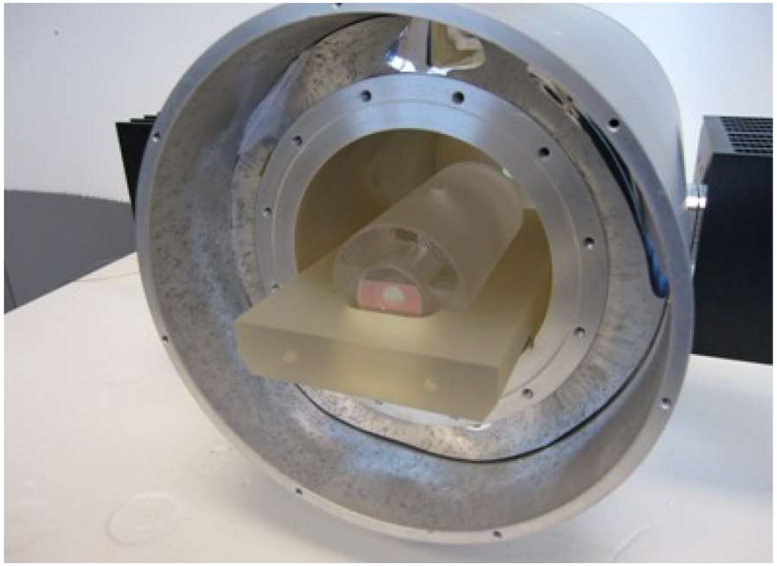

Cavity for frequency stabilization
Finesse around 30000

Fabry-perot cavity

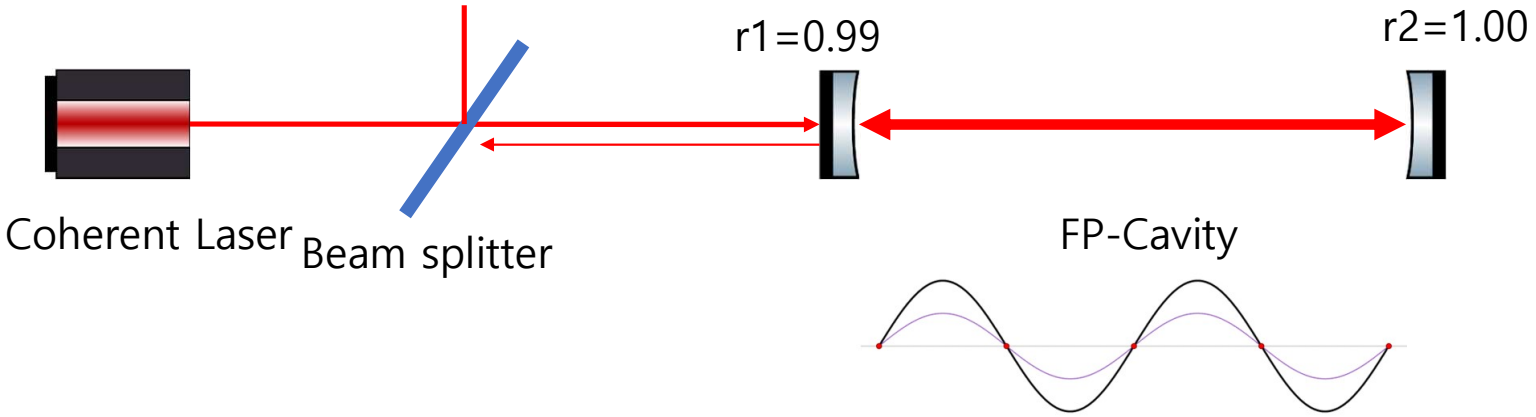

Laser frequency stabilization

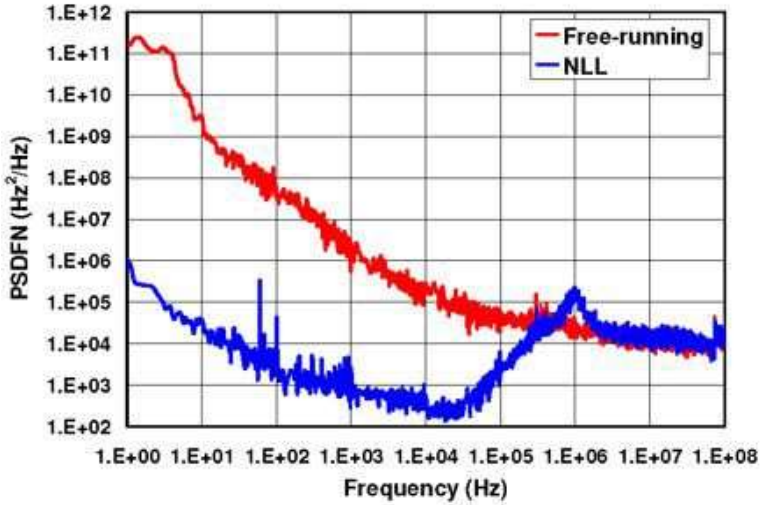

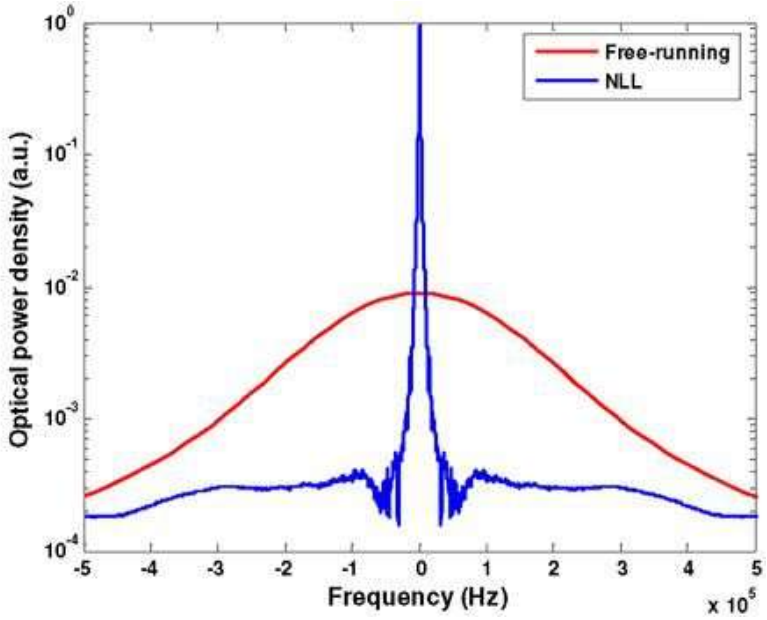

Beam stabilization

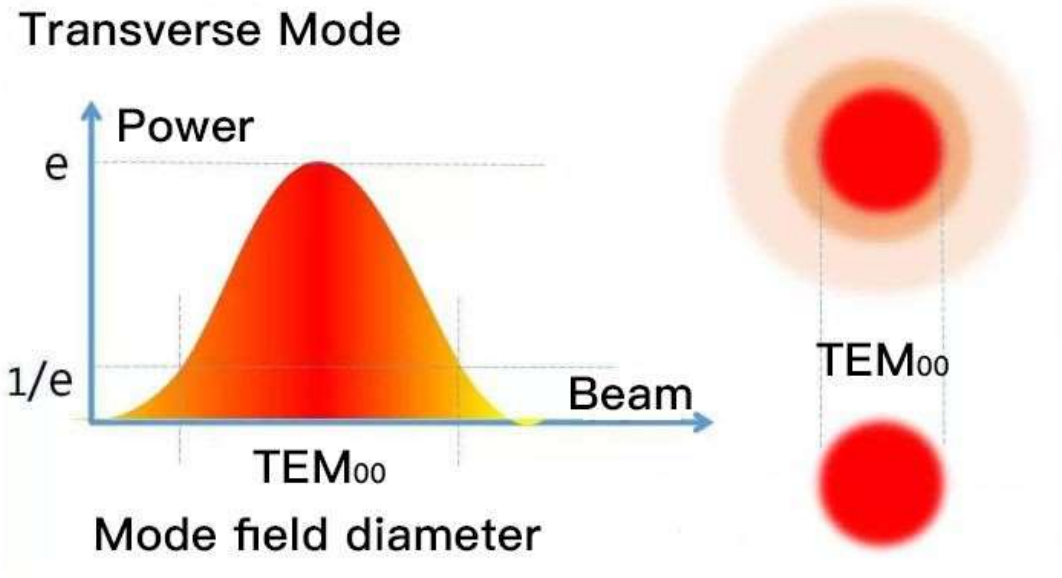

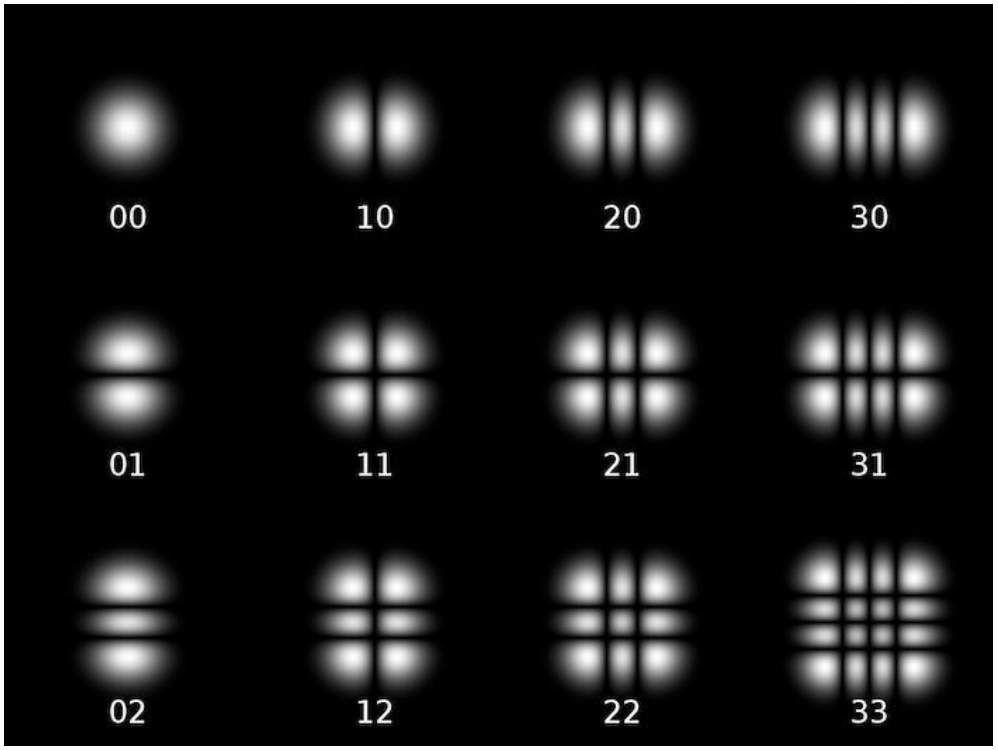

PSL room of KAGRA

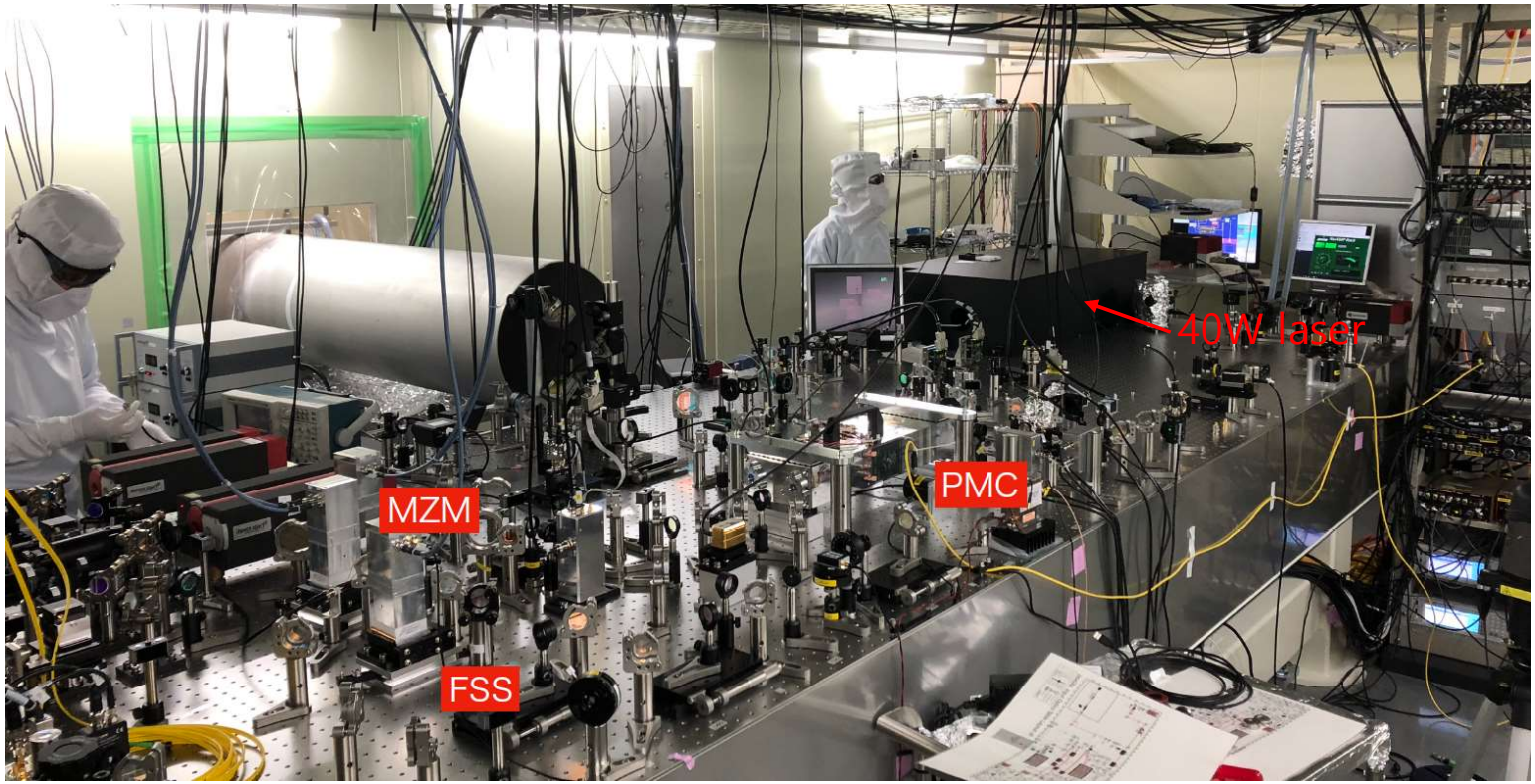

JGW-G1910363 – Masayuki Nakano

LIGO interferometer

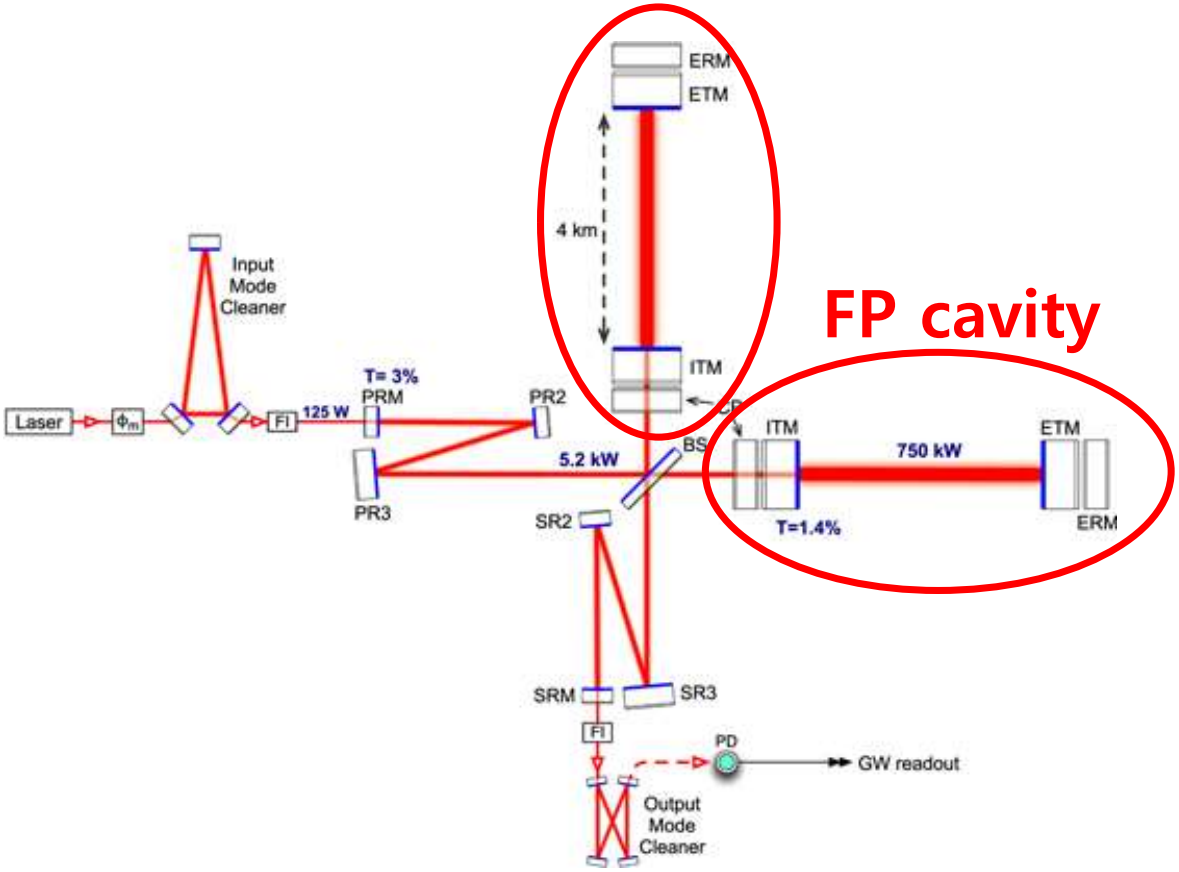

Key component of LIGO

- Stabilized laser
- Michelson interferometer
- Fabry-perot cavity
- Test mass
- Suspended system
- Dual recycling system

4 km FP cavity

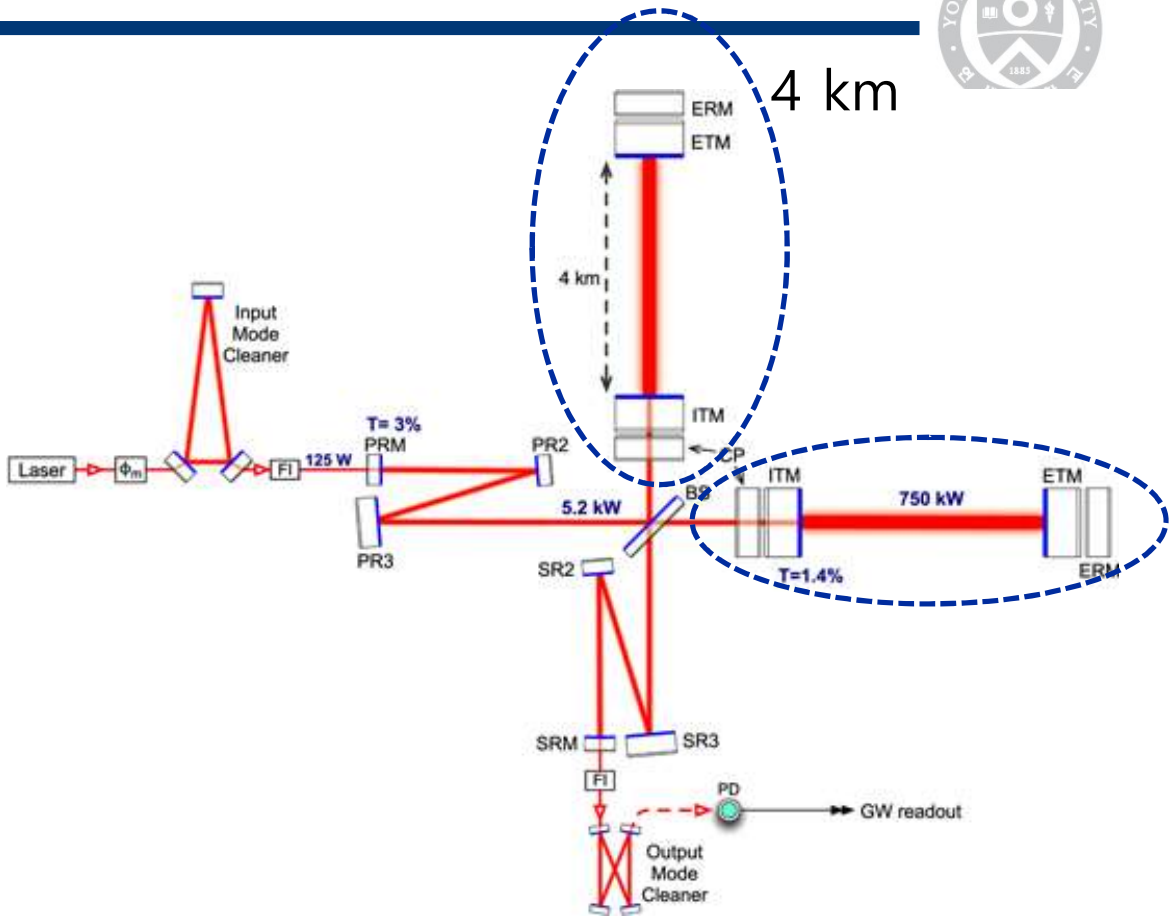

LIGO interferometer / Livingston

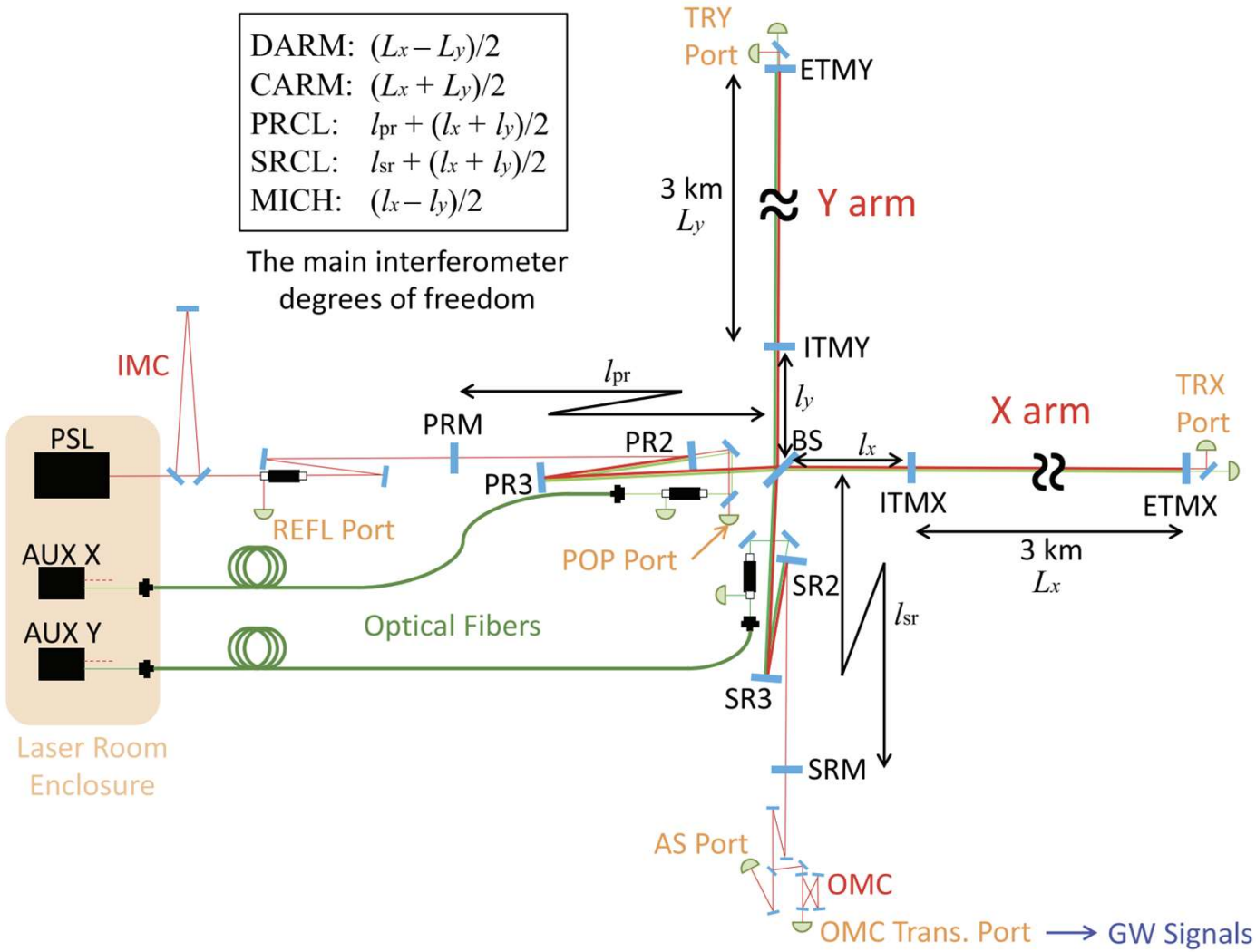
DARM: $(L_x - L_y)/2$
CARM: $(L_x + L_y)/2$
PRCL: $l_{pr} + (l_x + l_y)/2$
SRCL: $l_{sr} + (l_x + l_y)/2$
MICH: $(l_x - l_y)/2$
The main interferometer degrees of freedom
TRY Port
ETMY
3 km
L_y
Y arm
ITMY
l_{pr}
l_y
IMC
PRM
PR2
BS
l_x
X arm
TRX Port
PSL
PR3
ITMX
ETMX
REFL Port
POP Port
3 km
L_x
AUX X
SR2
l_{sr}
AUX Y
Optical Fibers
SR3
Laser Room Enclosure
SRM
AS Port
OMC
OMC Trans. Port → GW Signals

Arm length control

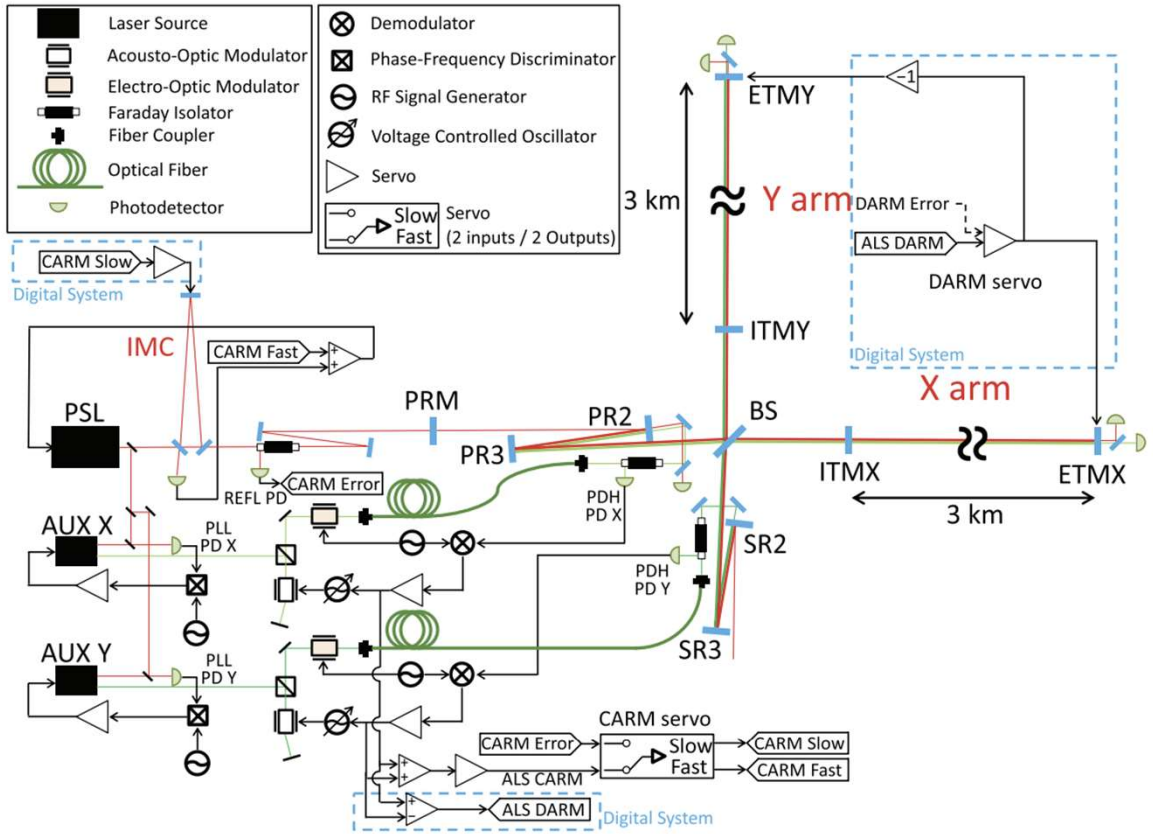

Arm length control

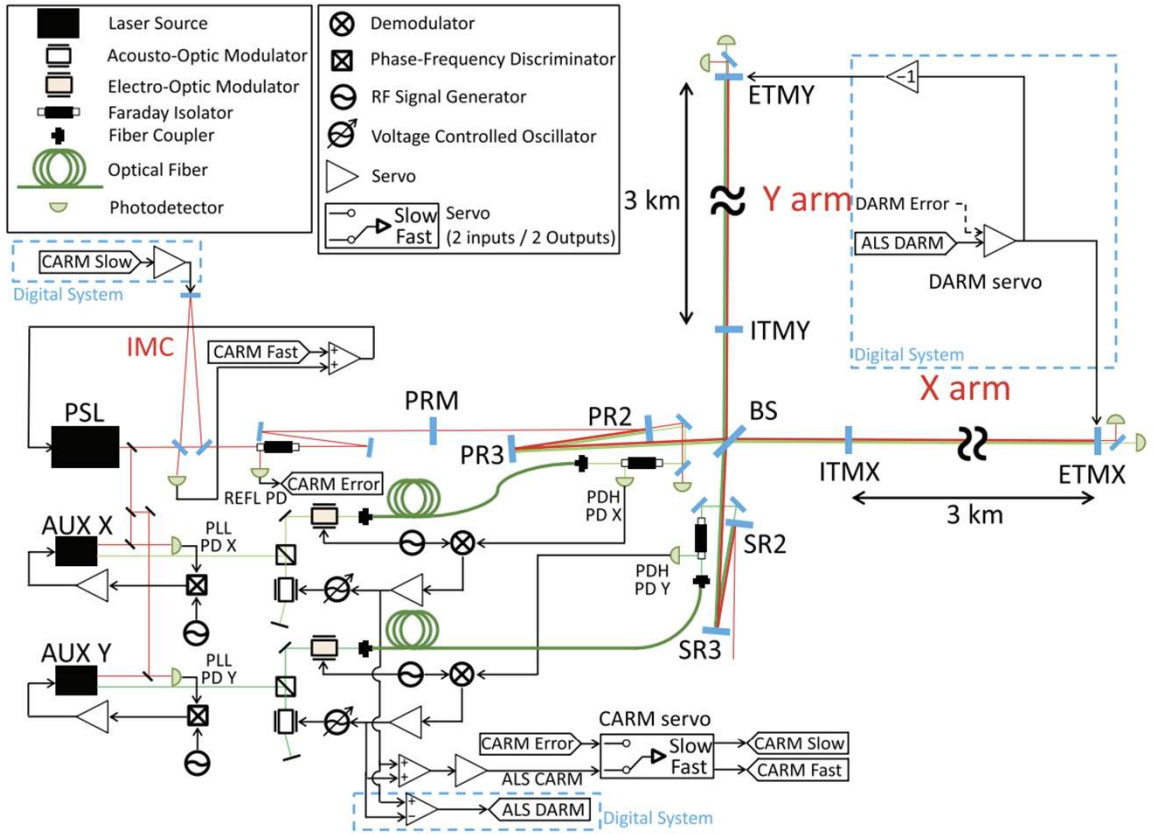

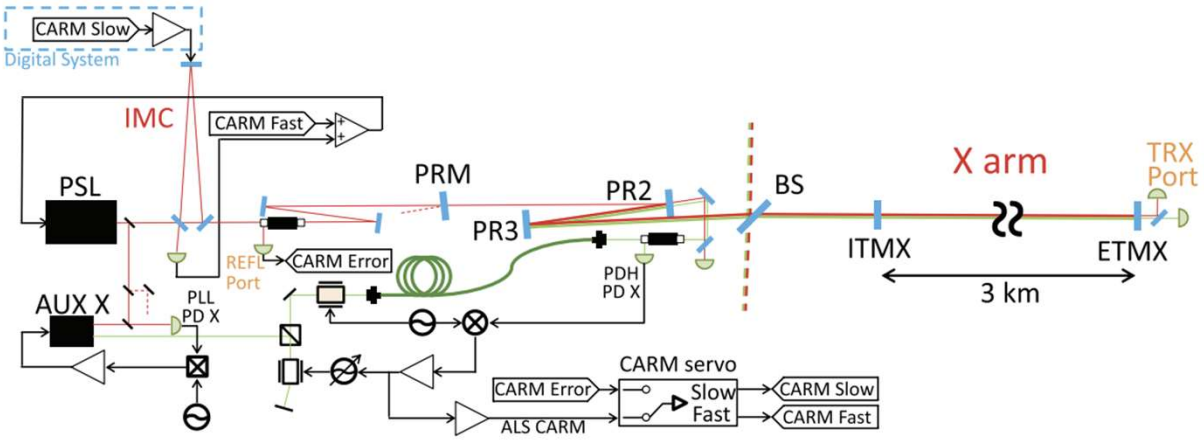

Figure 4. Schematic view of the configuration of the interferometer and the control for the X arm lock experiment. The PRM was misaligned, and the Y arm and the signal recycling mirrors were not involved in the experiment. The legend for the symbols in the figure can be found in figure 2.

Table 2. Optical parameters of the X arm cavity. The values measured in the X arm experiment are shown along with the design values.

Parameter name	Designed	Measured
Cavity length[a]	3000 m [25]	2999.990(2) m
Finesse for 1064 nm[b]	1530 [25]	1410(30)
Roundtrip loss for 1064 nm[a,c]	<100 ppm [25]	86(3) ppm
Mode matching ratio for 1064 nm[a]	—	0.91(1)
Transverse mode spacing[a]	34.80 kHz [25]	34.79(5) kHz
Finesse for 532 nm[d]	49.2	41.0(3)

- **Largest FP cavity**
- **Length control**
- **DOF control**

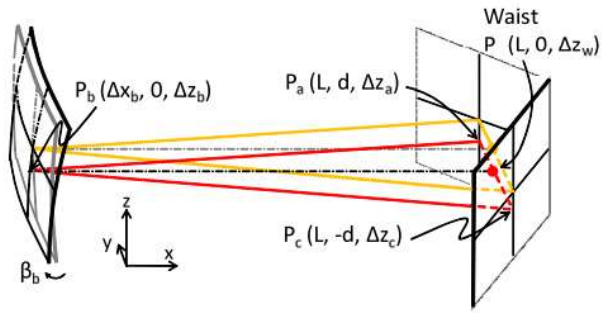

Figure 16. Cavity eigenmodes of the aligned (lighter colored triangle) and the misaligned by β_b (darker colored triangle) cases. This type of misalignment does not affect the mirror alignment in the y direction, hence the eigenmode changes only along the z axis.

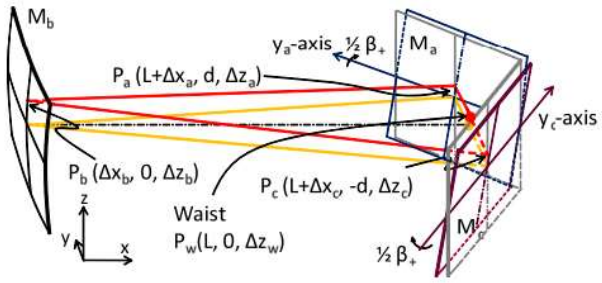

Figure 18. Cavity eigenmodes of the aligned and the misaligned (β_+) cases. This type of misalignment does not affect the mirror alignment in the y di
along the z axis.

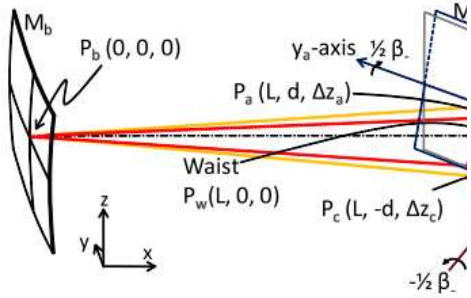

Figure 20. Cavity eigenmodes of the aligned and
(β_-) cases. The beam spot position and the waist
unchanged.

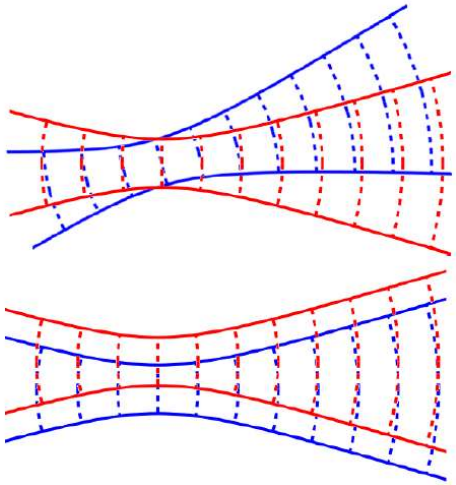

Wavefront sensor

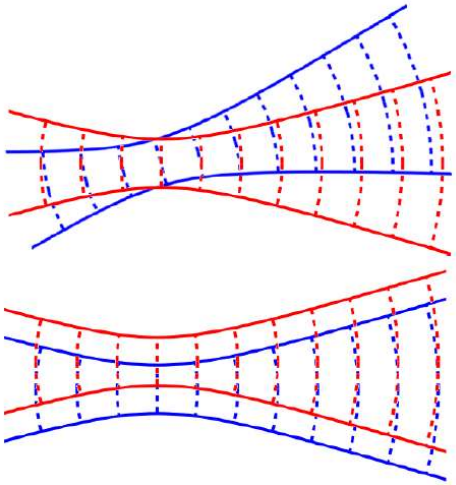

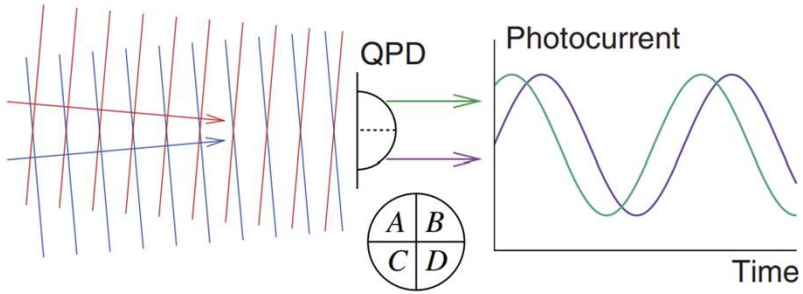

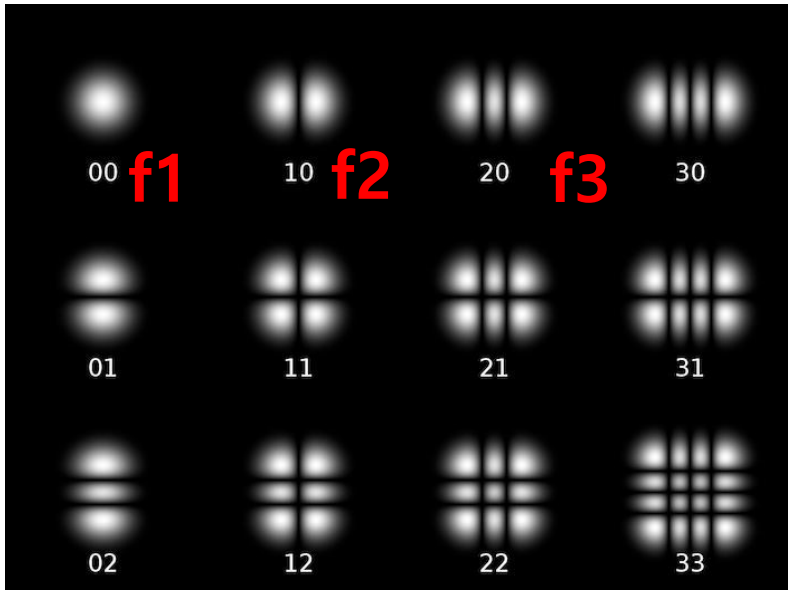

Wavefront sensor

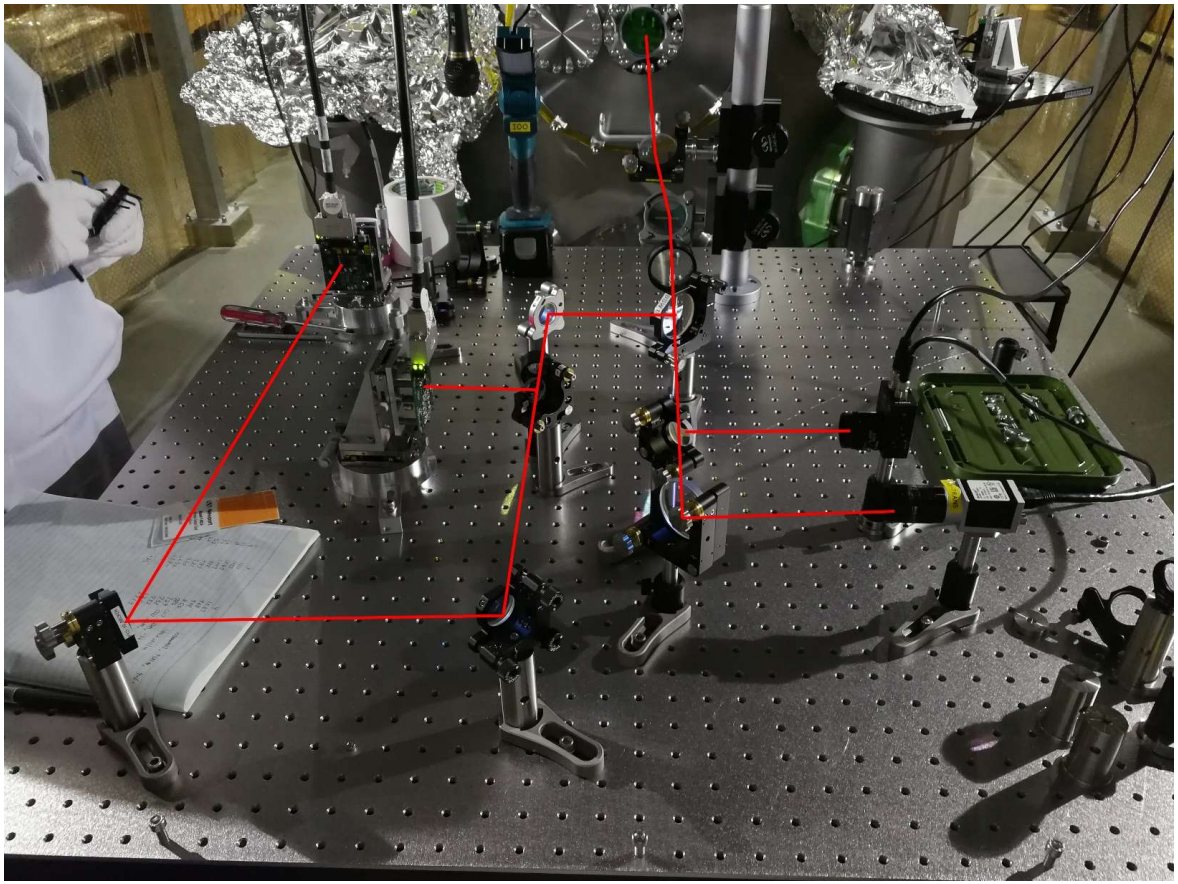

LIGO interferometer

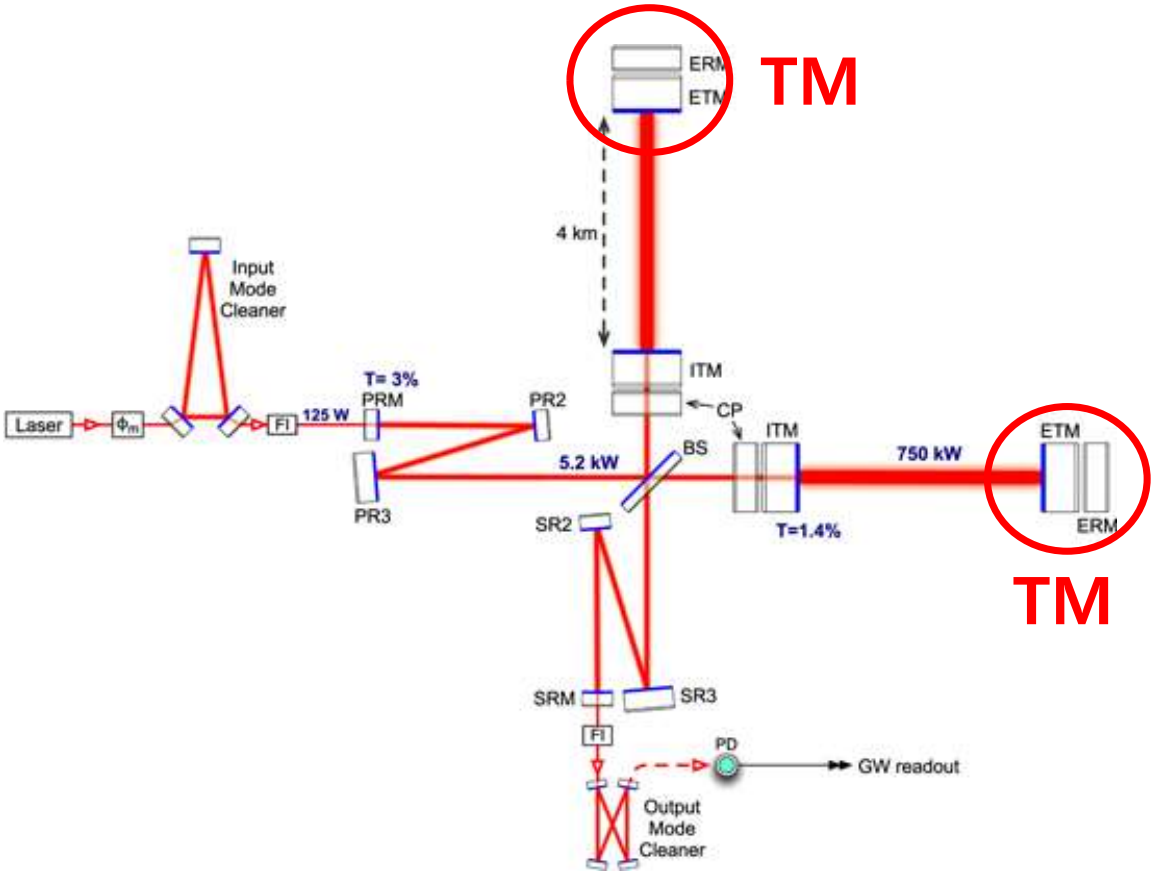

Key component of LIGO

- Stabilized laser
- Michelson interferometer
- Fabry-perot cavity
- Test mass
- Suspended system
- Dual recycling system

Test mass of LIGO (40 kg)

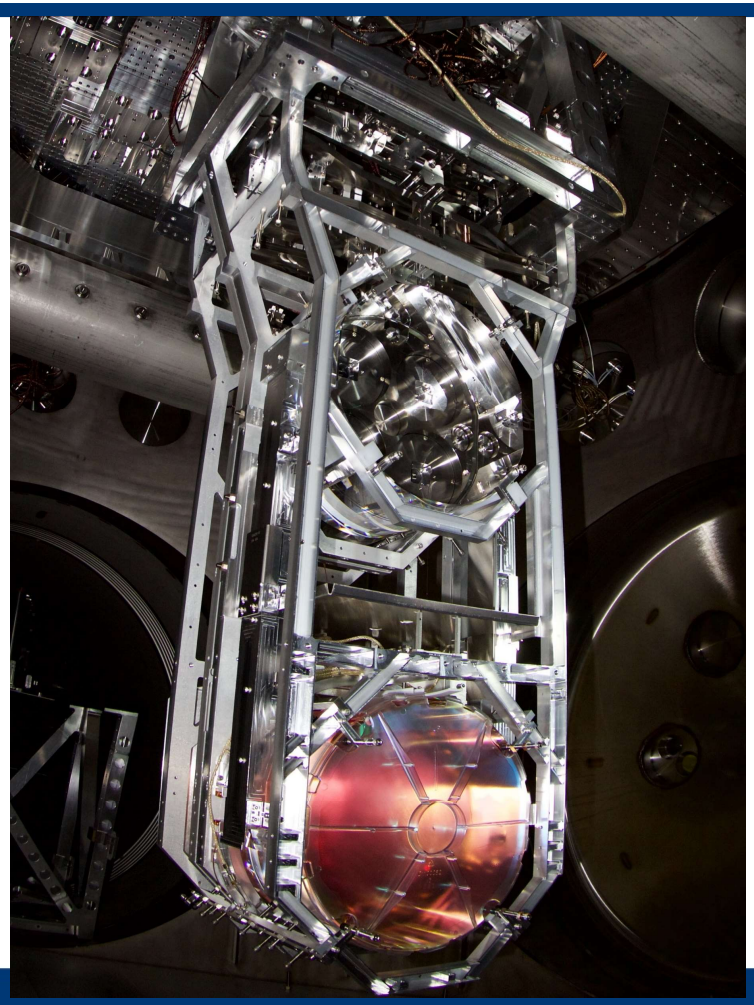

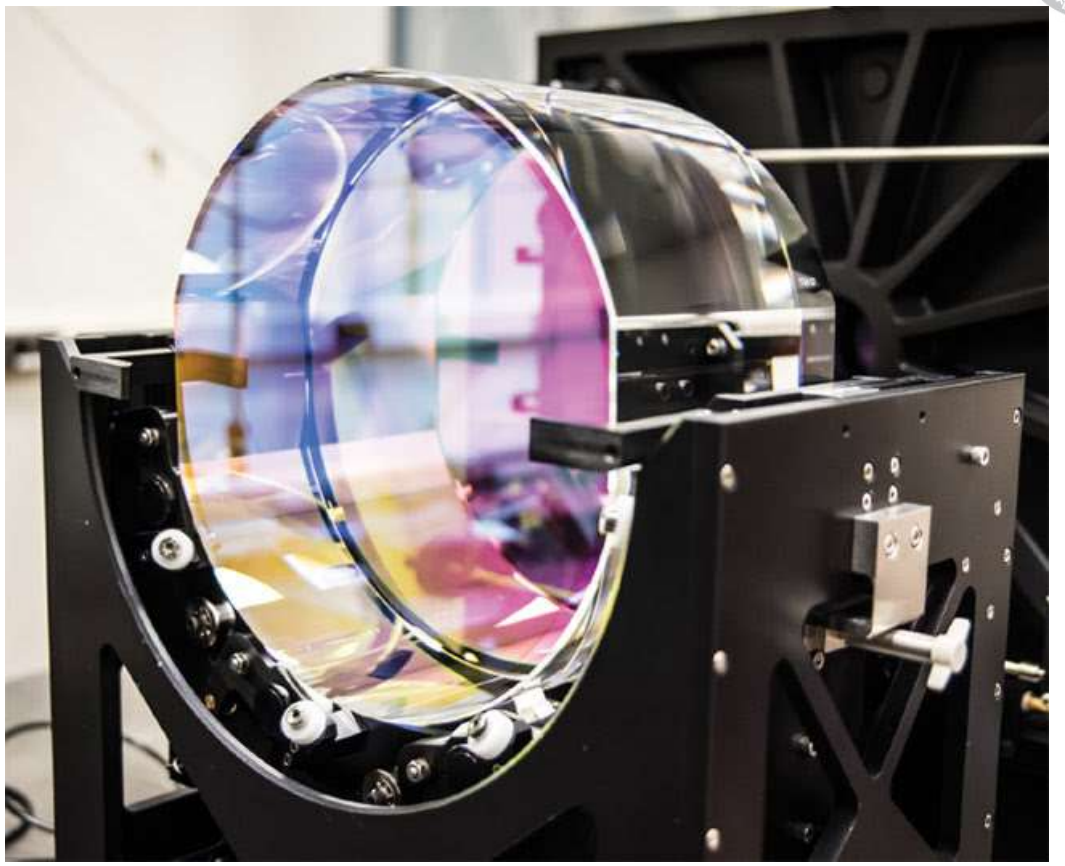

Test mass

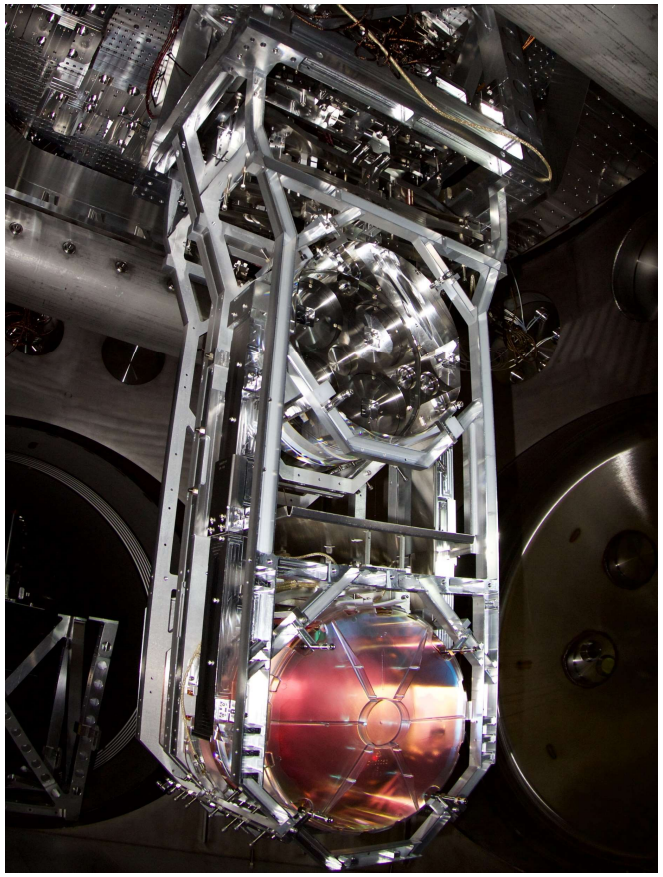

LASER INTERFEROMETER GRAVITATIONAL WAVE OBSERVATORY

LIGO

SPECIFICATION

E080511- V3 -D
Drawing No Rev. Group

Sheet 3 of 4

Advanced LIGO Input Test Mass (ITM)

Surface Error, Low Spatial Frequency: measurement aperture to 1 mm^{-1}

The following root mean square standard deviation (σ_{rms}) values are calculated from the phase maps which are to be provided with each optic. For this calculation the amplitudes for the best fit Zernike terms $Z_{0,0}$, $Z_{1,1}$, $Z_{2,0}$ and $Z_{2,2}$ or corresponding Seidel aberrations are subtracted from the phase map. Known bad pixels may be excluded from this calculation.

Surface 1, Frequency Band: $< 1\ mm^{-1}$
Measured over the central 300 mm diameter aperture: $\sigma_{rms} < 2.5$nanometers
Measured over the central 160 mm diameter aperture: $\sigma_{rms} < 0.3$ nanometers

Surface 2 - Frequency Band: $< 1\ mm^{-1}$
Measured over the central 300 mm diameter aperture: $\sigma_{rms} < 4$ nanometers
Measured over the central 160 mm diameter aperture: $\sigma_{rms} < 2$ nanometers

Suspended system

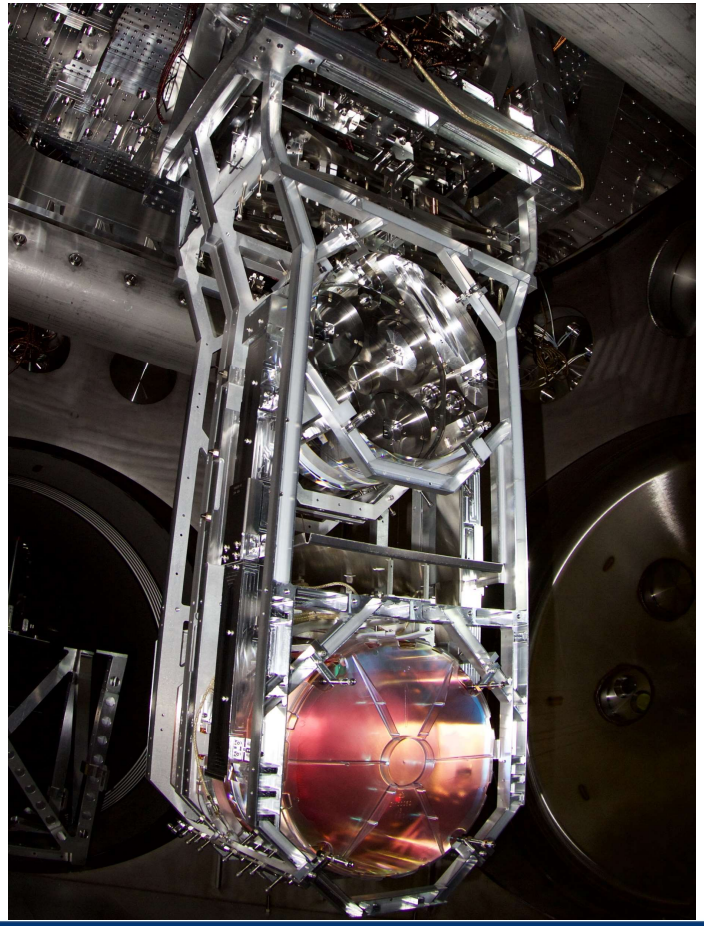

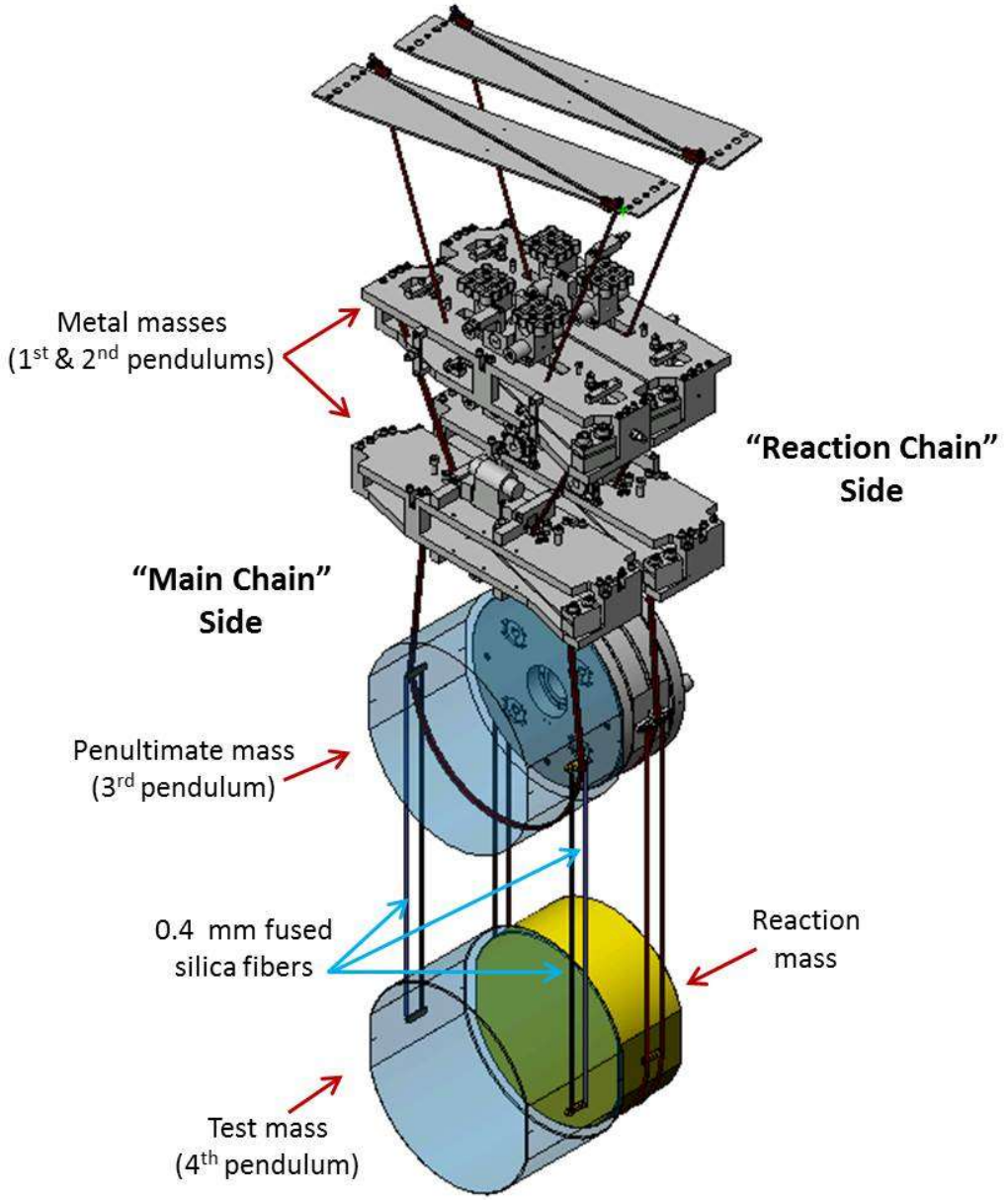

First detection of gravitational wave

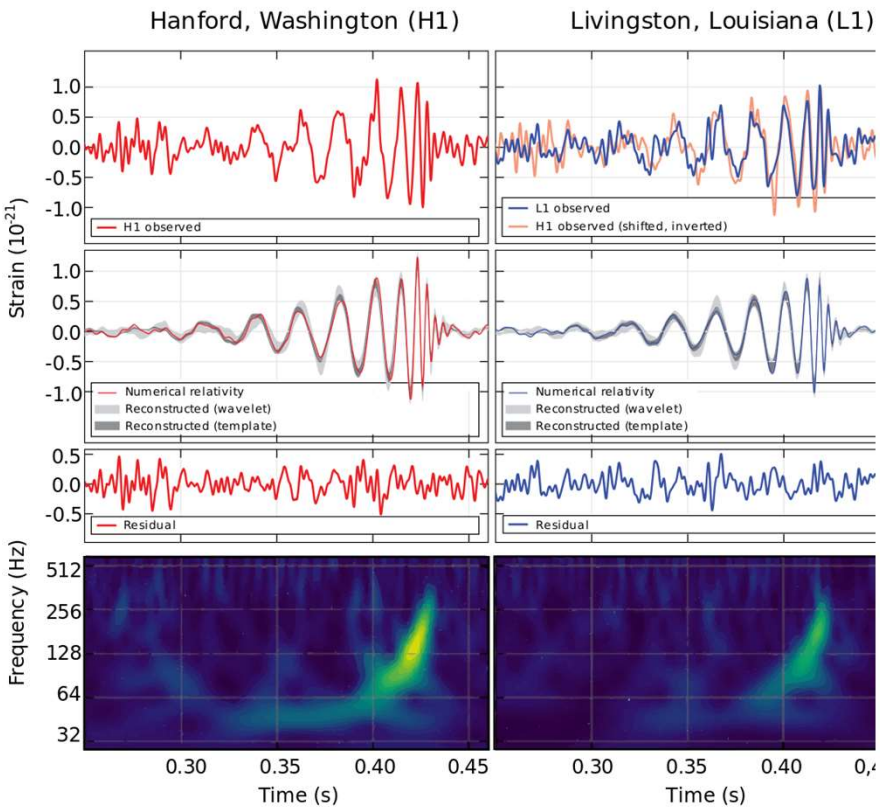

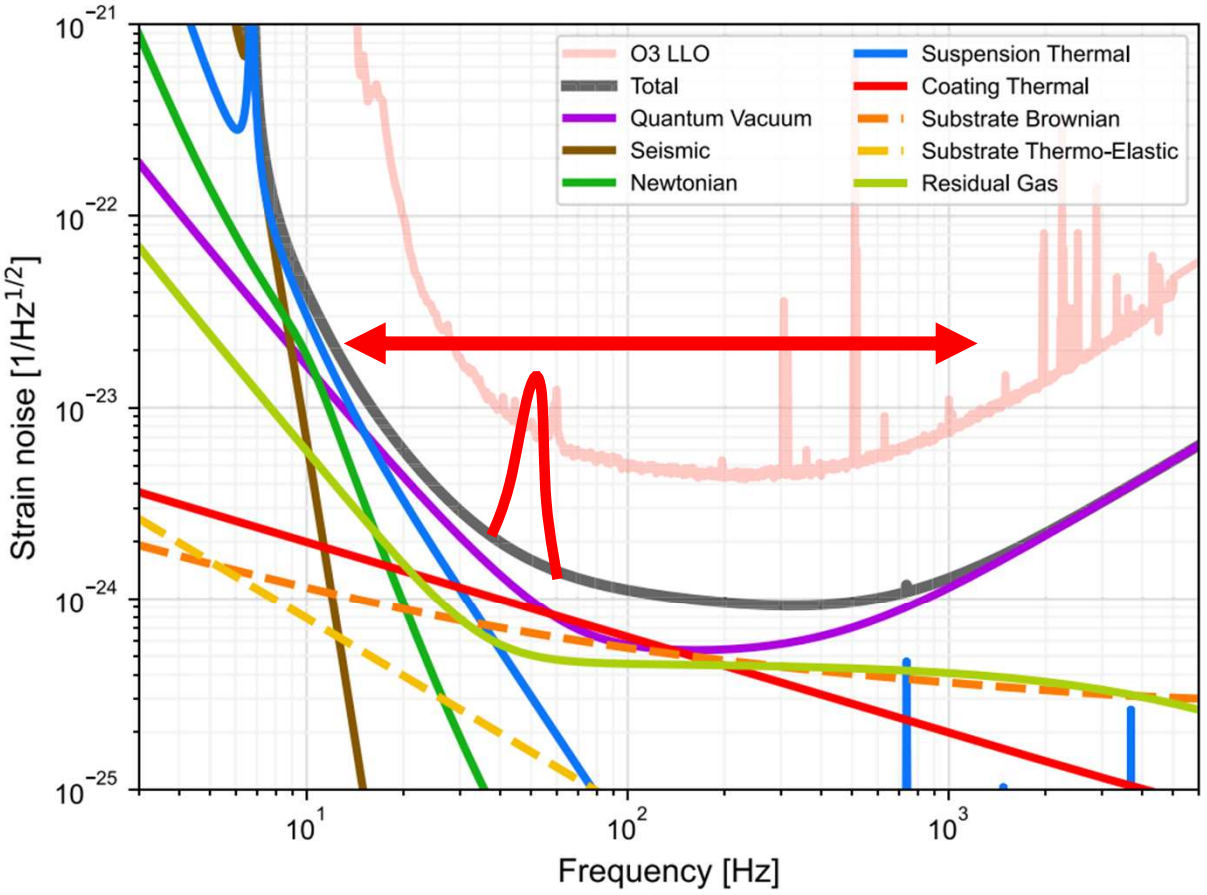

Suspended system

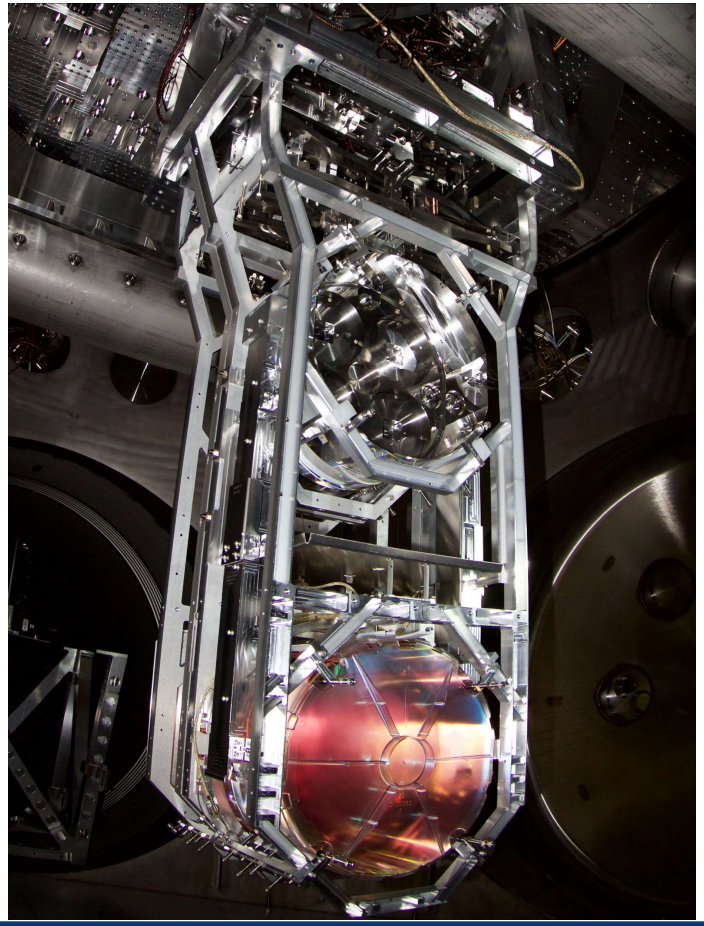

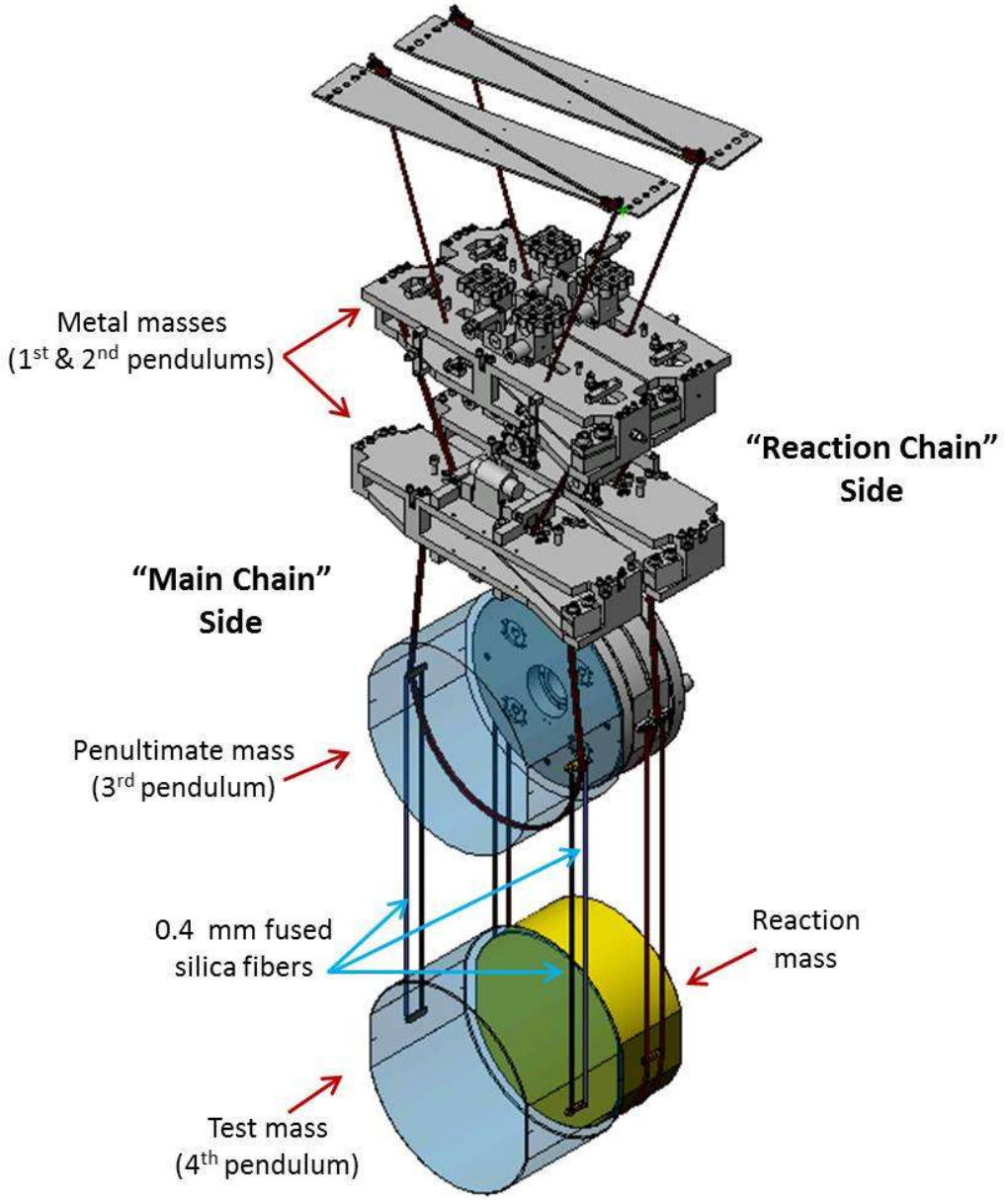

Sensitivity curve of KAGRA

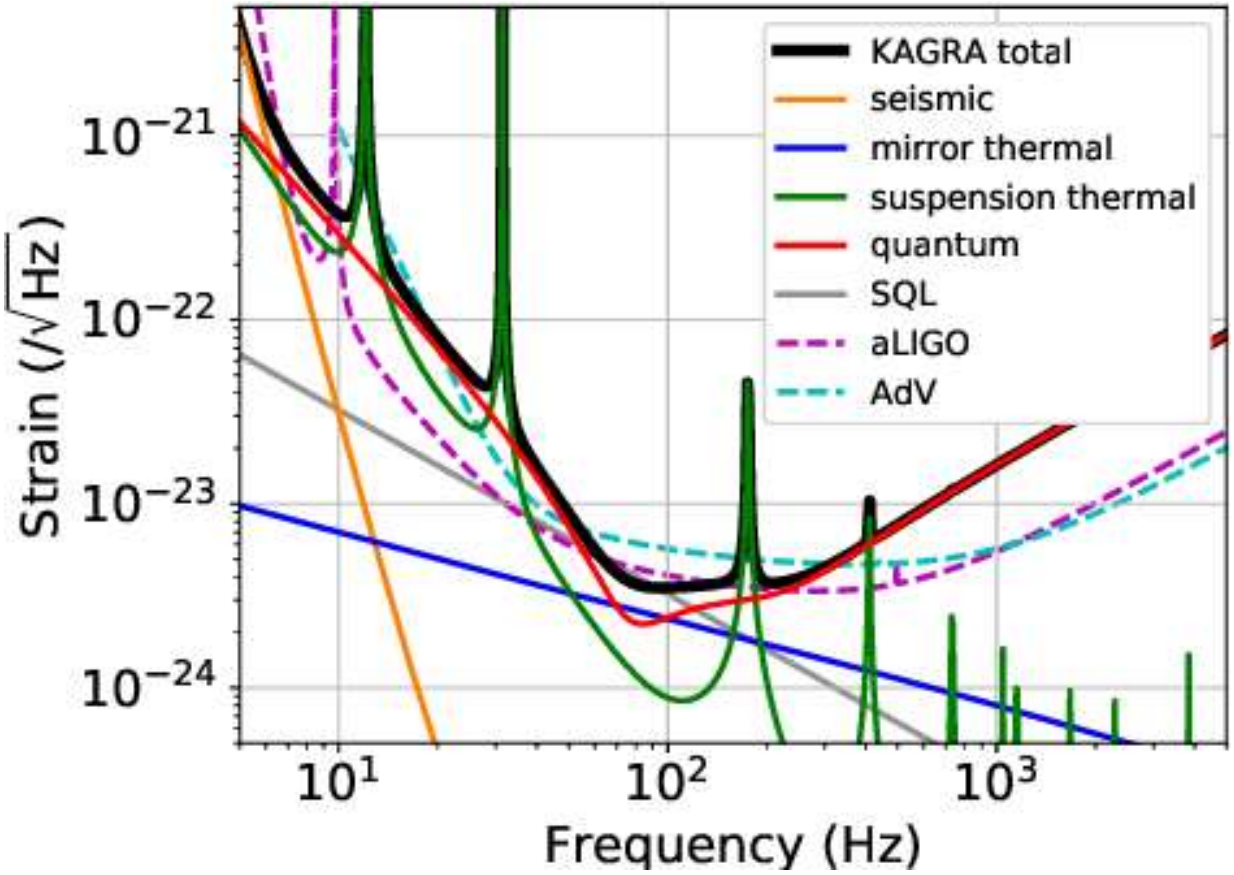

First detection of gravitational wave

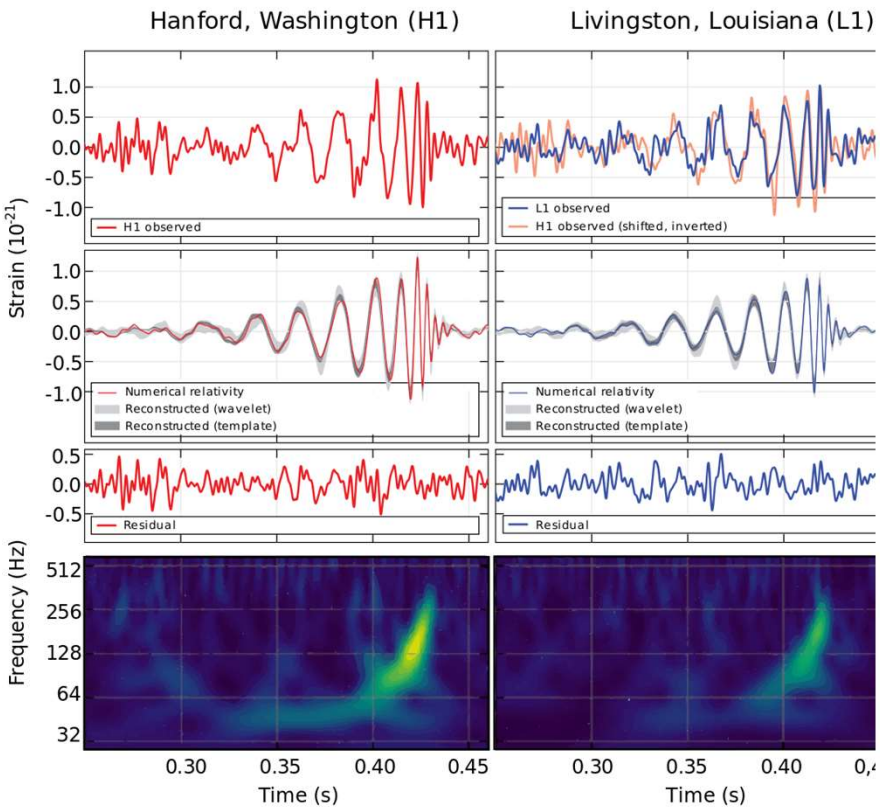

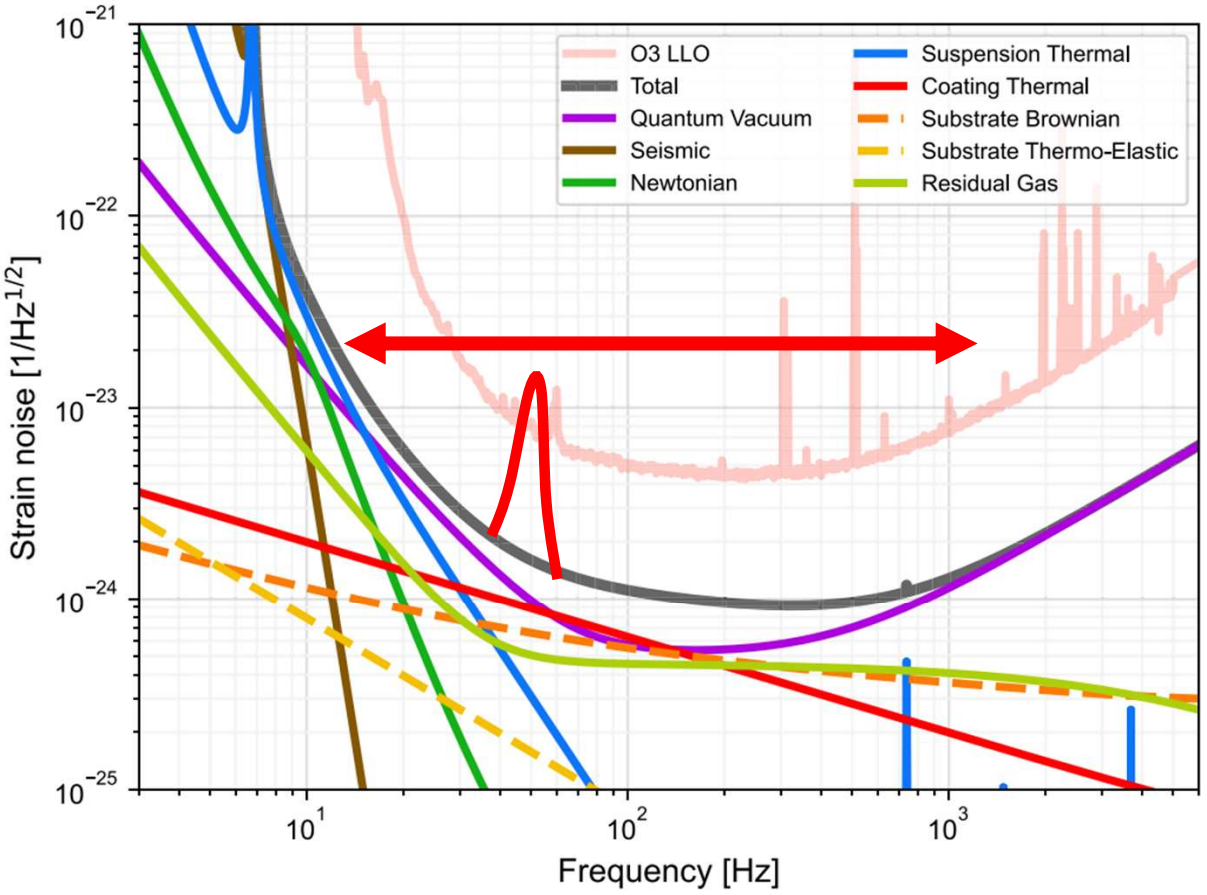

LIGO interferometer

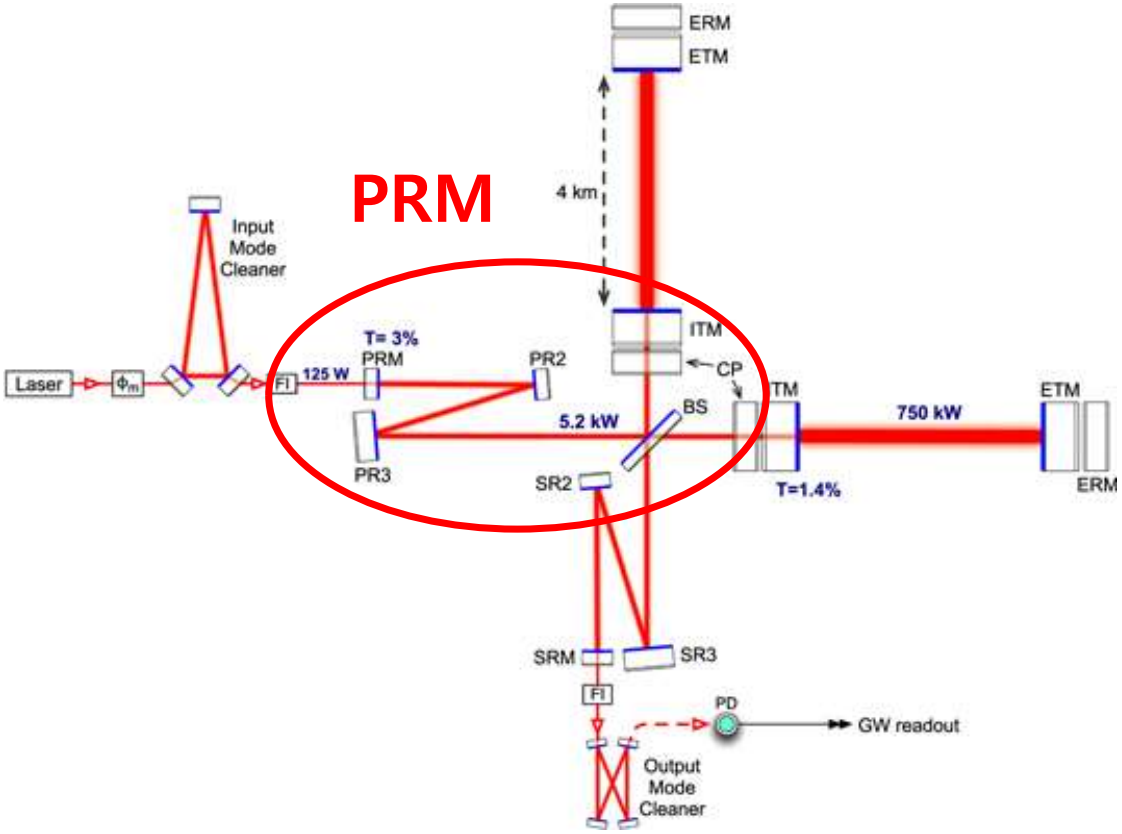

Key component of LIGO

- Stabilized laser
- Michelson interferometer
- Fabry-perot cavity
- Test mass
- Suspended system
- Dual recycling system

LIGO interferometer

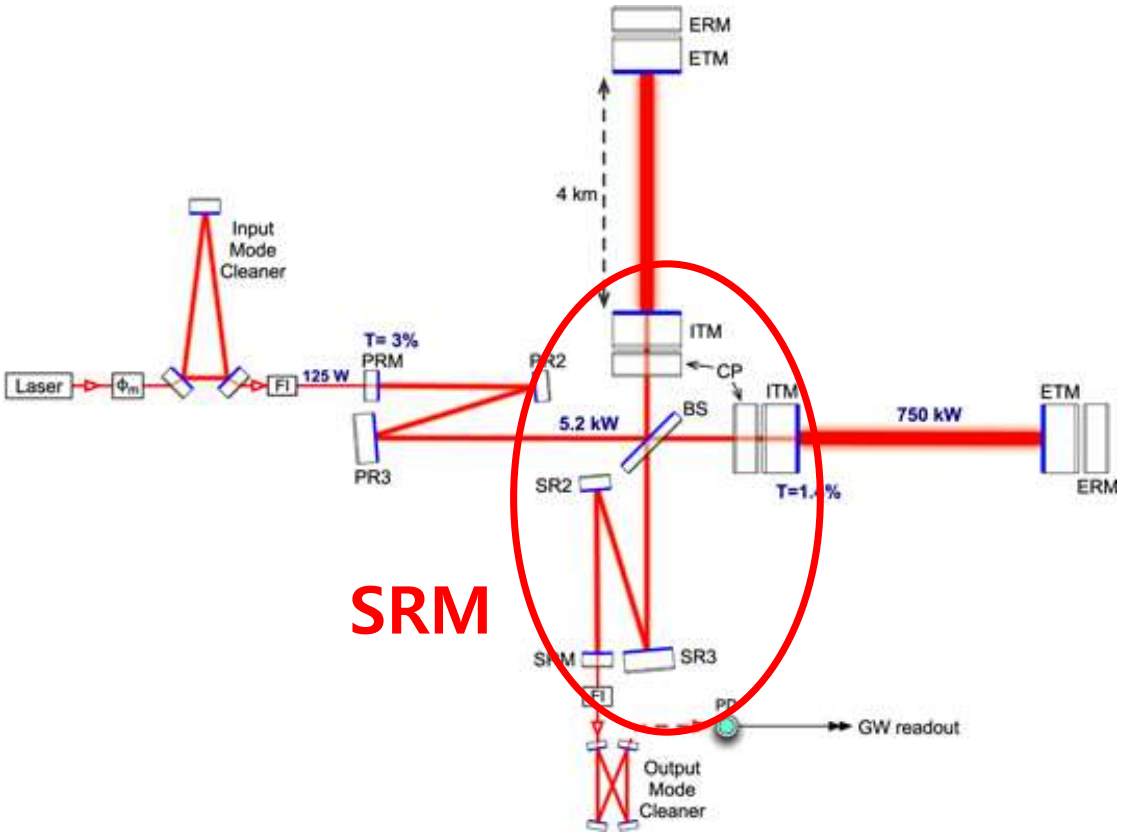

Key component of LIGO

- Stabilized laser
- Michelson interferometer
- Fabry-perot cavity
- Test mass
- Suspended system
- Dual recycling system

PHYSICAL REVIEW D
PARTICLES AND FIELDS

THIRD SERIES, VOLUME 38, NUMBER 8 15 OCTOBER 1988

Recycling in laser-interferometric gravitational-wave detectors

Brian J. Meers
Department of Physics and Astronomy, University of Glasgow, Glasgow G12 8QQ, Scotland
(Received 31 March 1988)

Laser interferometers may detect gravitational waves by sensing the strain in space produced by their passage. The resultant change in intensity of an interference fringe must be observable against a background noise due to the statistical fluctuations in the number of detected photons. Optimization of the detector sensitivity thus involves devising an optical system which both maximizes the signal and minimizes the noise. This is attempted in the various arrangements known collectively as light recycling. Here, the performance of these systems is quantitatively assessed. Standard or broadband recycling functions essentially by making efficient use of the available light, but it is shown that it may also be made to further enhance the sensitivity within a narrow bandwidth, becoming tuned recycling. This works, as do all the narrow-band variants, by arranging for both the laser light and a gravitational-wave-induced sideband to be resonant in the optical system. The original narrow-band system, resonant recycling, can also be made broadband; the various sensitivity-bandwidth combinations, together with the tuning properties of such a system, are discussed. Furthermore, a new optical arrangement, dual recycling, is proposed. Its optical layout is an extension of standard recycling and its strength lies in its flexibility. It is shown that, relatively simply, it may be made into either a broadband or a narrow-band system, in each case with the same performance as the best of the other schemes. It may be tuned more efficiently and easily over a wide range of frequencies. Uniquely, optimum performance may be obtained with dual recycling without the requirement that the storage time of the optical elements in each arm of the interferometer be comparable with the period of the gravitational wave. This may allow the operation of delay line interferometers down to much lower gravitational-wave frequency and will provide great operational flexibility. Finally, it is shown that dual recycling, together with resonant recycling, is relatively insensitive to imperfections in the geometrical quality of the optical system. When implemented on interferometers with lengths greater than about a kilometer, recycling should allow the attainment of the sensitivity required in order to observe gravitational waves and open up a new window to the Universe.

LIGO interferometer

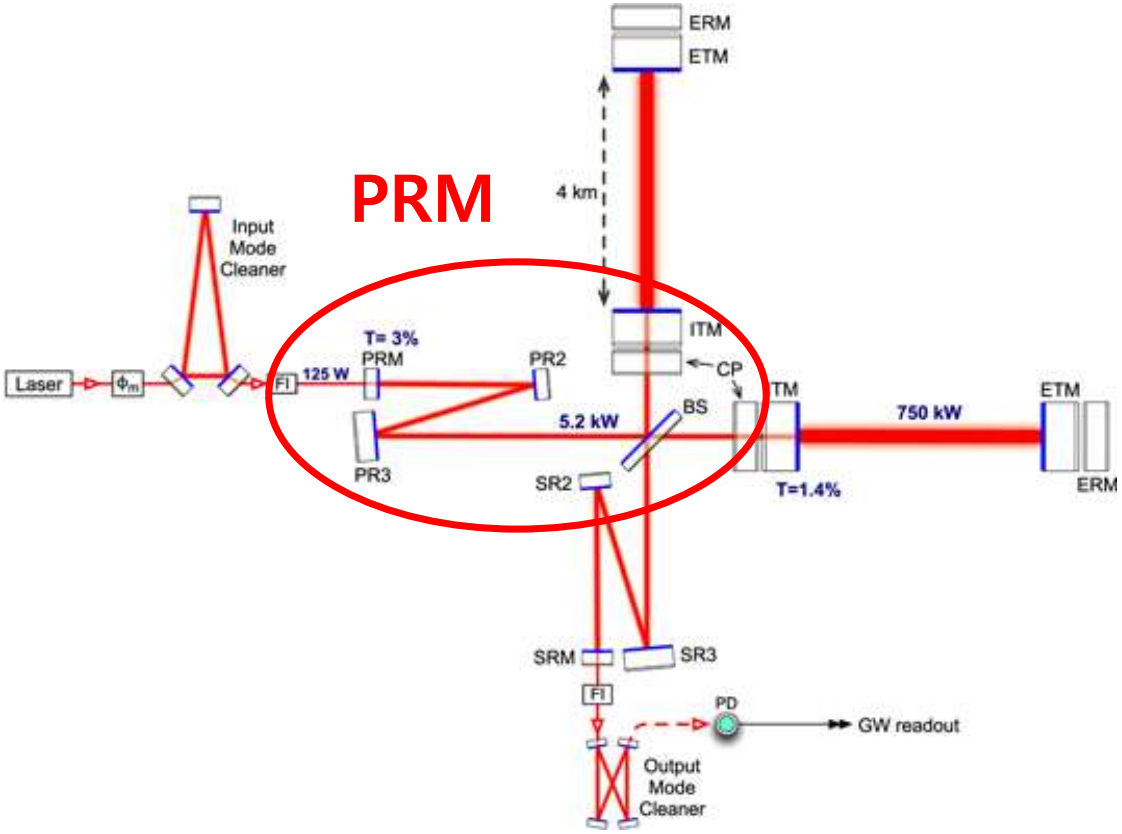

Key component of LIGO

- Stabilized laser
- Michelson interferometer
- Fabry-perot cavity
- Test mass
- Suspended system
- Dual recycling system

LIGO interferometer

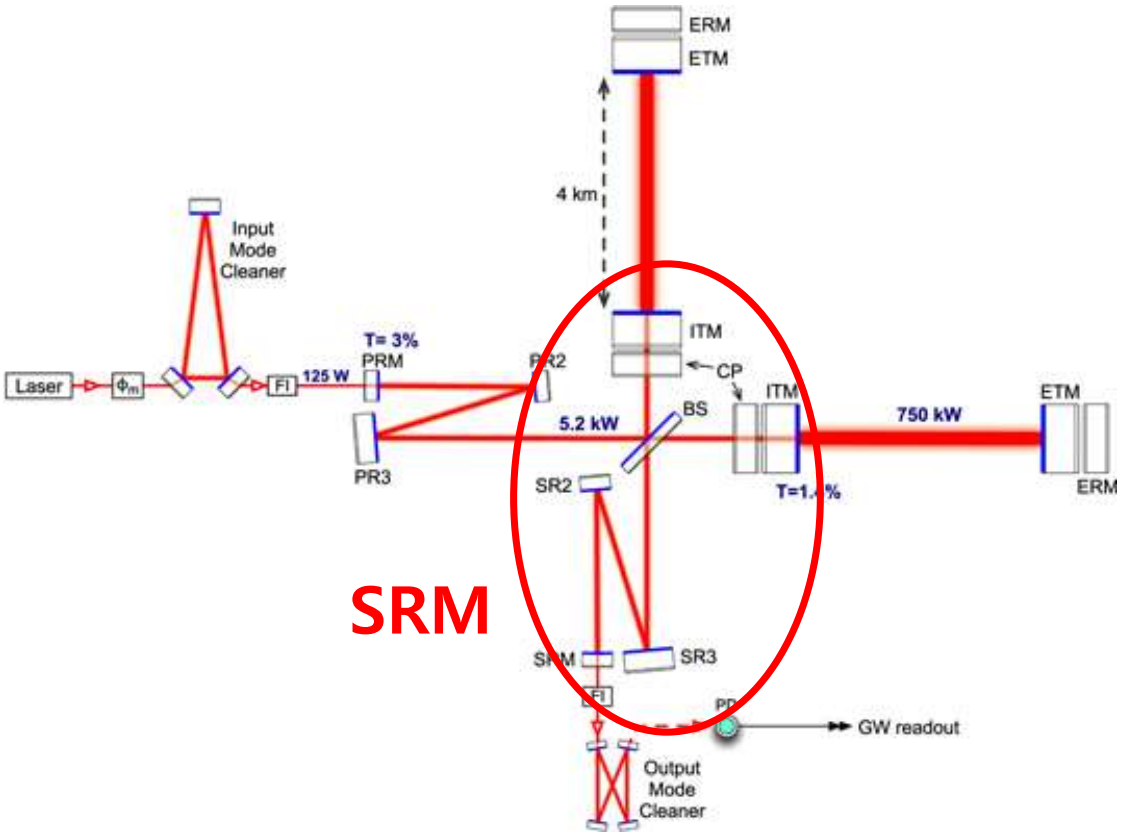

Key component of LIGO

- Stabilized laser
- Michelson interferometer
- Fabry-perot cavity
- Test mass
- Suspended system
- Dual recycling system

KAGRA interferometer

Power recycling cavity

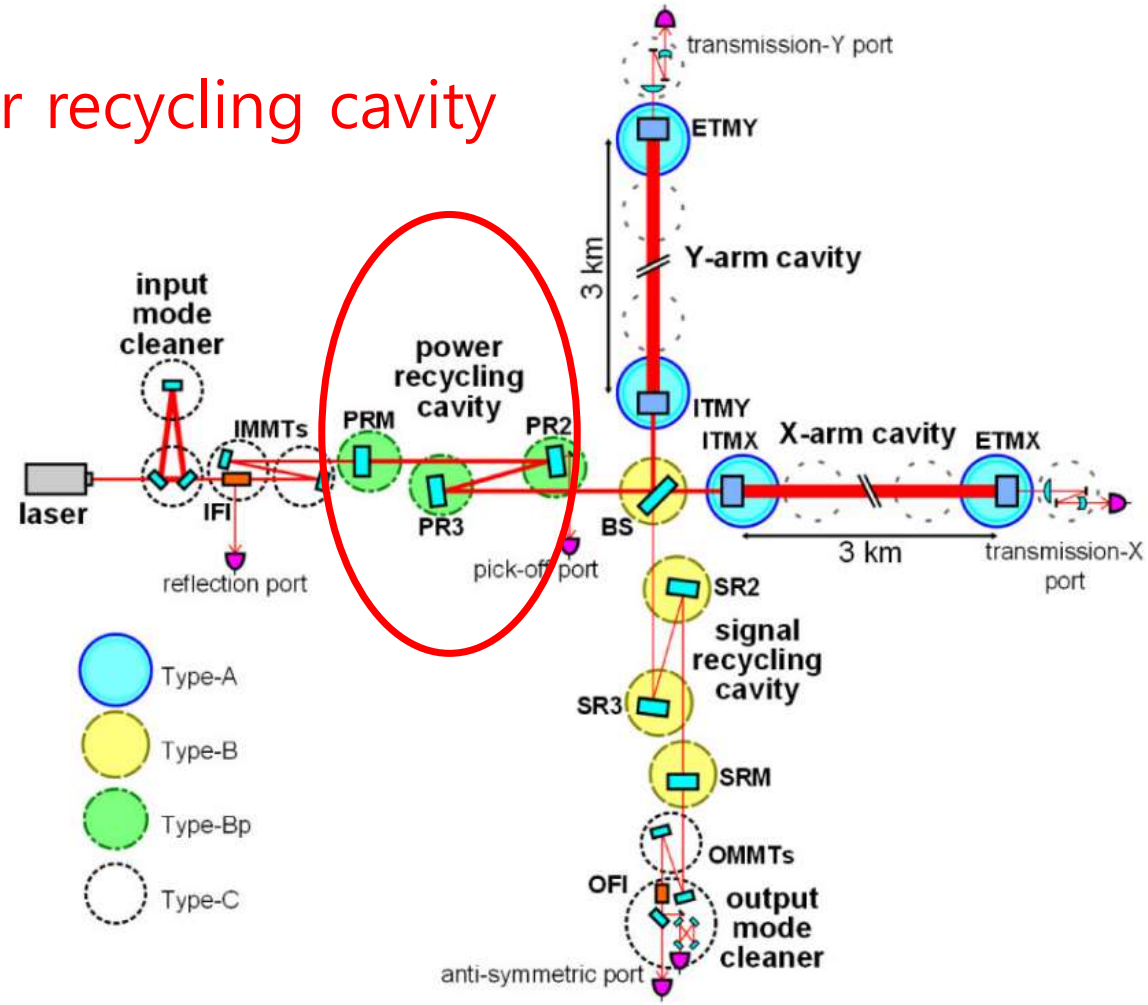

Power recycling cavity

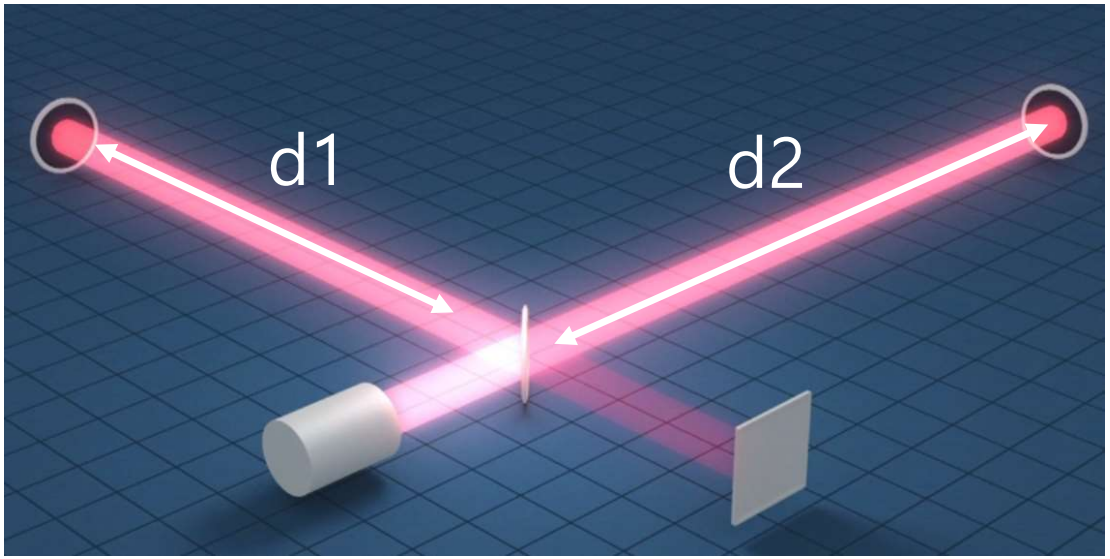

Power recycling cavity

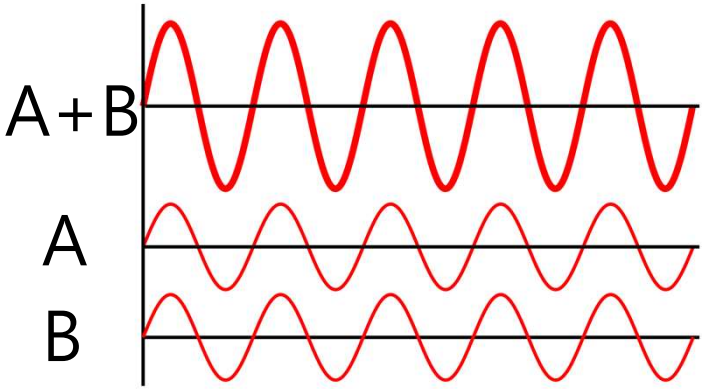

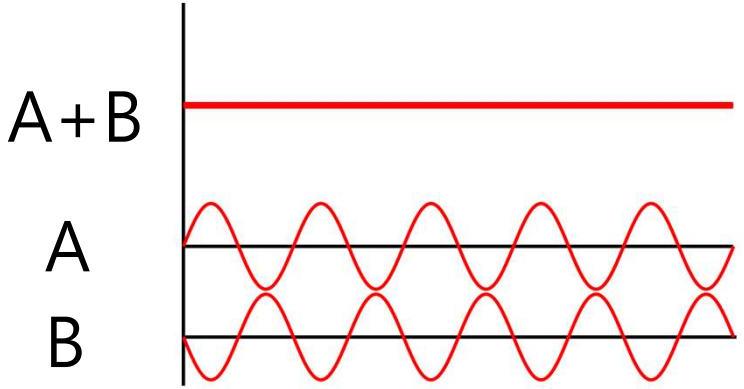

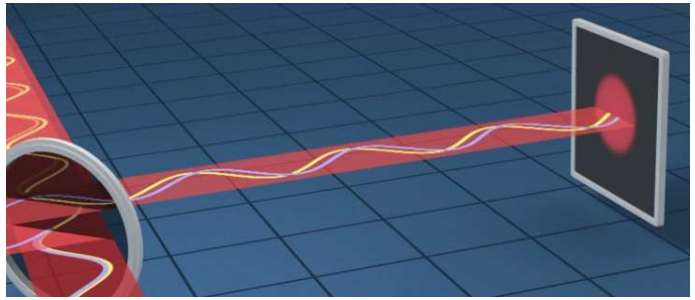

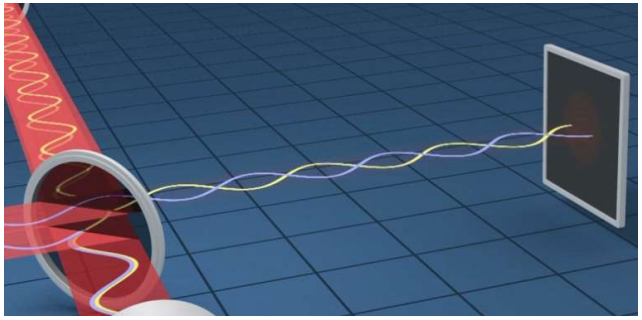

Constructive

Destructive

Power recycling cavity

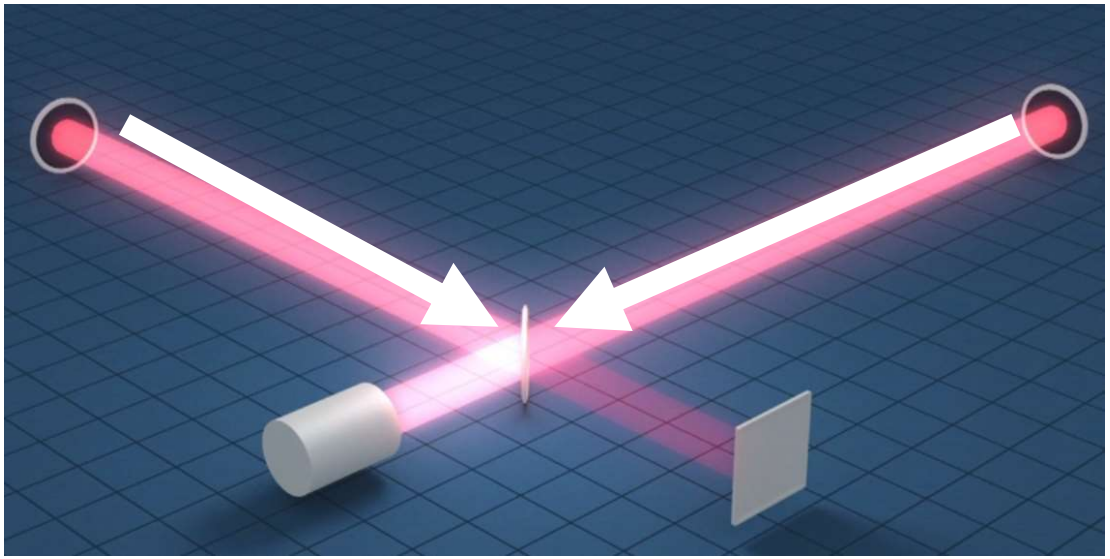

Power recycling cavity

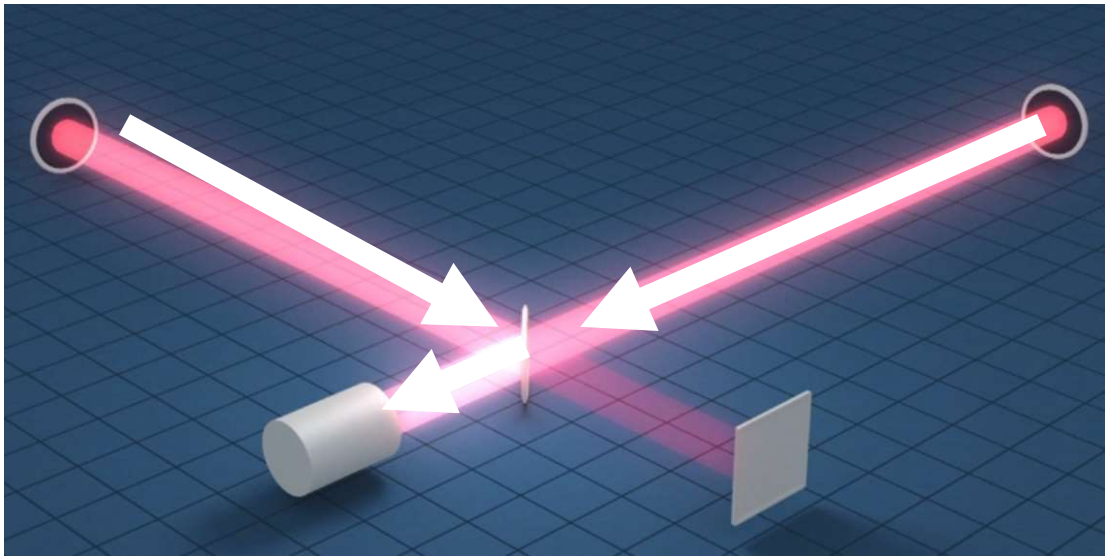

KAGRA interferometer

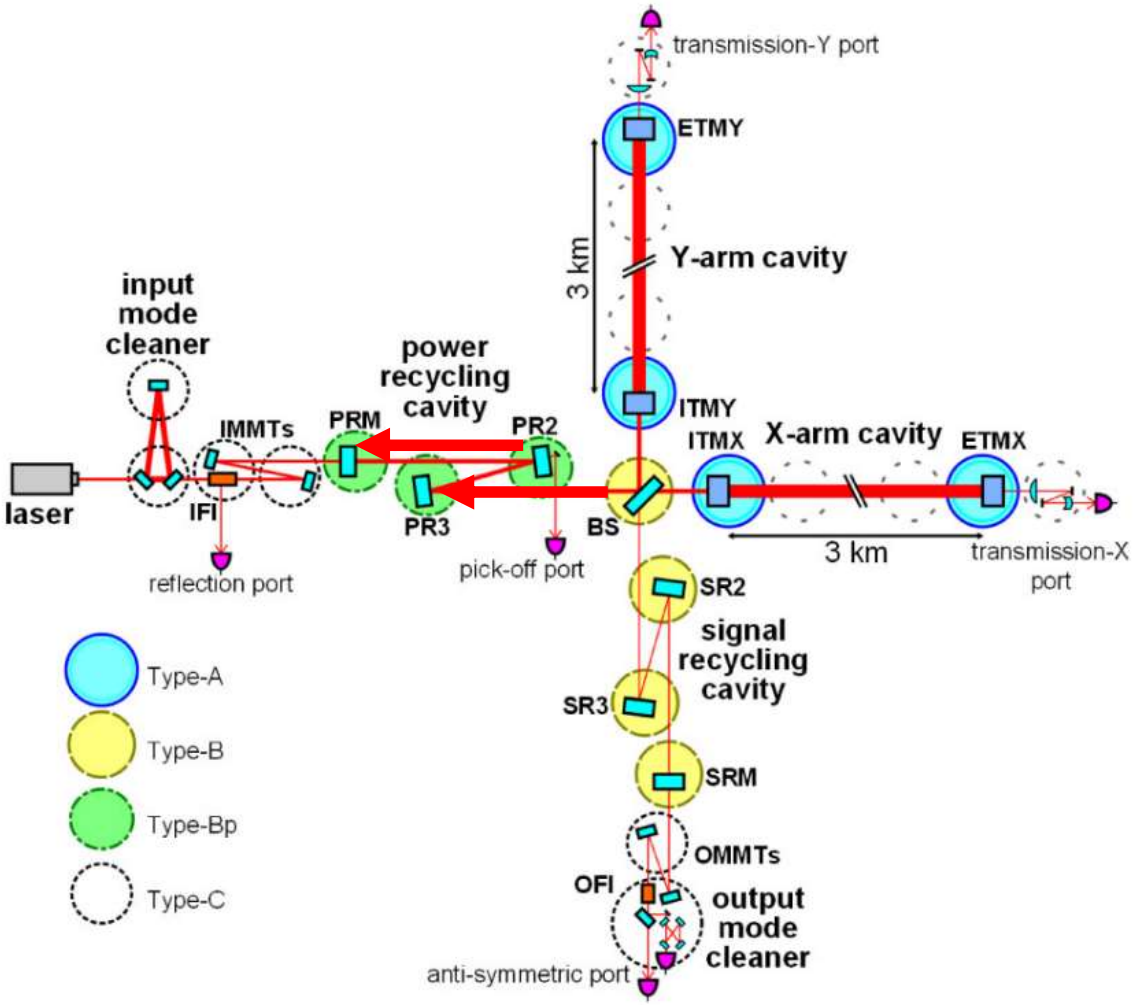

IOO : Input output optics
MIF : Main interferometer
MIR : Mirror
MMT : Mode matching telescope
OMC : Output mode cleaner

KAGRA interferometer

Power recycling cavity

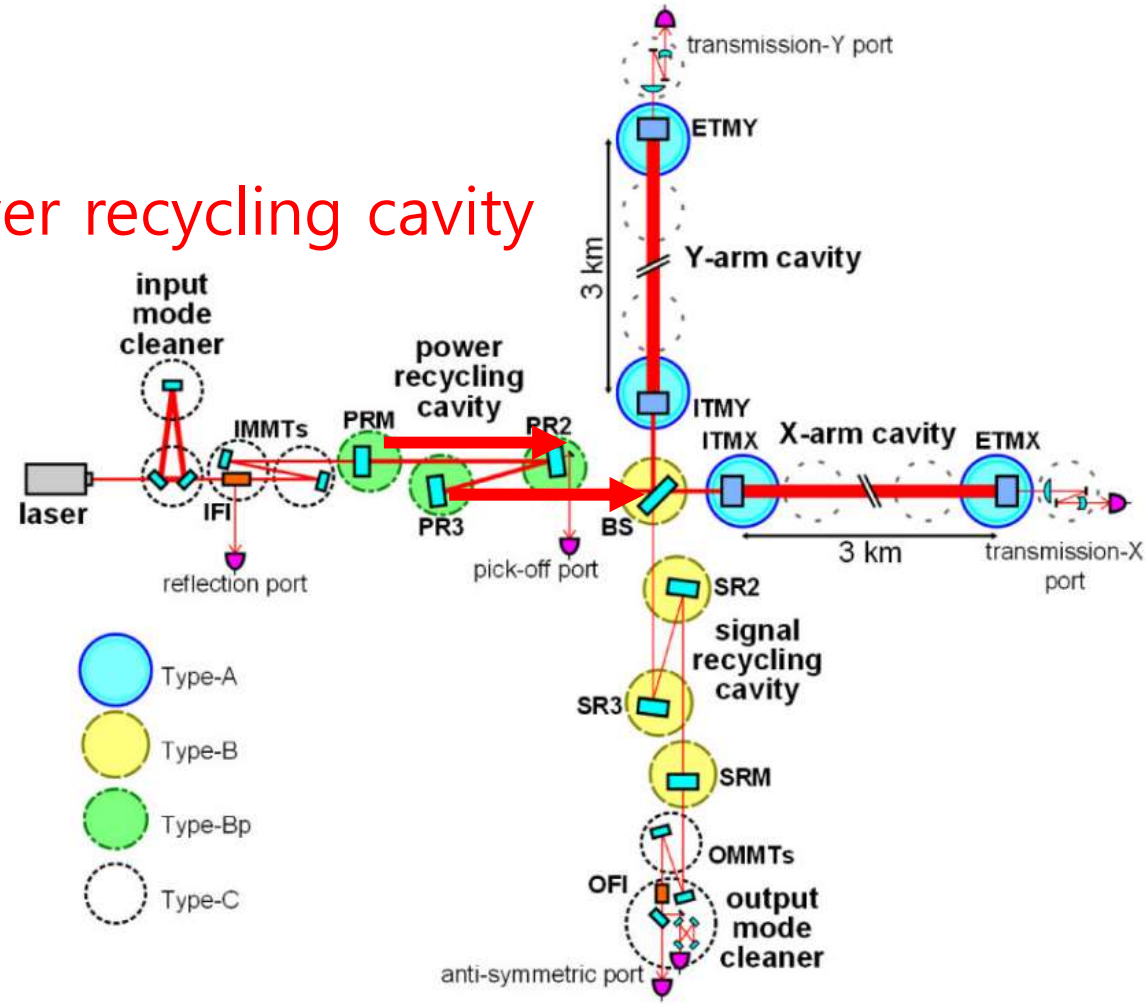

IOO : Input output optics
MIF : Main interferometer
MIR : Mirror
MMT : Mode matching telescope
OMC : Output mode cleaner

LIGO interferometer

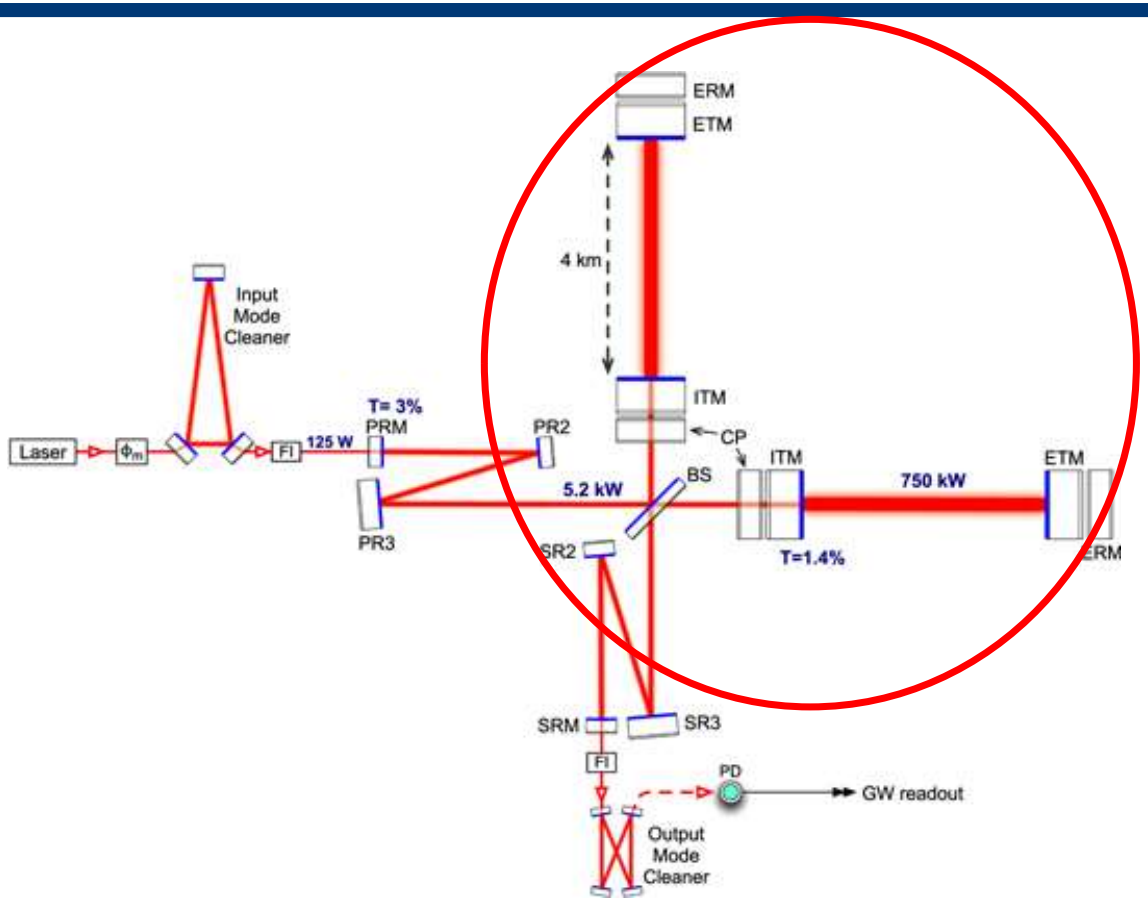

Increase Power

inside main arm cavity

-> sensitivity improvement

KAGRA interferometer

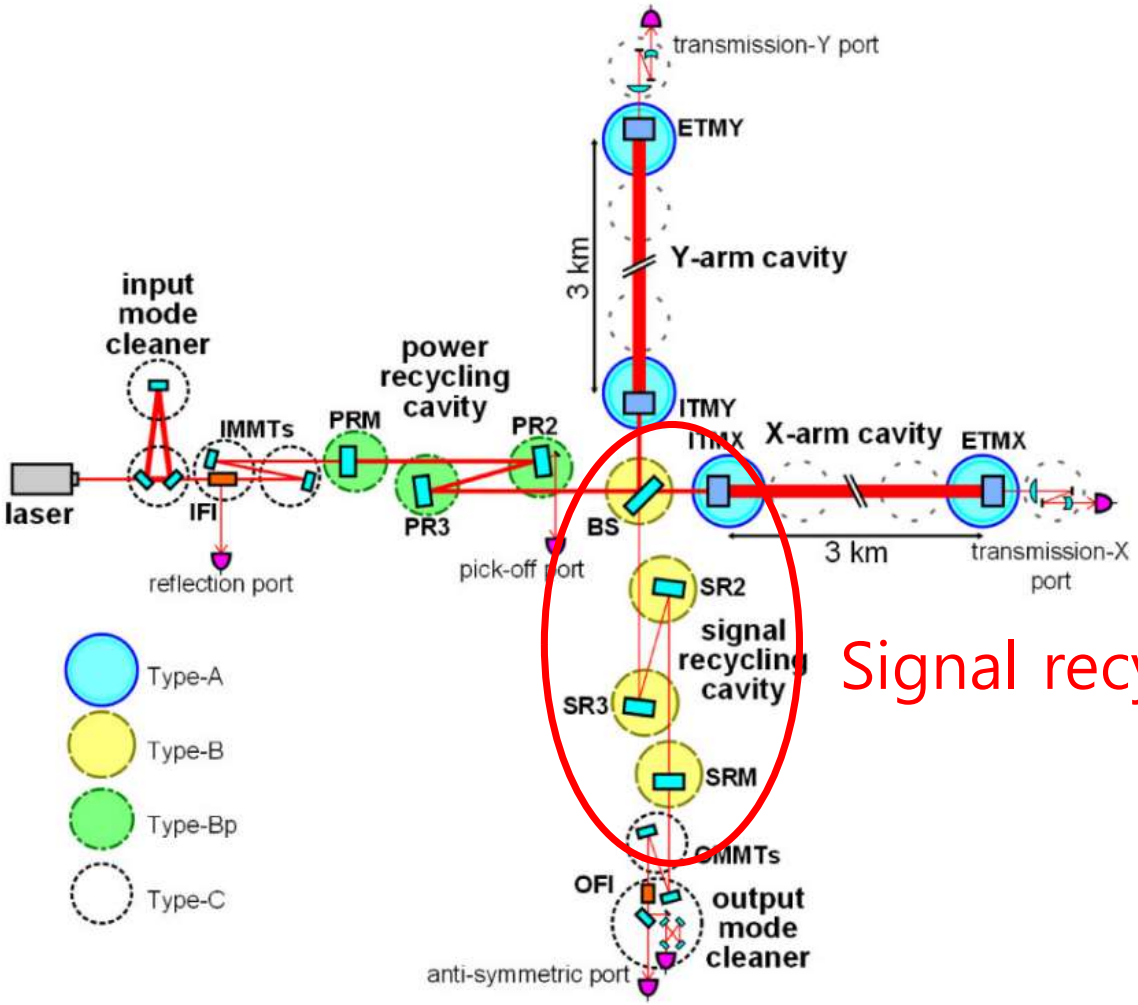

Signal recycling cavity

Signal recycling cavity

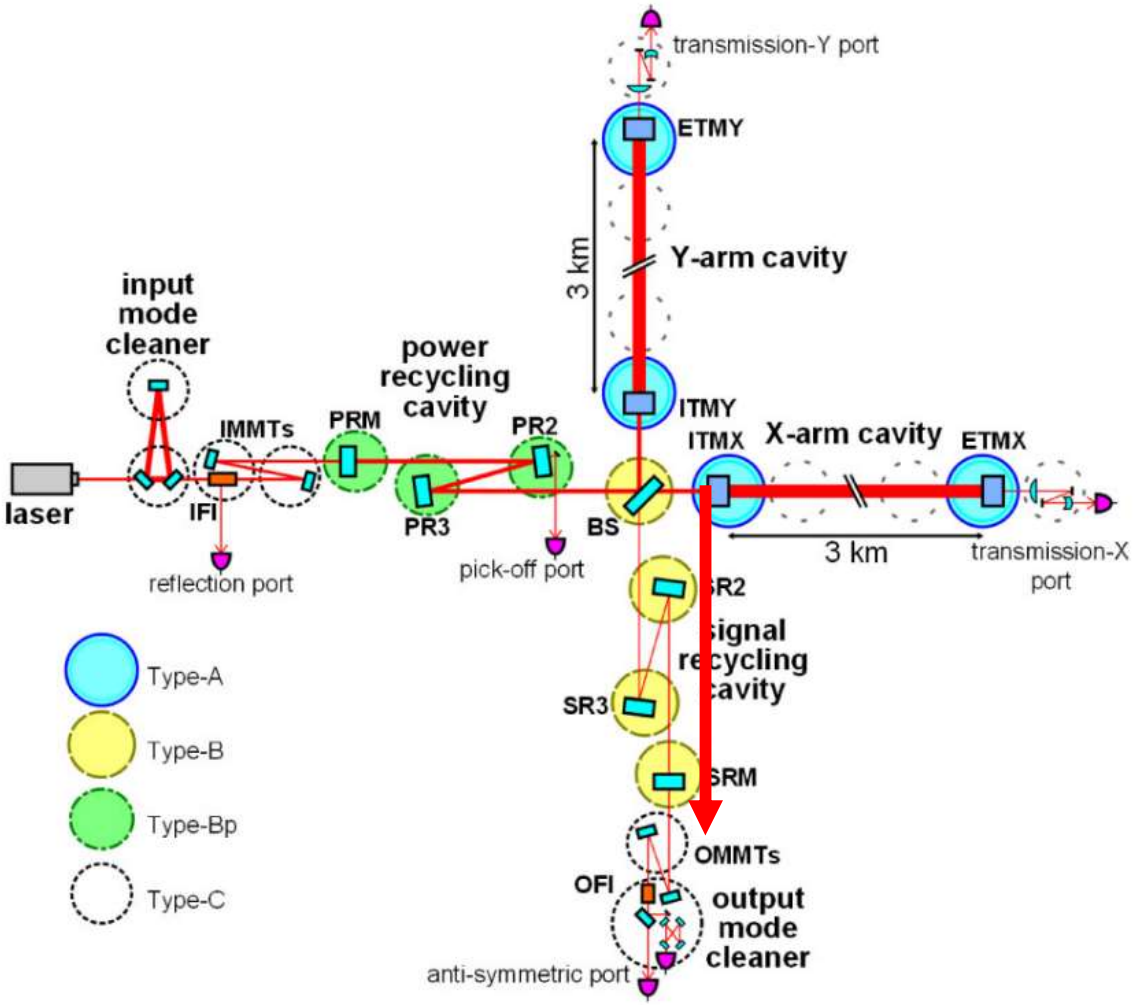

KAGRA interferometer

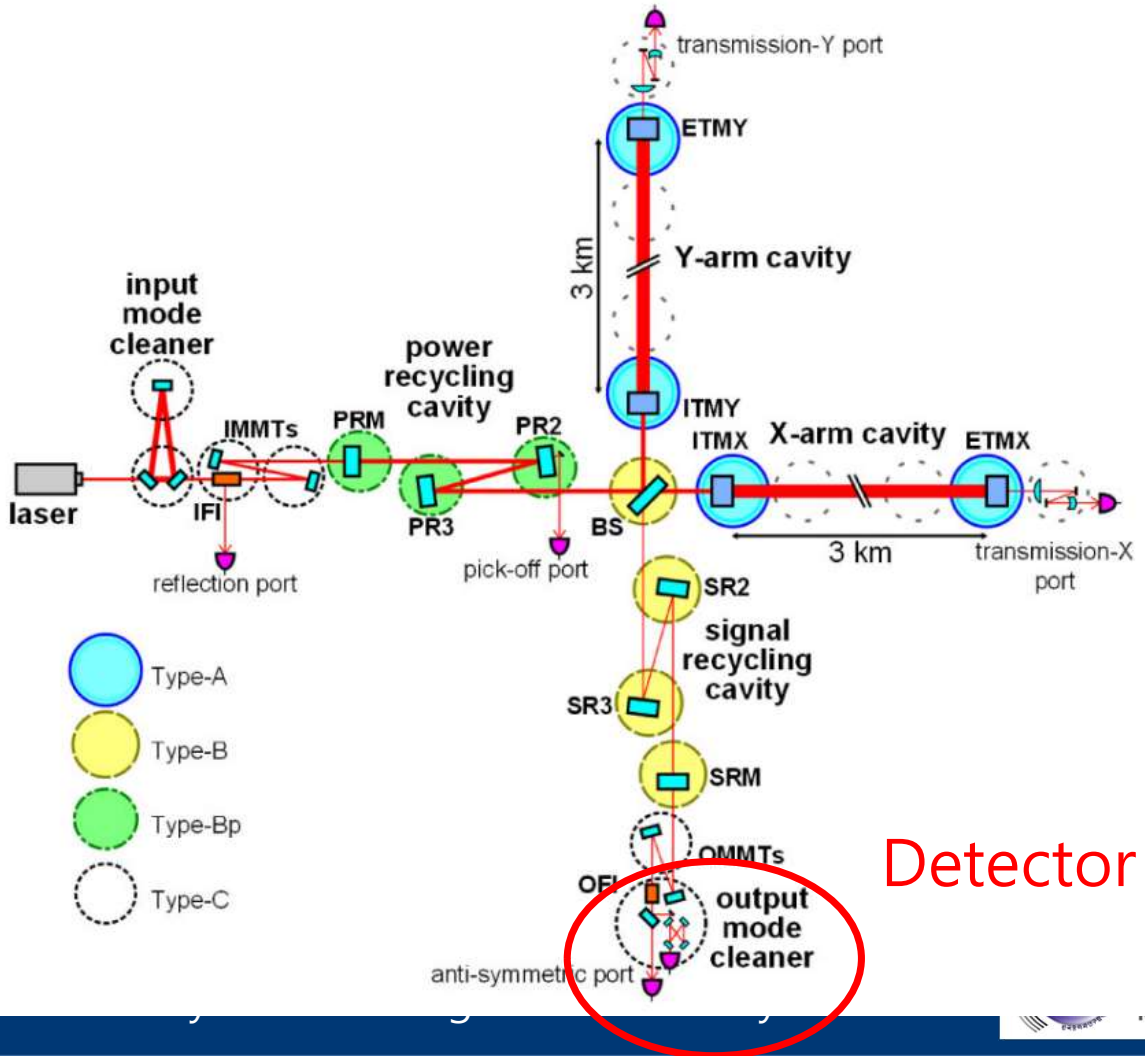

IOO : Input output optics
MIF : Main interferometer
MIR : Mirror
MMT : Mode matching telescope
OMC : Output mode cleaner

Detector

First detection of gravitational wave

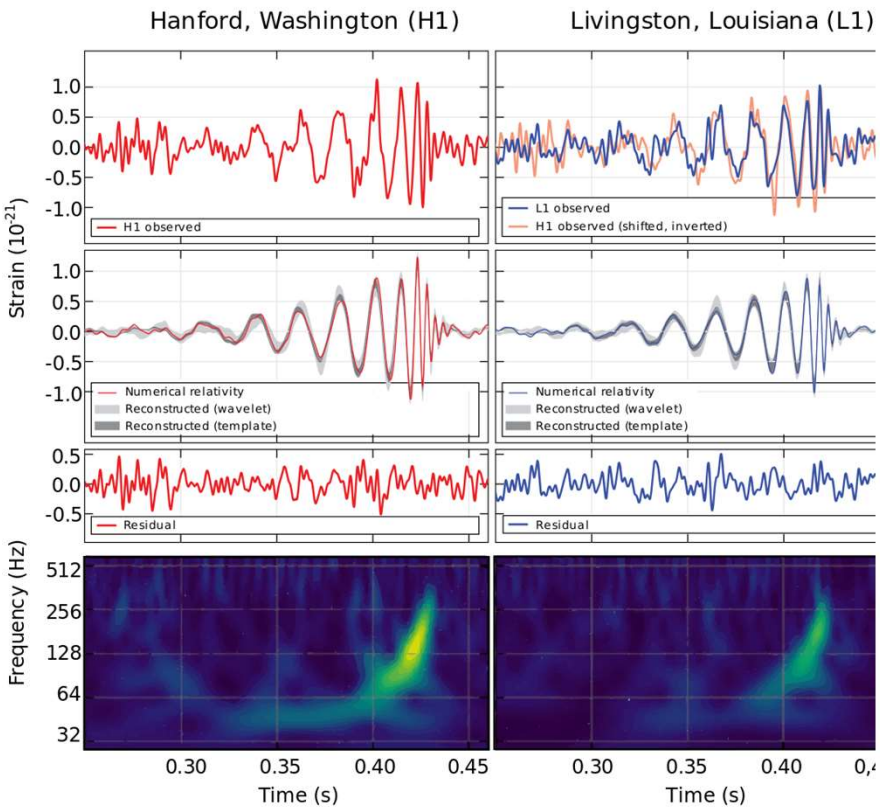

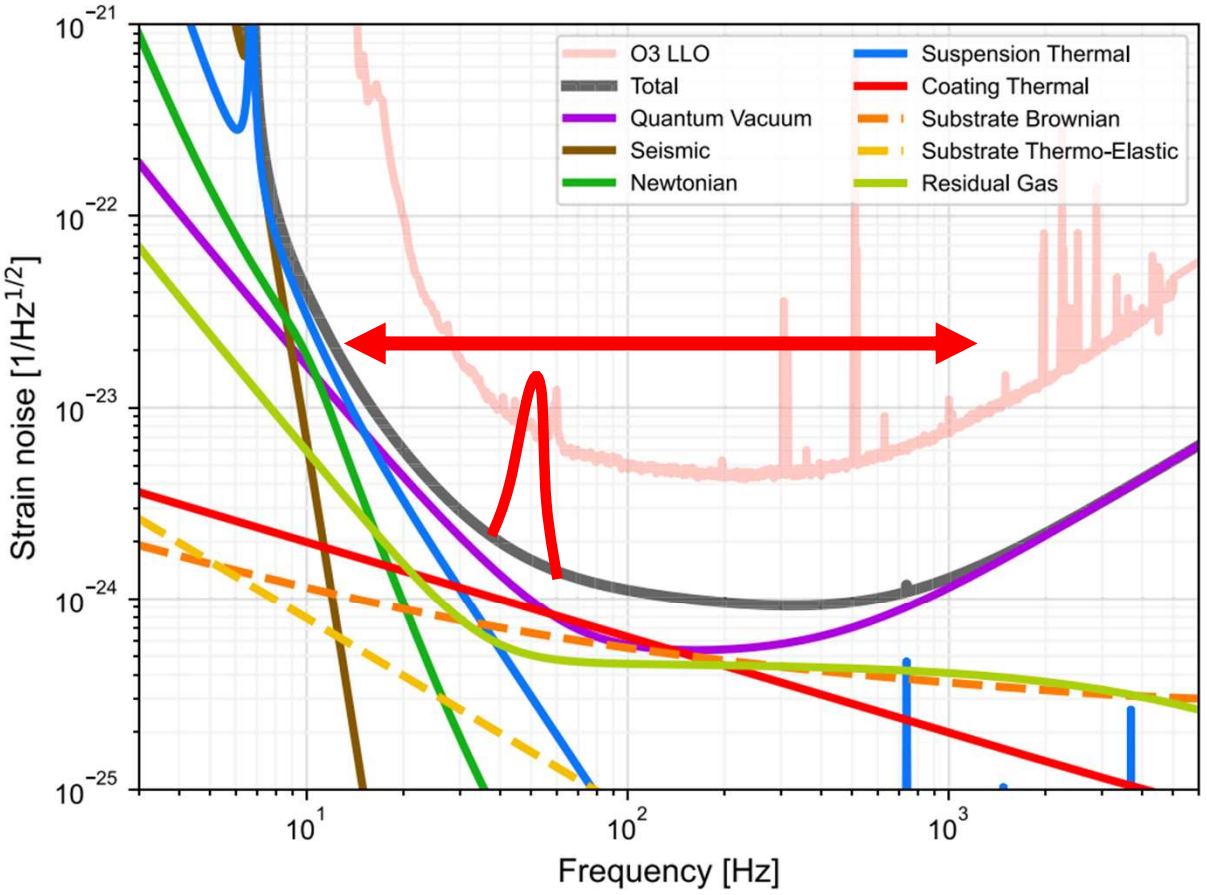

Signal recycling cavity

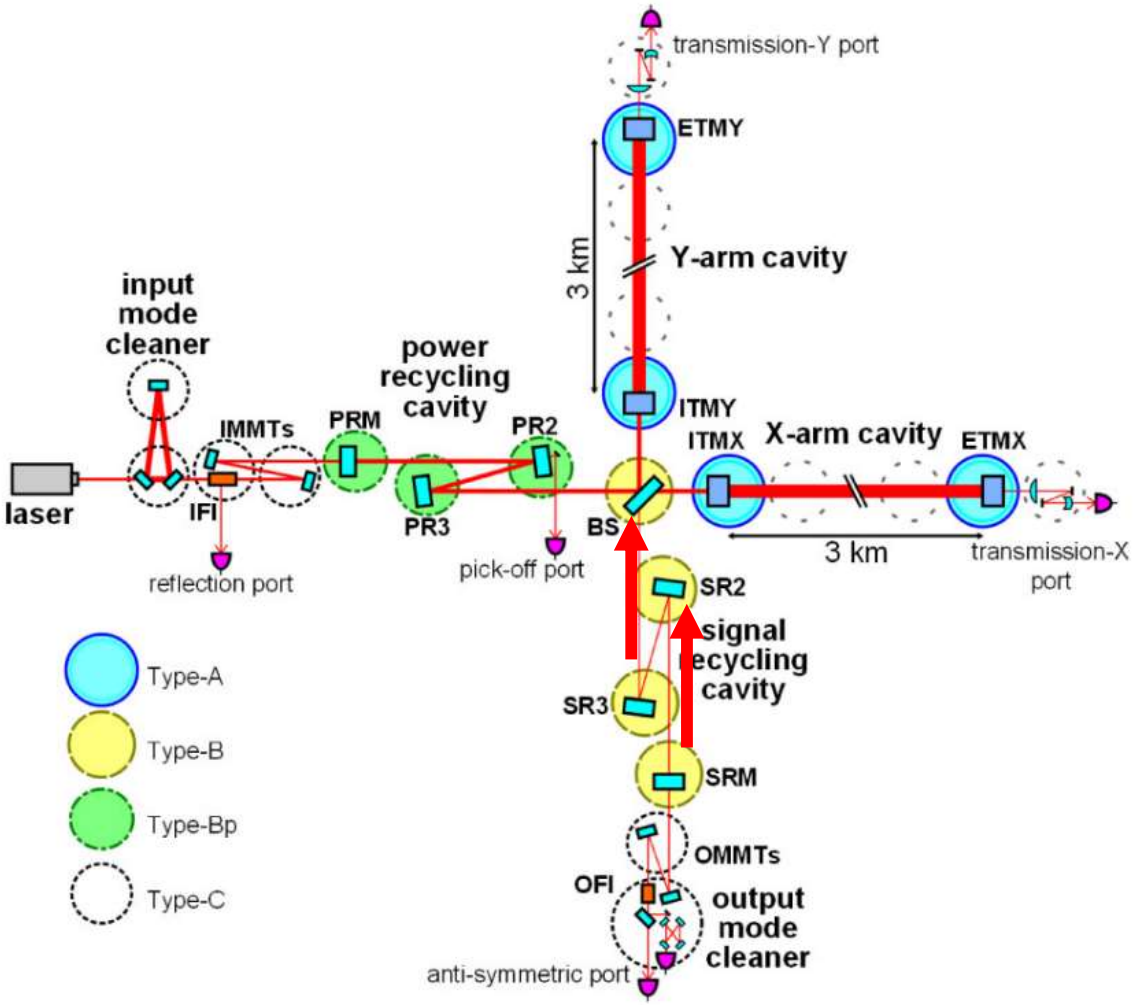

Cavity between SRM and ITMS

FFT

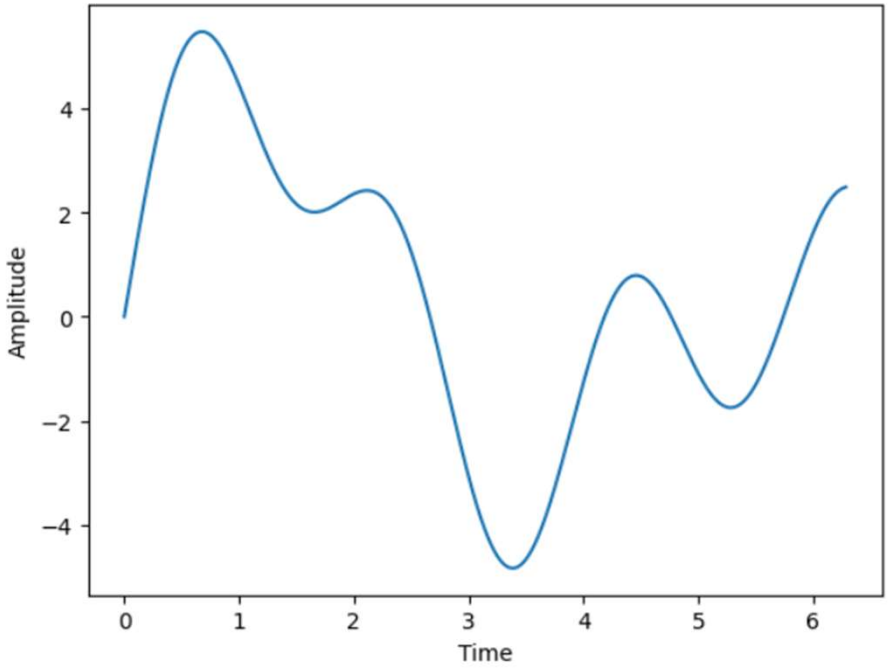

$$f(x) = \sum_{n=-\infty}^{\infty} a_n e^{inx}$$

$$= \text{asin k}x \quad + \text{asin 2k}x$$

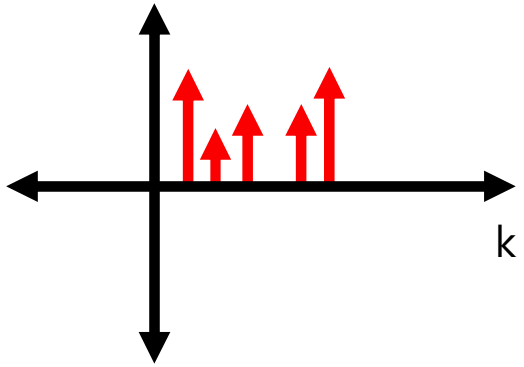

First detection of gravitational wave

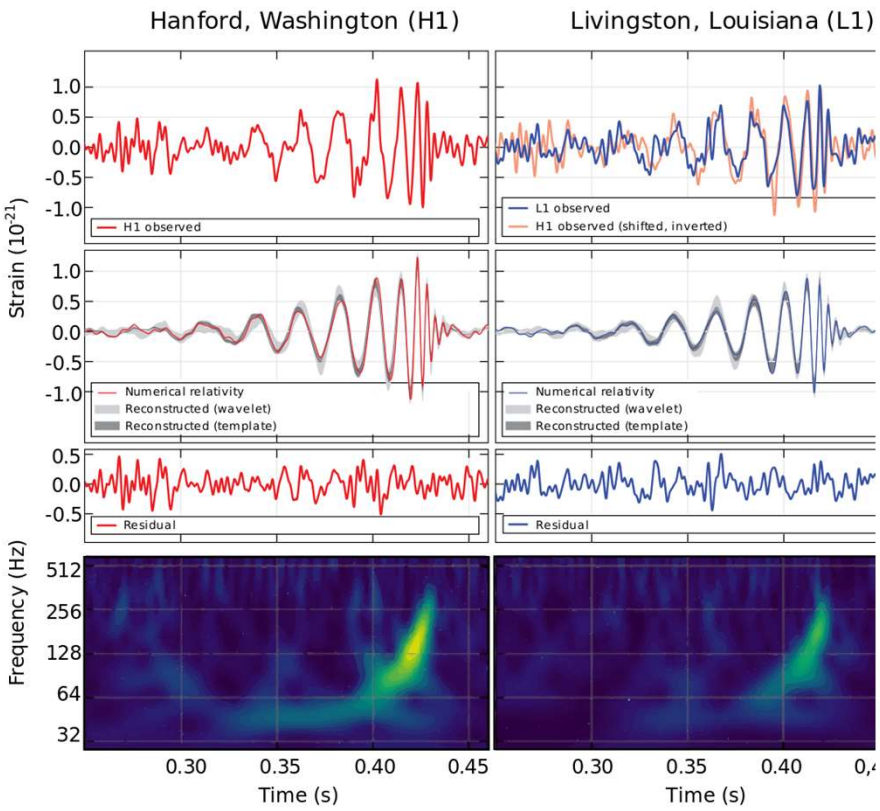

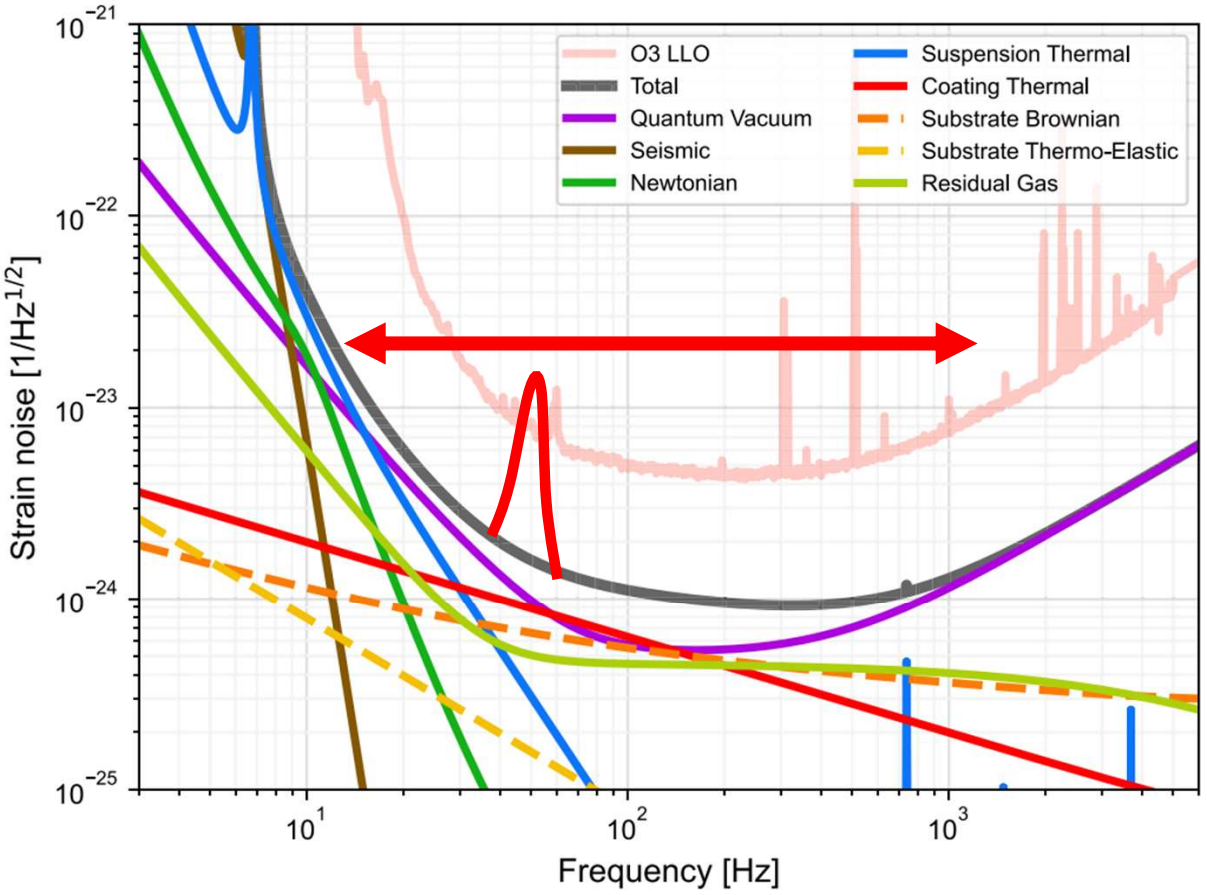

SRC tuning

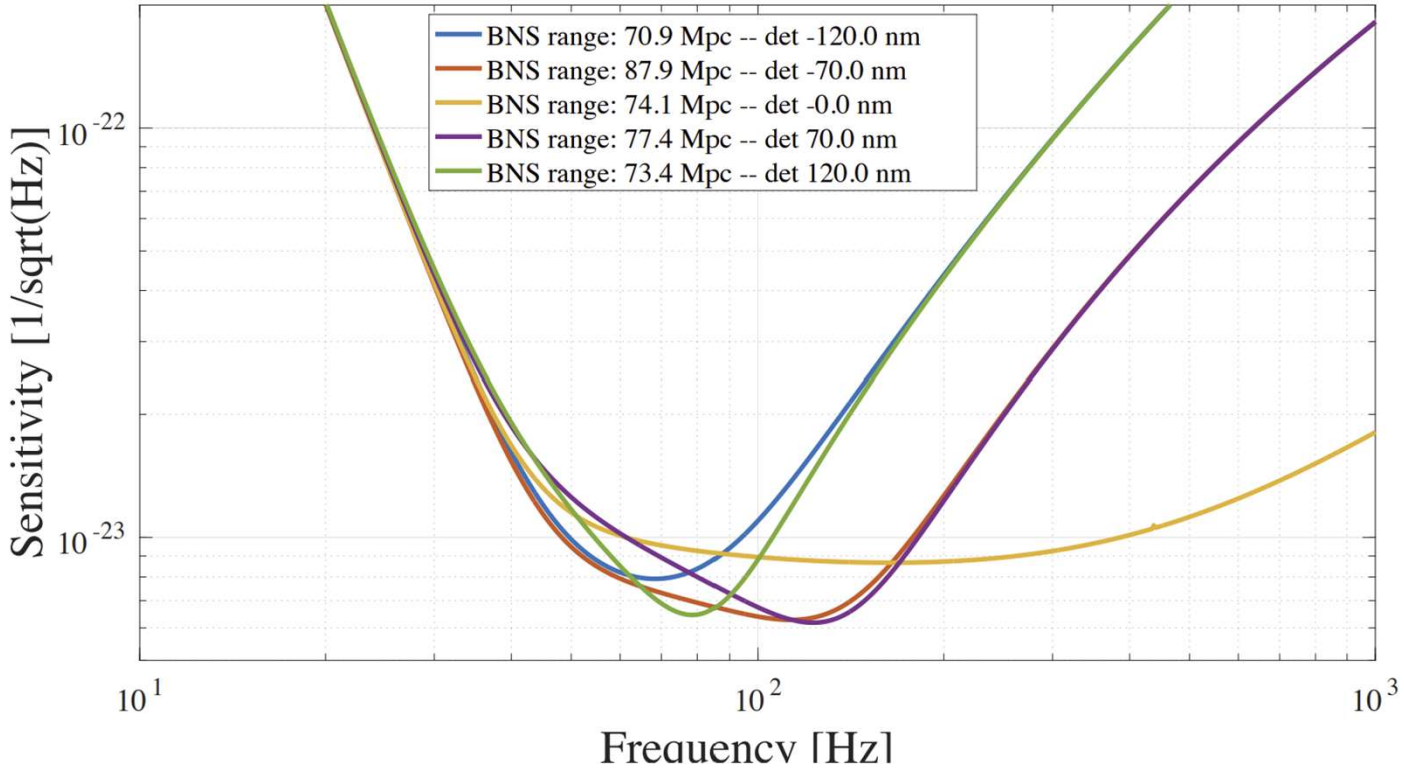
BNS range: 70.9 Mpc -- det -120.0 nm
BNS range: 87.9 Mpc -- det -70.0 nm
BNS range: 74.1 Mpc -- det -0.0 nm
BNS range: 77.4 Mpc -- det 70.0 nm
BNS range: 73.4 Mpc -- det 120.0 nm
Sensitivity [1/sqrt(Hz)]
10^-22
10^-23
10^1
10^2
10^3
Frequency [Hz]

Dual recycling system

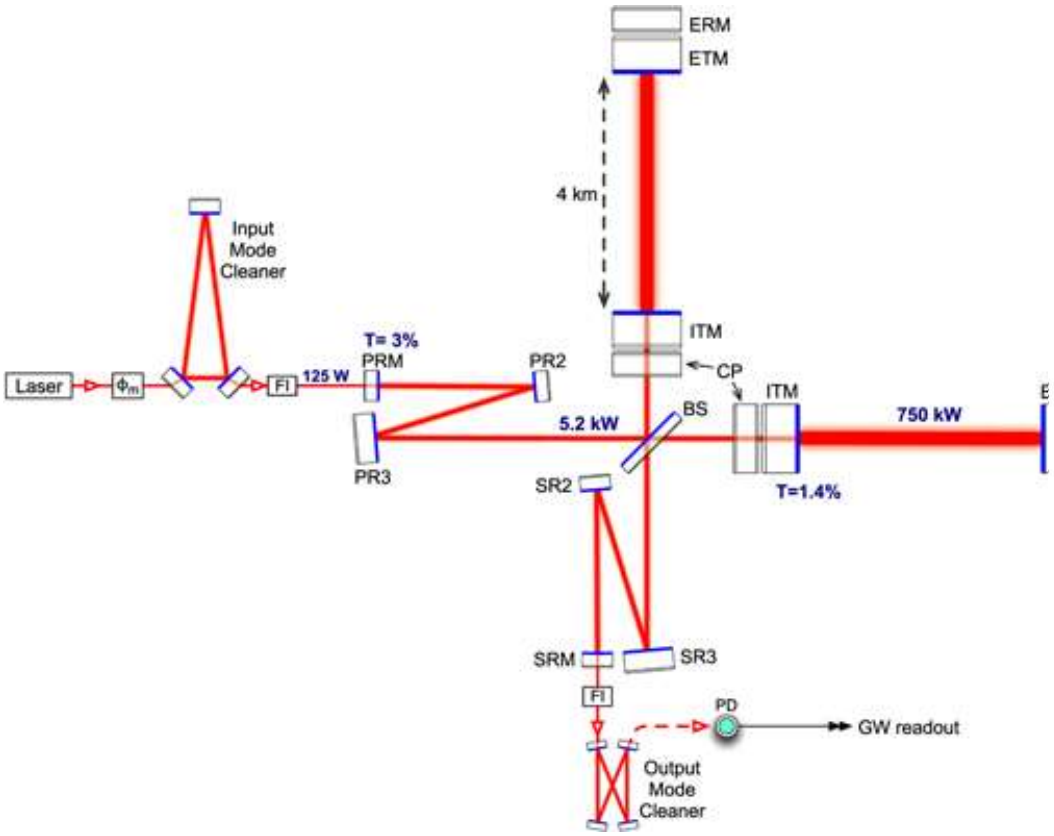

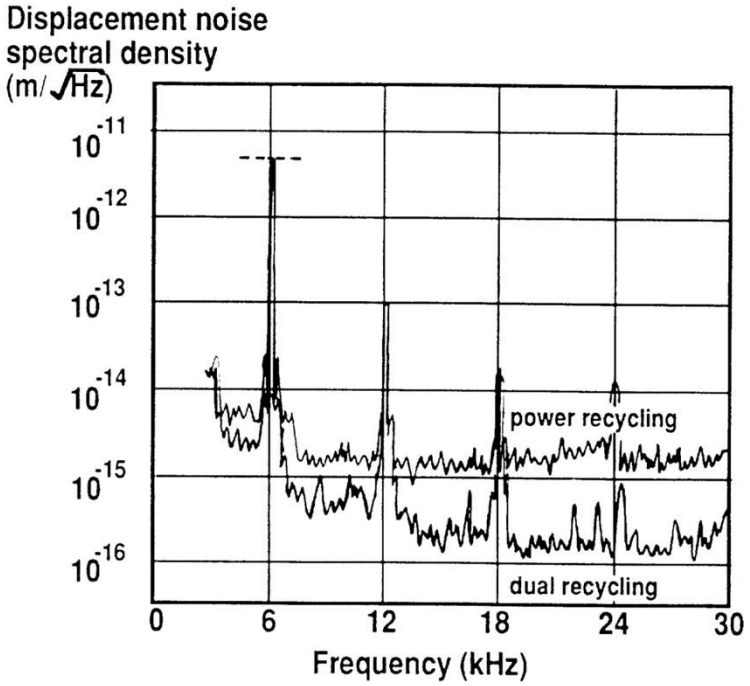

FIG. 4. The equivalent displacement of the noise at the output of the power- and dual-recycling systems. The 6-kHz peak was used as calibration.

Photon calibration in GWD

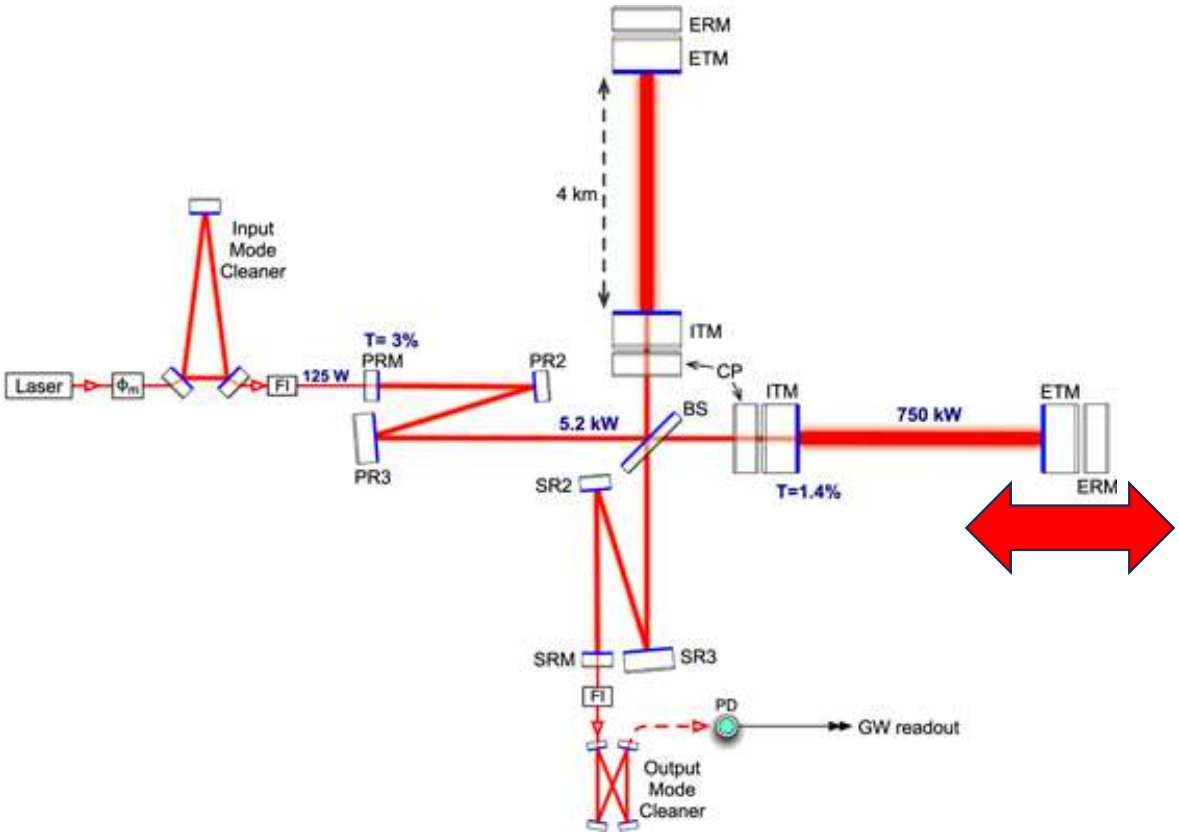

Interference

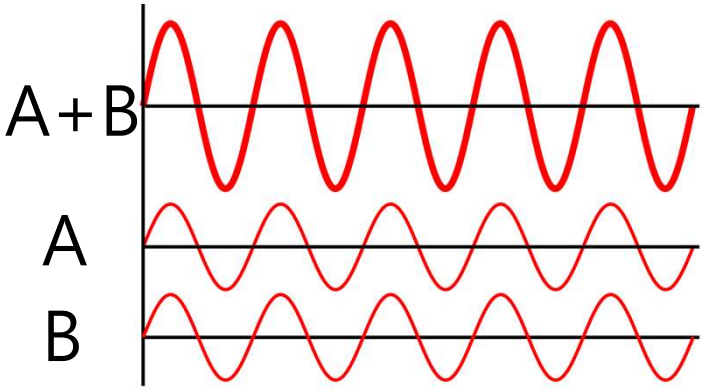

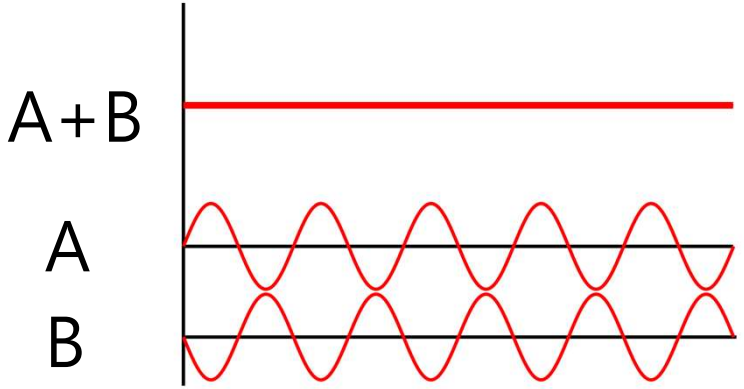

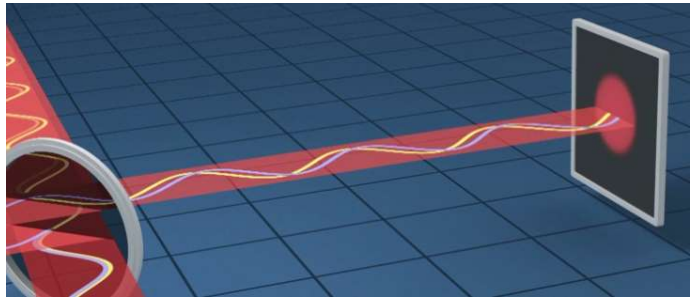

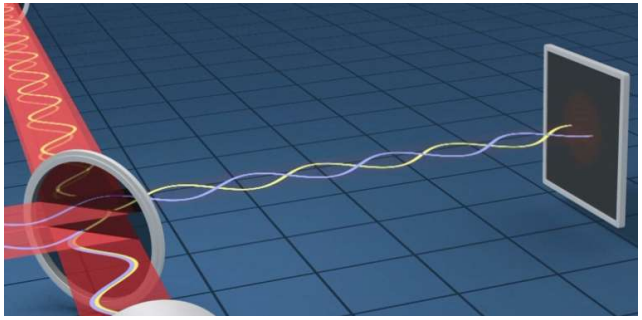

Constructive

Destructive

Interference signal

$$i_{PD1} - i_{PD2} \propto |E_S||E_R|\cos(\Delta\phi)$$

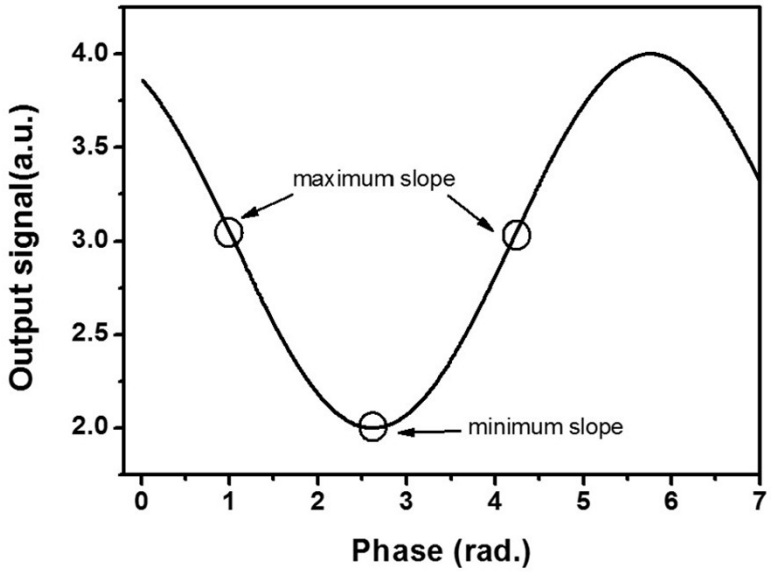

by intensity change?

by phase change?

Photon calibration

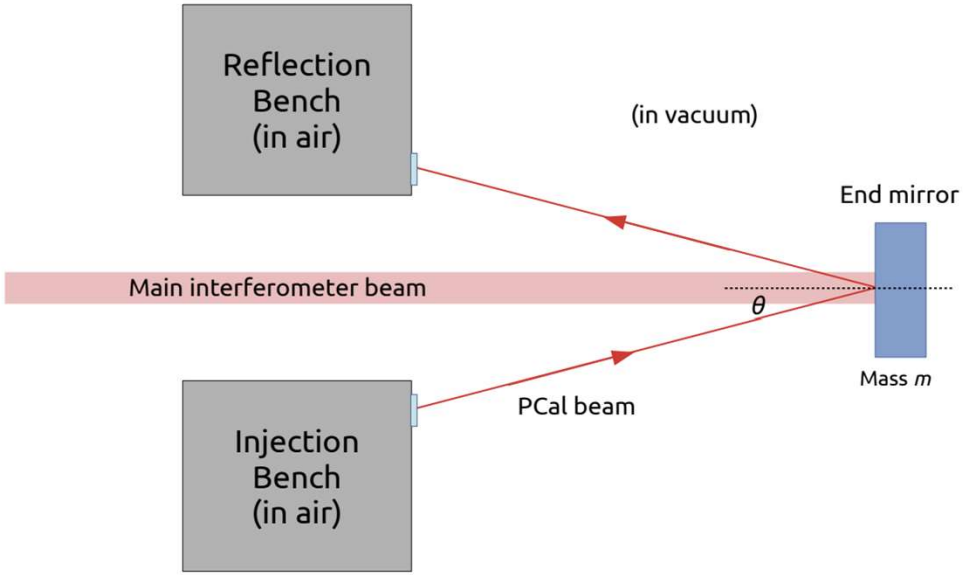

Figure 2: Schematic of an Advanced Virgo photon calibrator viewed from the top.

$$p = \frac{h}{\lambda}$$

We know momentum
We know mass of test mass

Photon calibration

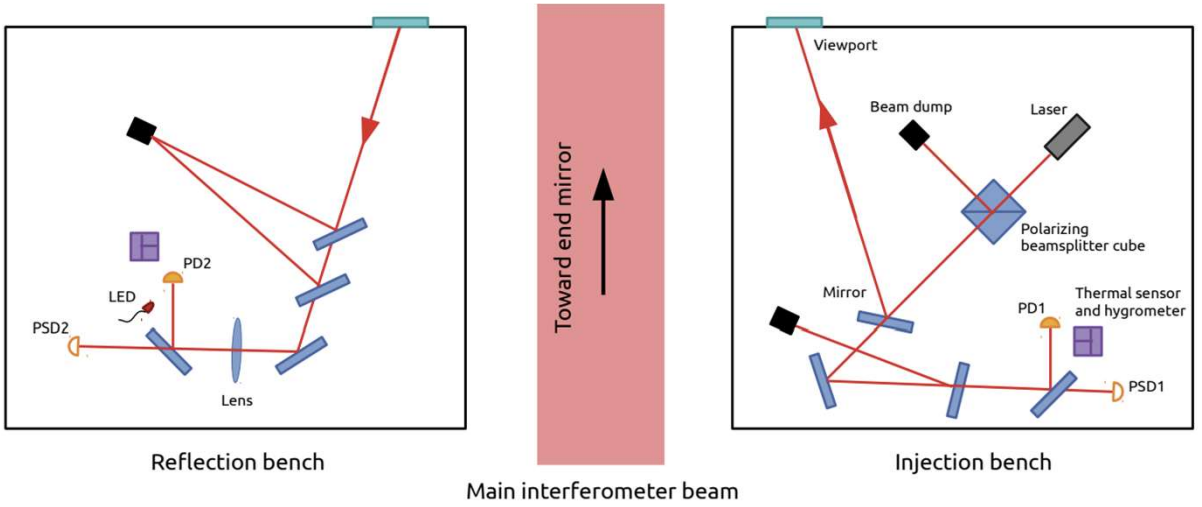

Figure 3: Detailed schematic of an Avanced Virgo photon calibrator viewed from the top. The size of the benches is 40 cm × 40 cm.

Global Pcal network

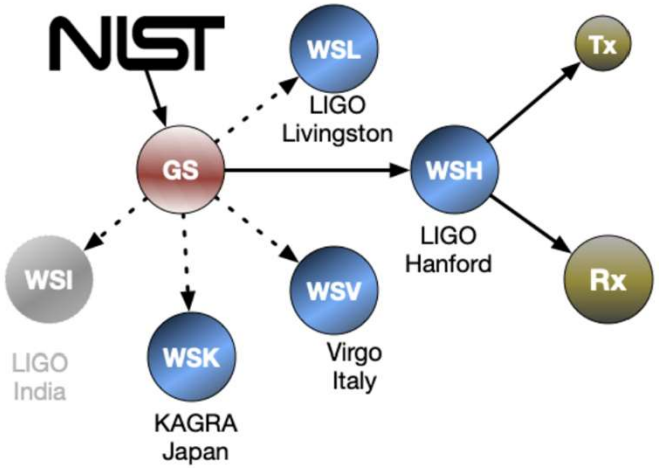

Figure 3. Schematic diagram showing the transfer of laser power calibration from NIST to the Pcal receiver (Rx) and transmitter (Tx) module power sensors (Rx and Tx) at the observatory end stations via a single Gold Standard (GS) and Working Standards (WSi) at each observatory. The Virgo, KAGRA and two LIGO detectors were actively involved in this scheme during the O3 observing run. LIGO India was expected to participate as soon as it became operational. Adapted from [21].

Frequency dependent squeezing

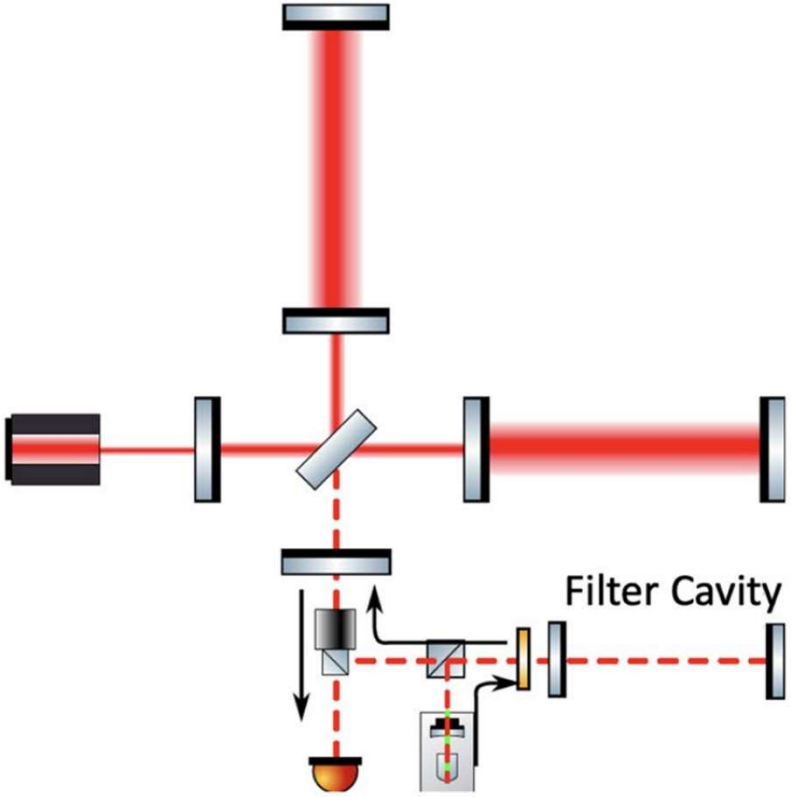

FDS using filter cavity

Standard quantum limit of GW detector

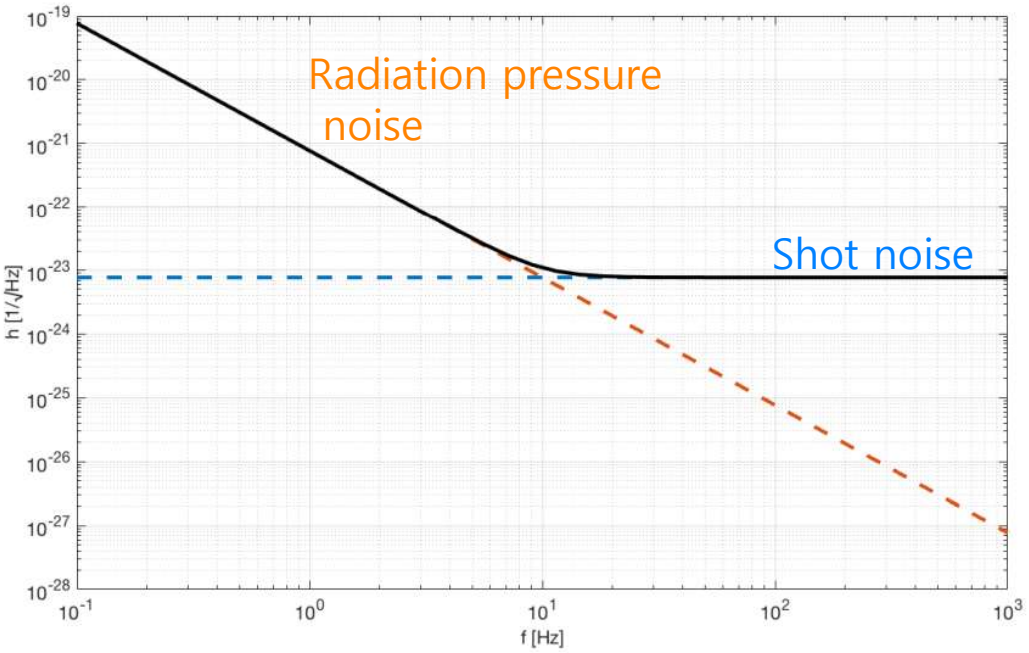

Standard quantum limit of gravitational wave detector
Shot noise + Radiation pressure noise

Shot noise of interferometer

$$E = h\nu$$

Photon energy

Laser power(W) = the number of photon(n) / time(s)

$nh\nu$ = / s

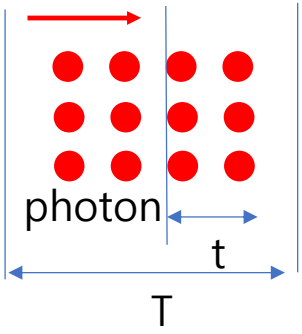

Shot noise

Shot noise of interferometer

$$E = h\nu$$

Photon energy

Laser power(W) = the number of photon(n) / time(s)

$nh\nu$ = / s

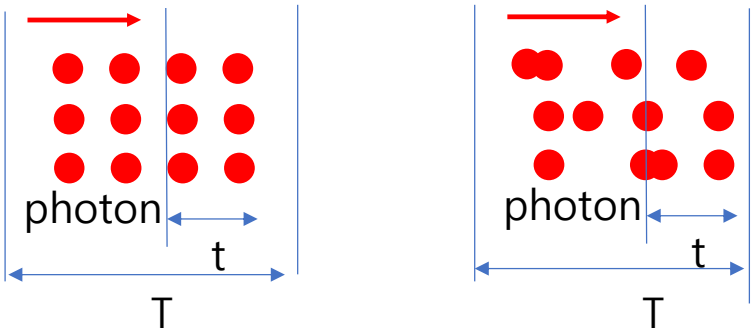

Shot noise

Shot noise of interferometer

h = 6.62607015×10^{-34} J·Hz^{-1}

Photon Counting Statistics

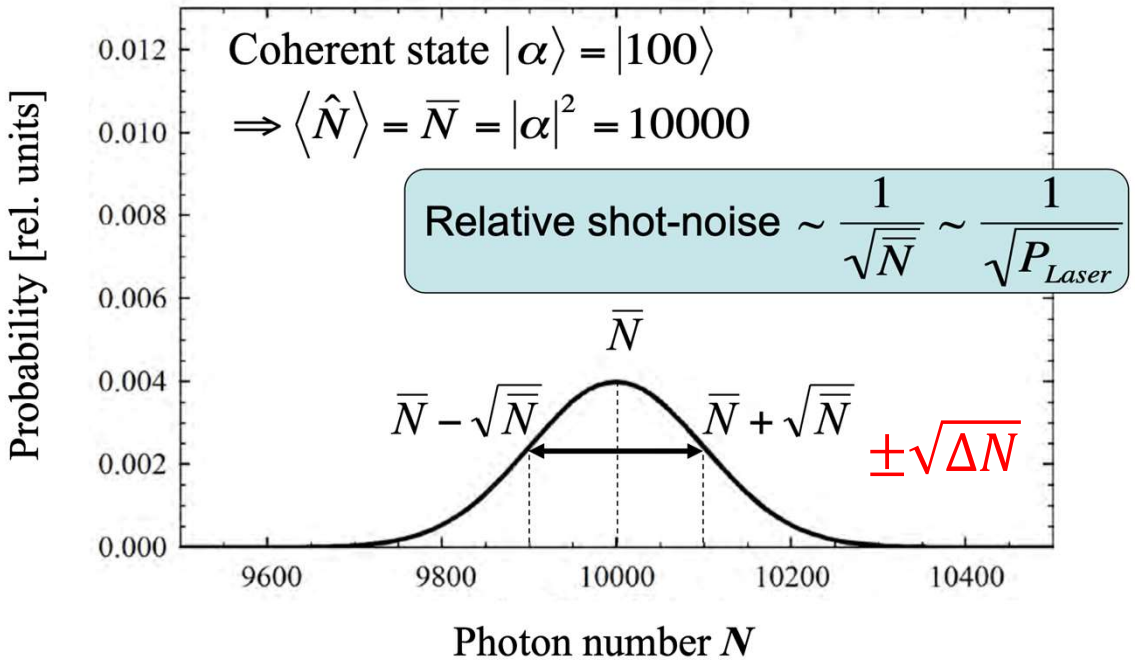

Standard quantum limit of GW detector

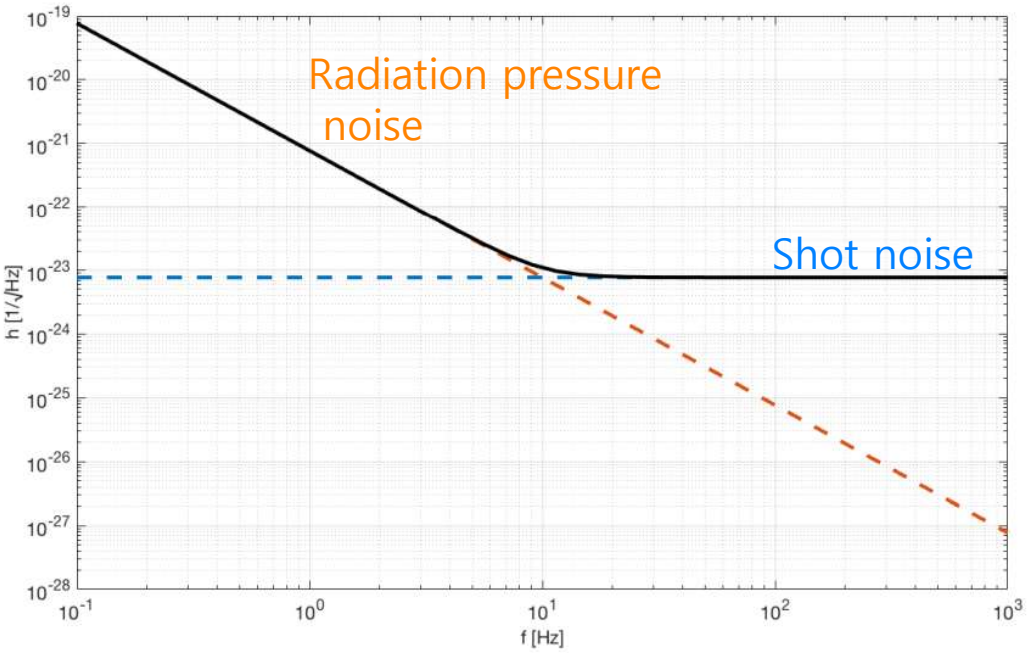

Standard quantum limit of gravitational wave detector
Shot noise + Radiation pressure noise

Radiation pressure noise

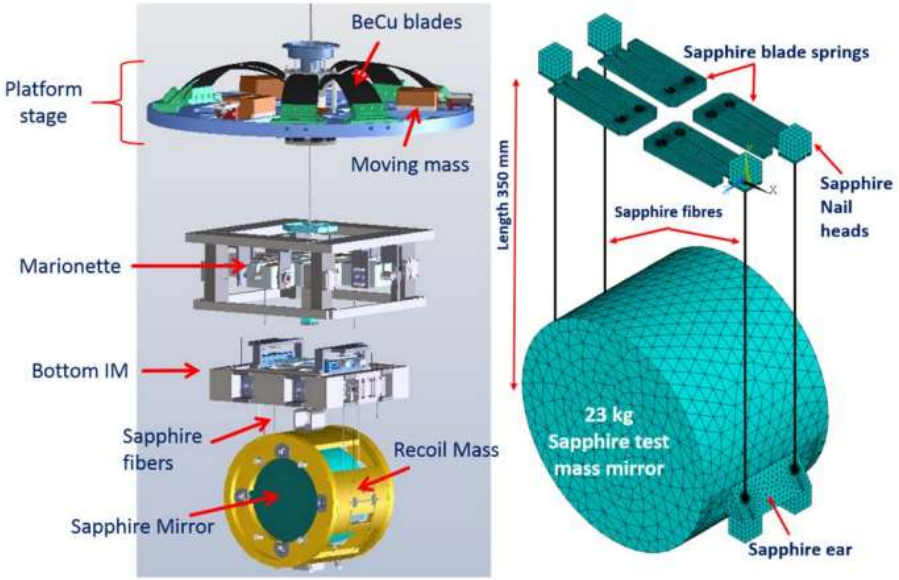

Radiation pressure noise

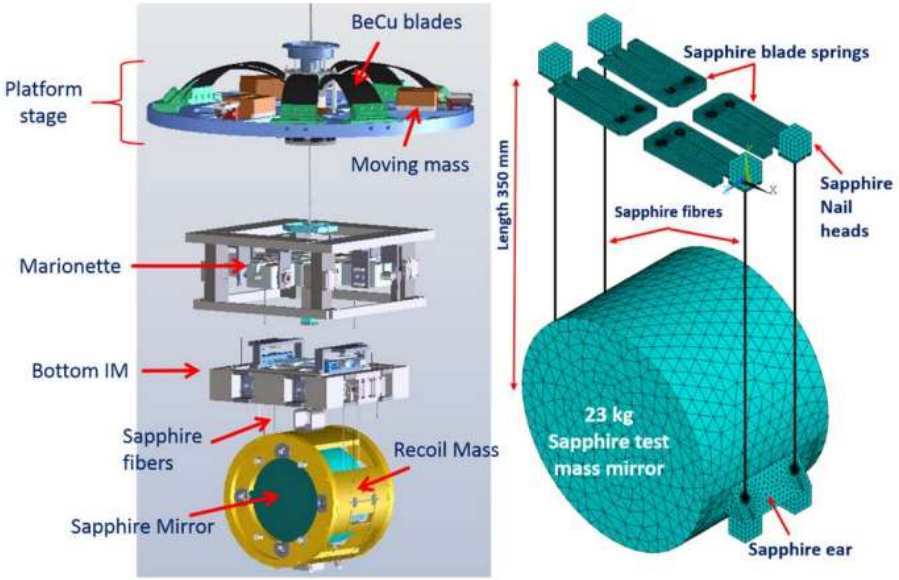

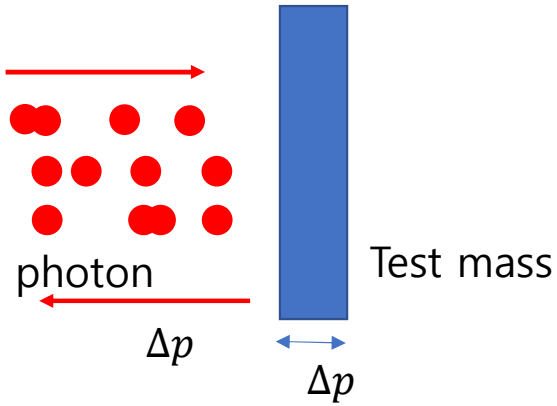

- Stored energy is very high (750 kW)
- Desired sensitivity is very high (10^{-21}~ 10^{-24})

Standard quantum limit of GW detector

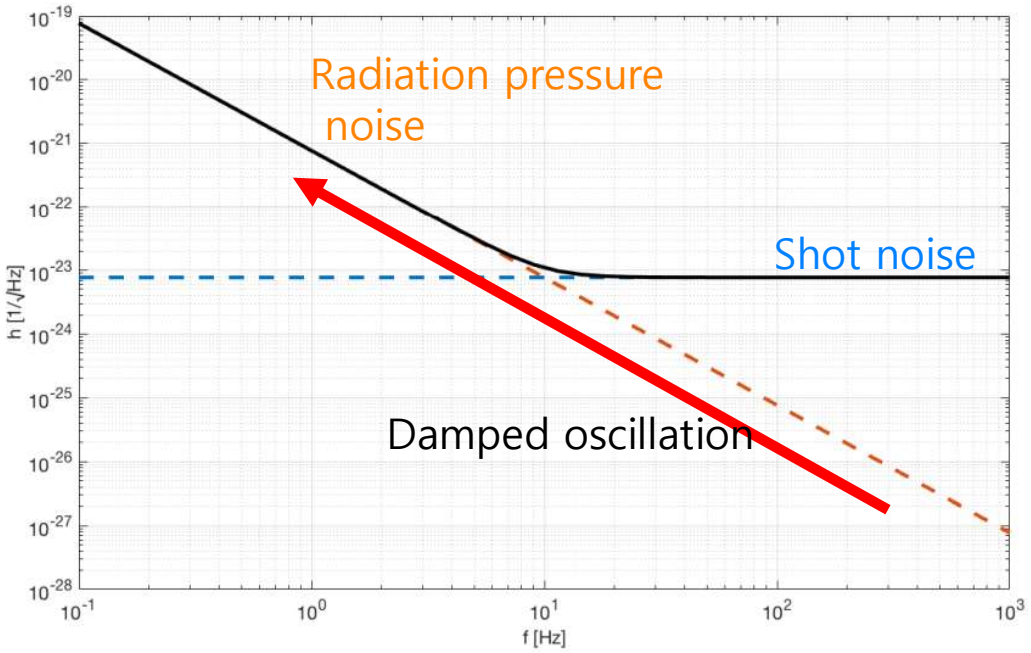

Standard quantum limit of gravitational wave detector
Shot noise + Radiation pressure noise

Radiation pressure noise
- Photon pressure fluctuation at **mirror**

-> Intensity noise

Shot noise
- Photon number fluctuation at **PD**

-> Phase noise

LIGO sensitivity

Radiation pressure

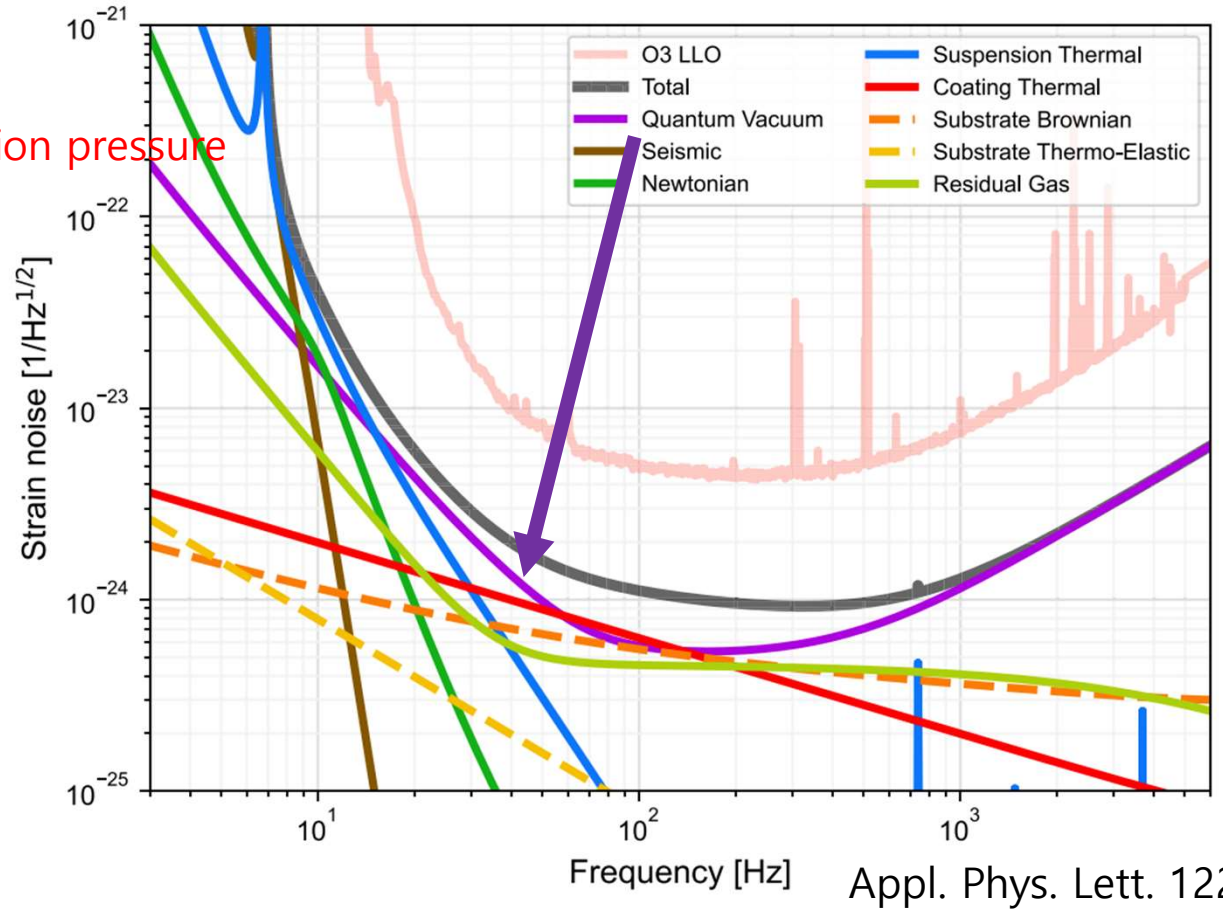

Shot noise

Appl. Phys. Lett. 122, 110502 (2023)

Quantum noise of gravitational wave detector

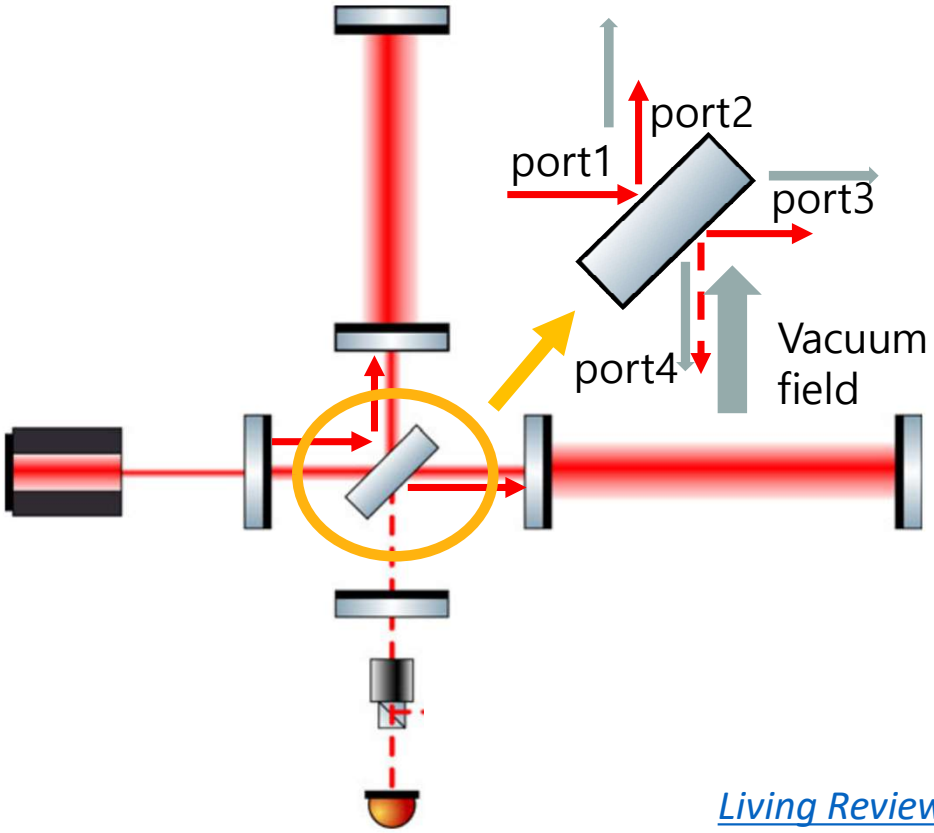

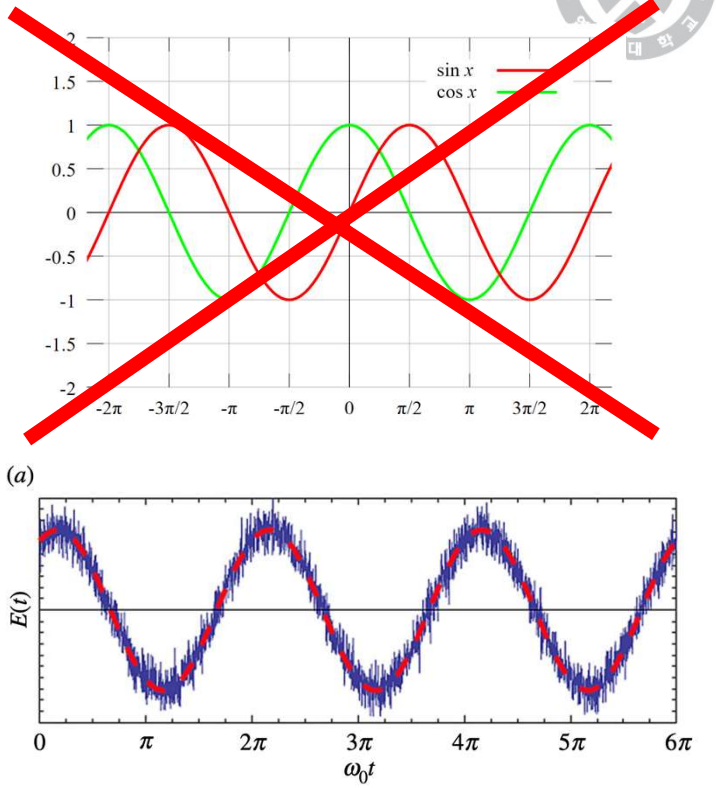

Living Reviews in Relativity **volume 22**, Article number: 2 (2019)

Gravitational wave detector

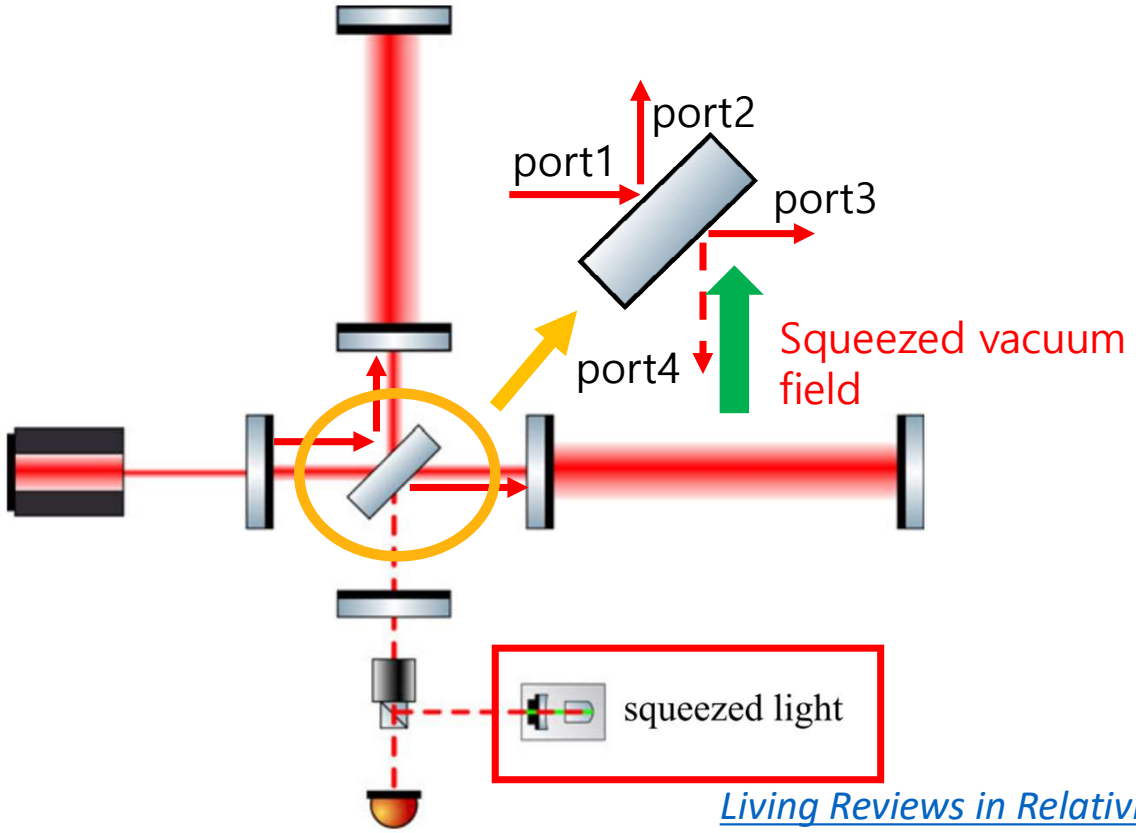

Living Reviews in Relativity **volume 22**, Article number: 2 (2019)

Squeezed light

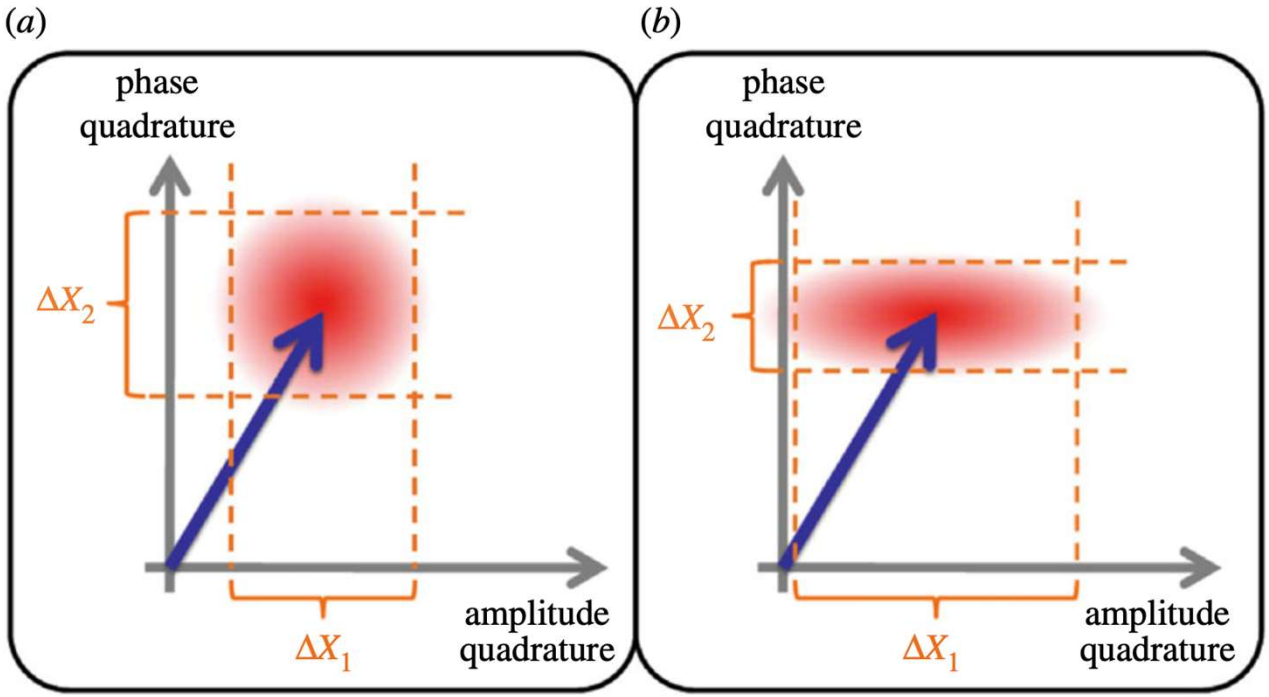

Heurs M. 2018 Gravitational wave detection u sing laser interferometry beyond the standard quantum limit.Phil. Trans. R. Soc. A 376: 20170 289.

O4 Squeezing status

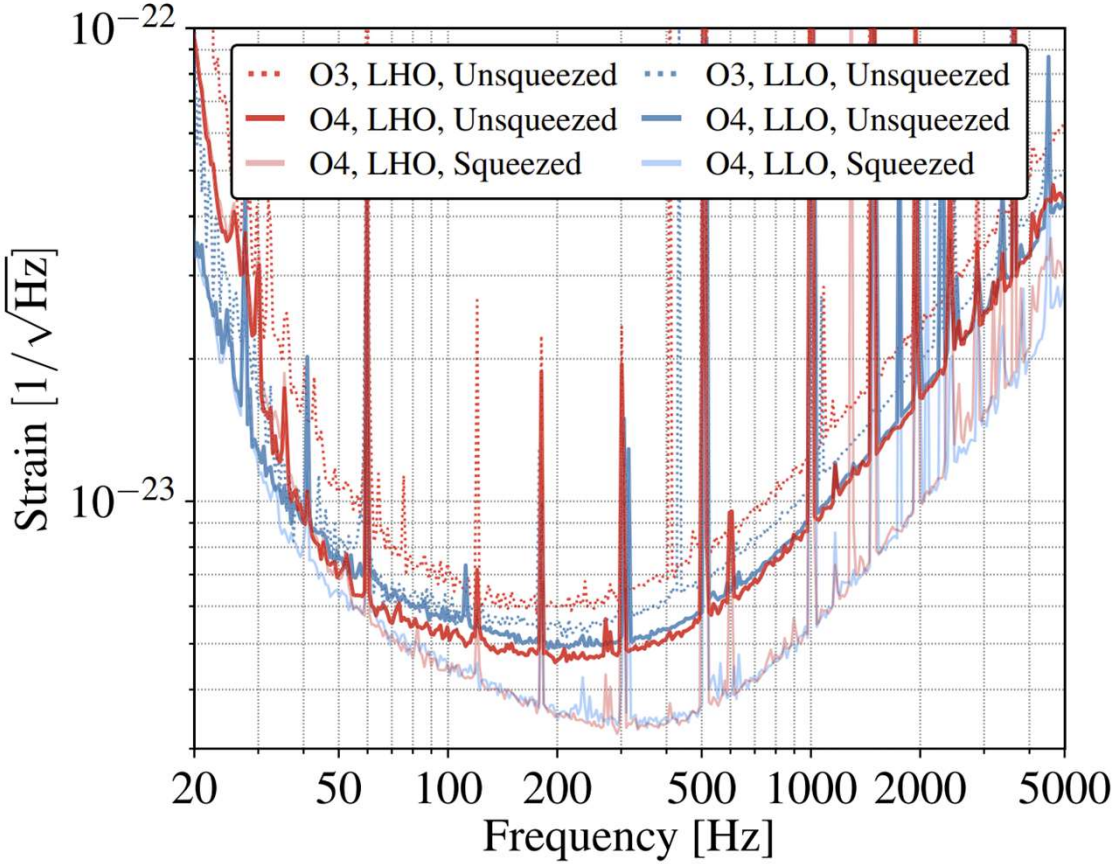

Frequency independent squeezing

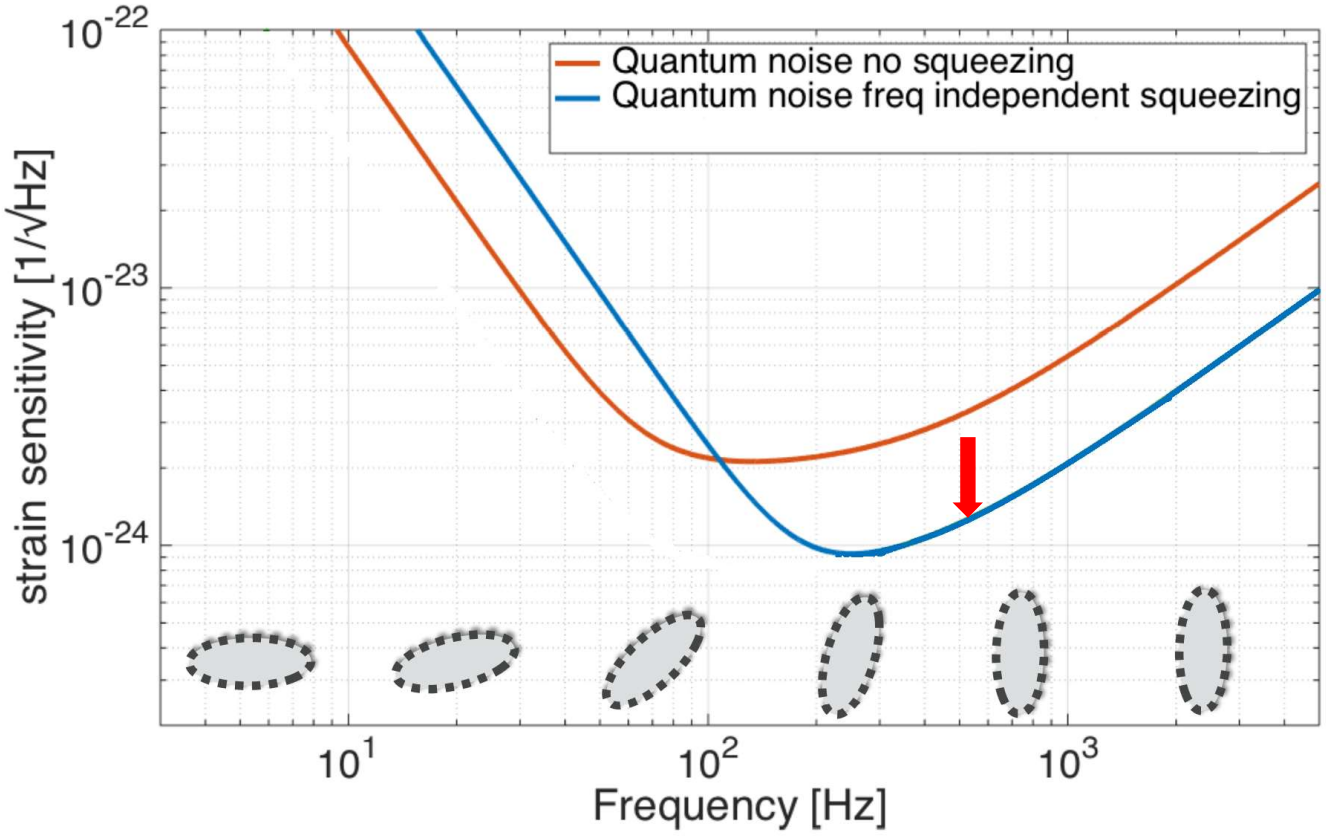

Optical and noise studies for Advanced Virgo and filter cavities for quantum noise reduction
in gravitational-wave interferometric detectors, Eleonora Capocasa, UNIVERSITÉ PARIS DIDEROT (2017)

Frequency independent squeezing

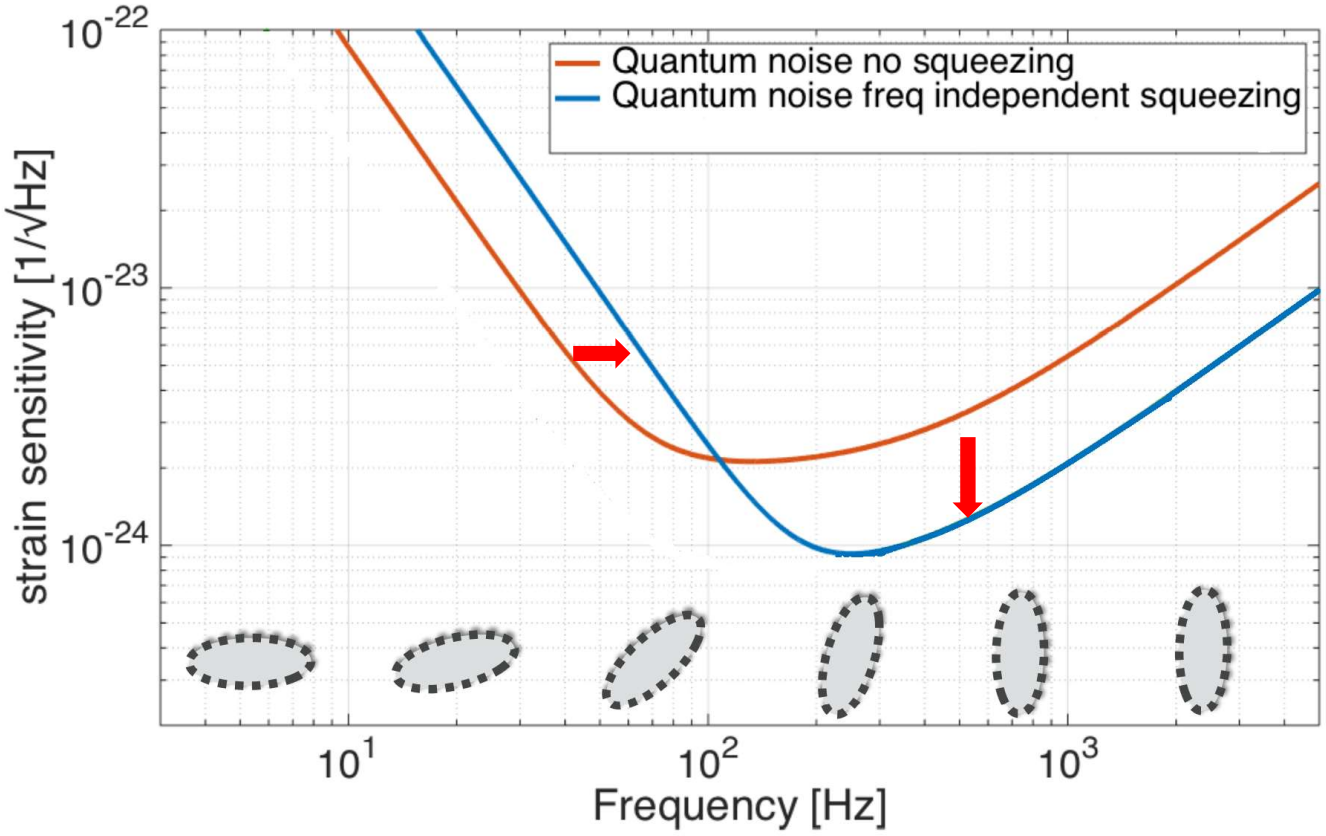

Optical and noise studies for Advanced Virgo and filter cavities for quantum noise reduction
in gravitational-wave interferometric detectors, Eleonora Capocasa, UNIVERSITÉ PARIS DIDEROT (2017)

Frequency independent squeezing

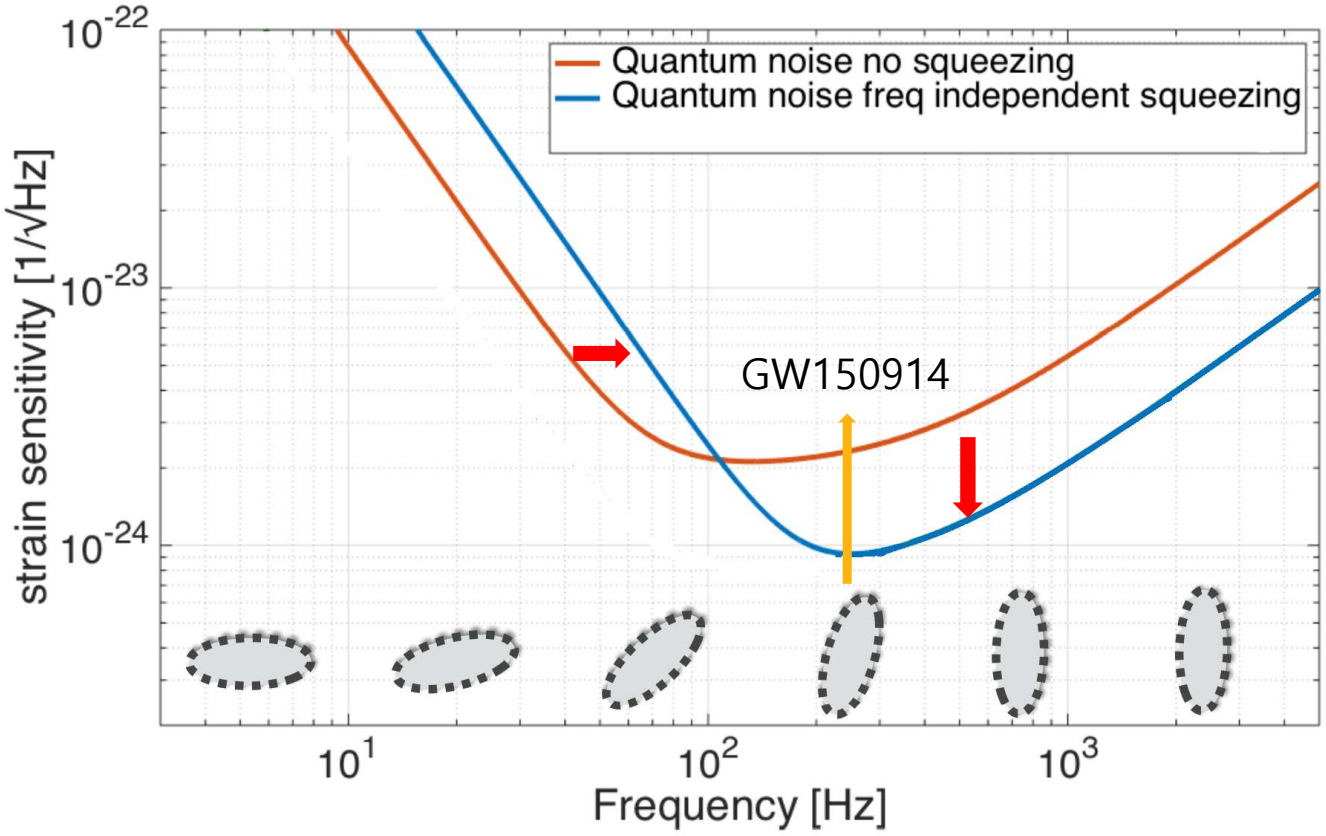

Optical and noise studies for Advanced Virgo and filter cavities for quantum noise reduction
in gravitational-wave interferometric detectors, Eleonora Capocasa, UNIVERSITÉ PARIS DIDEROT (2017)

Frequency independent squeezing

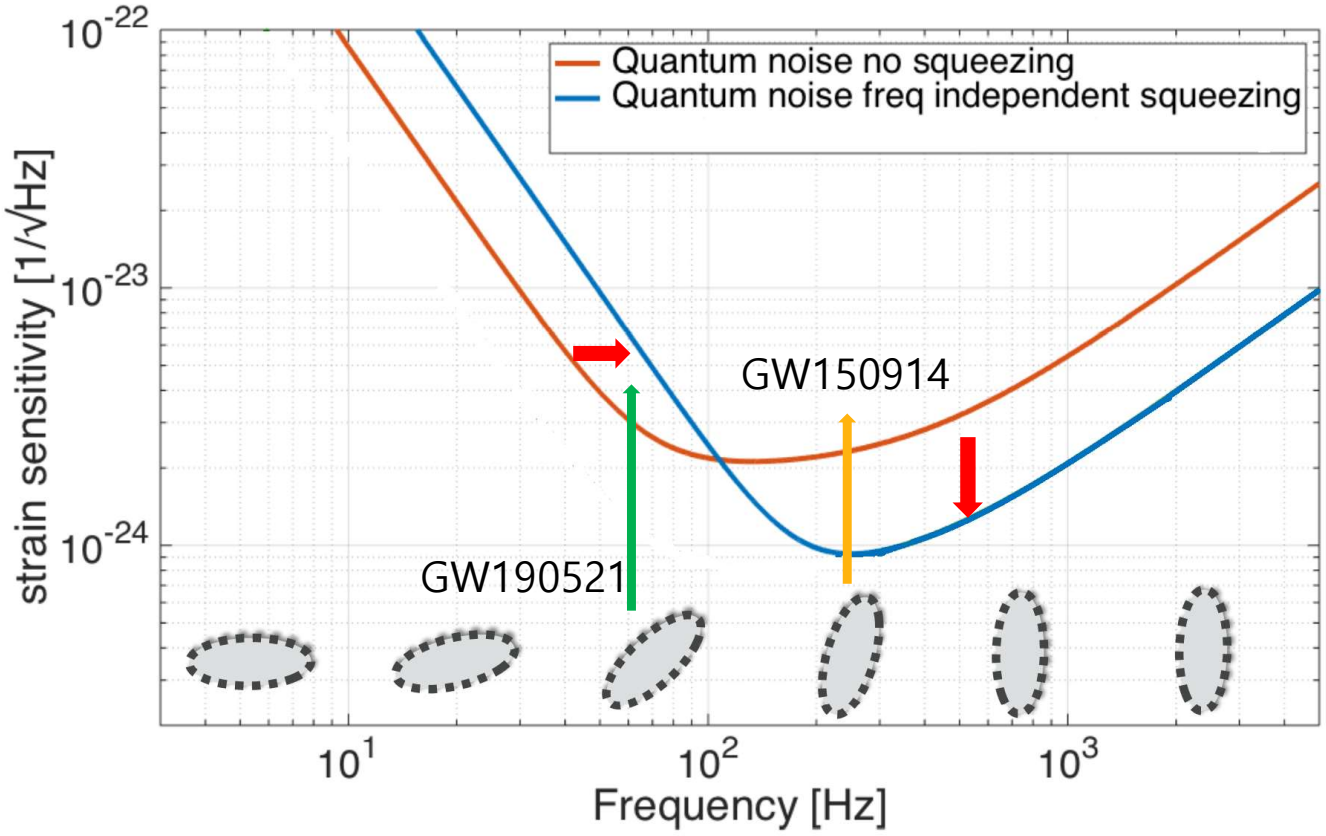

Optical and noise studies for Advanced Virgo and filter cavities for quantum noise reduction
in gravitational-wave interferometric detectors, Eleonora Capocasa, UNIVERSITÉ PARIS DIDEROT (2017)

Squeezed light

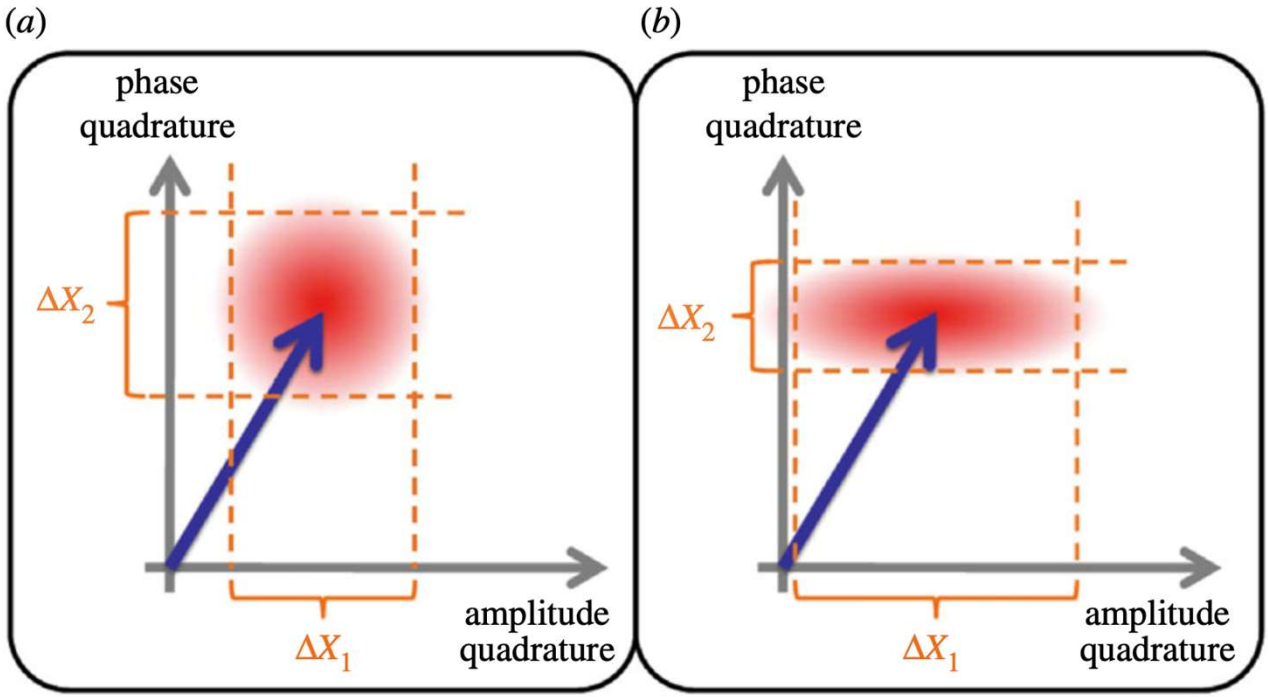

Heurs M. 2018 Gravitational wave detection u sing laser interferometry beyond the standard quantum limit.Phil. Trans. R. Soc. A 376: 20170 289.

Frequency independent squeezing

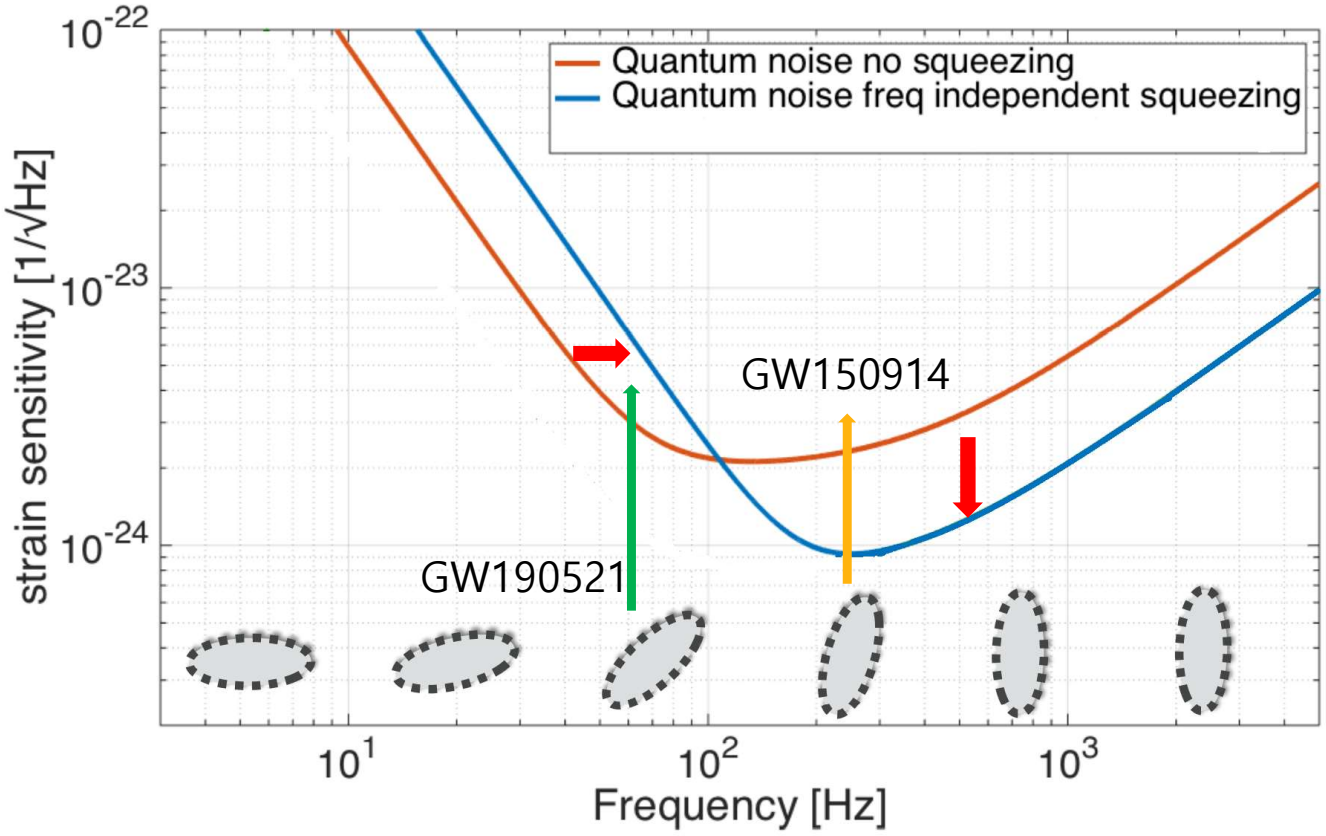

Optical and noise studies for Advanced Virgo and filter cavities for quantum noise reduction
in gravitational-wave interferometric detectors, Eleonora Capocasa, UNIVERSITÉ PARIS DIDEROT (2017)

Frequency dependent squeezing(FDS)

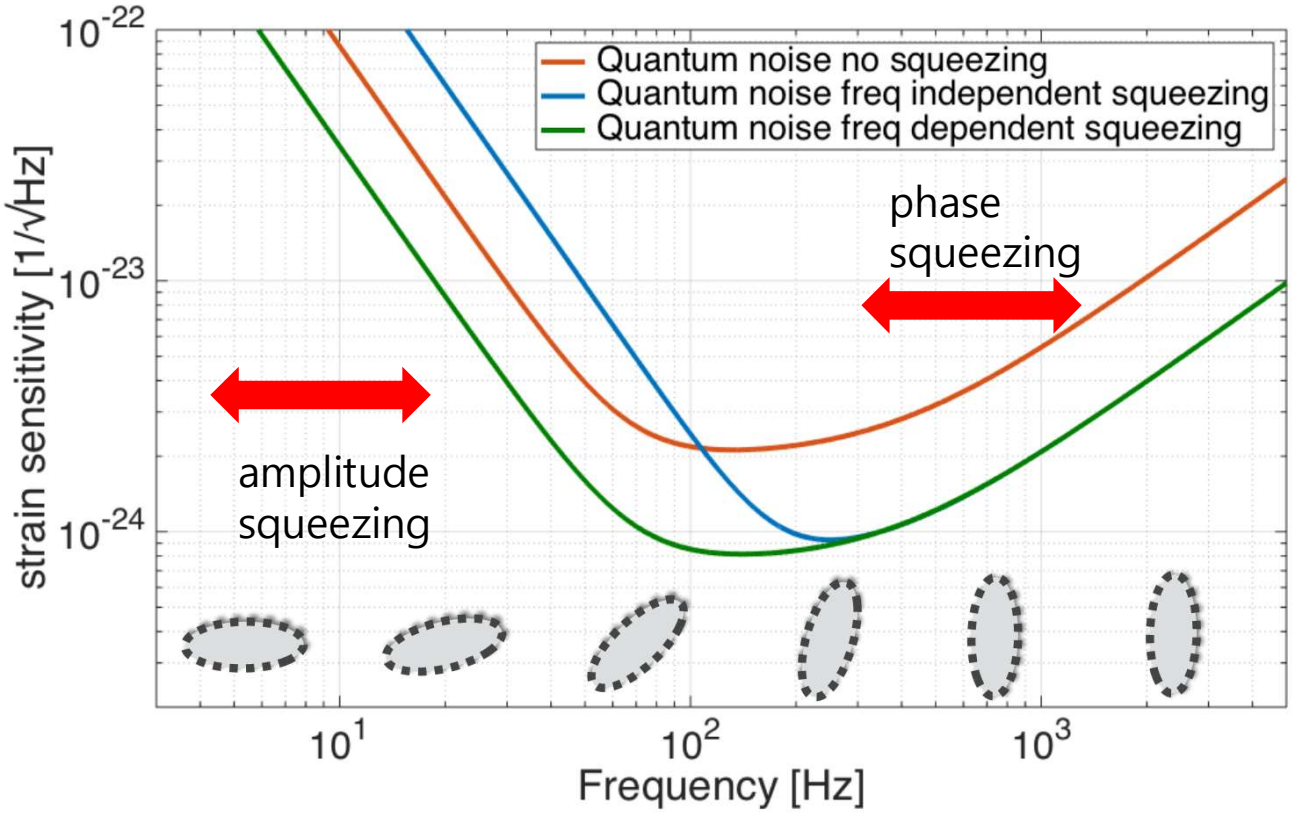

Optical and noise studies for Advanced Virgo and filter cavities for quantum noise reduction
in gravitational-wave interferometric detectors, Eleonora Capocasa, UNIVERSITÉ PARIS DIDEROT (2017)

Frequency dependent squeezing

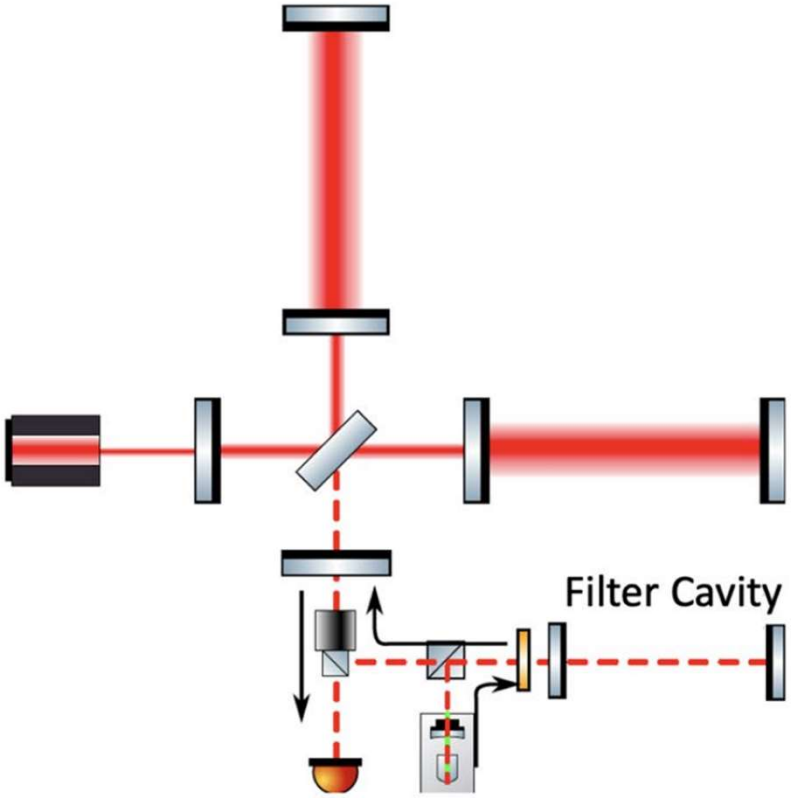

LIGO sensitivity

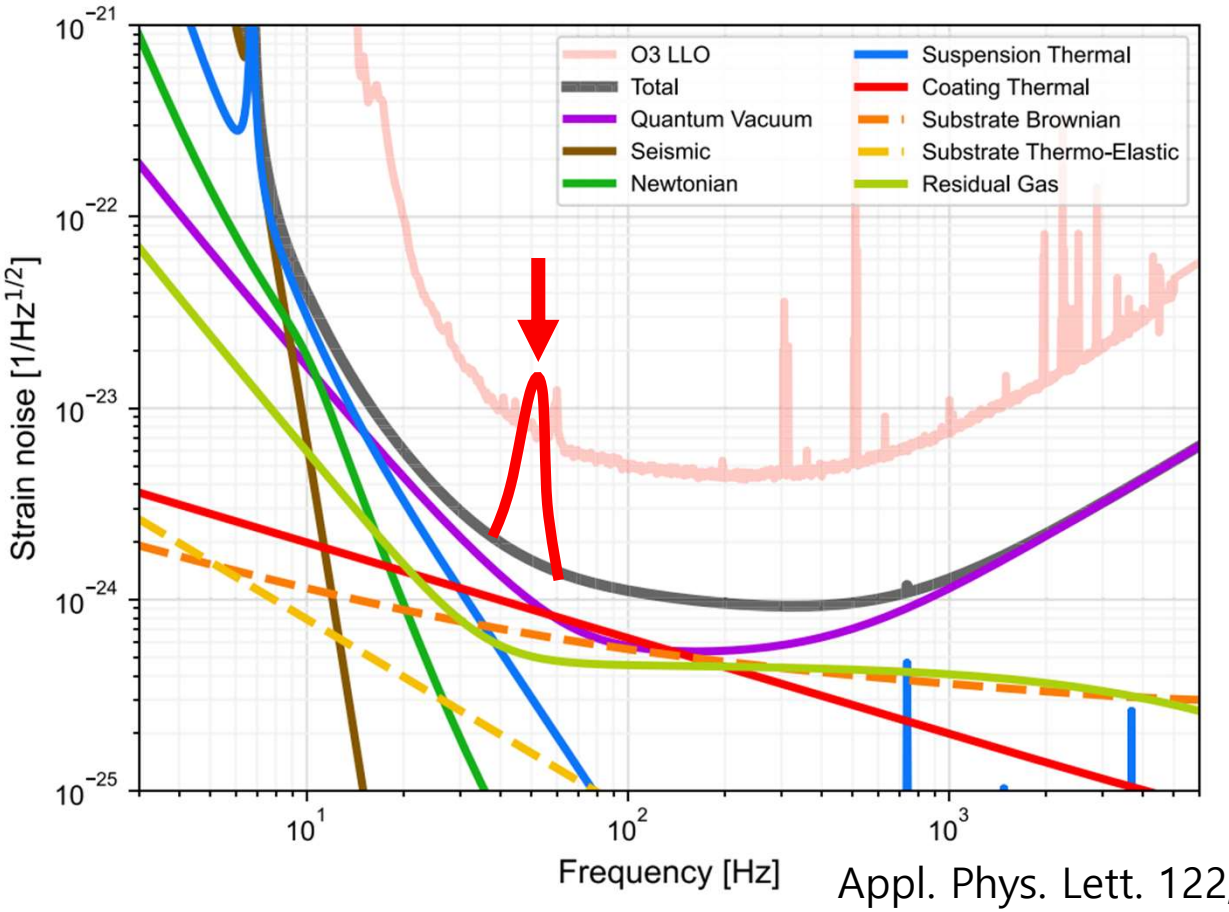

Appl. Phys. Lett. 122, 110502 (2023)

Frequency dependent squeezing using filter cavity

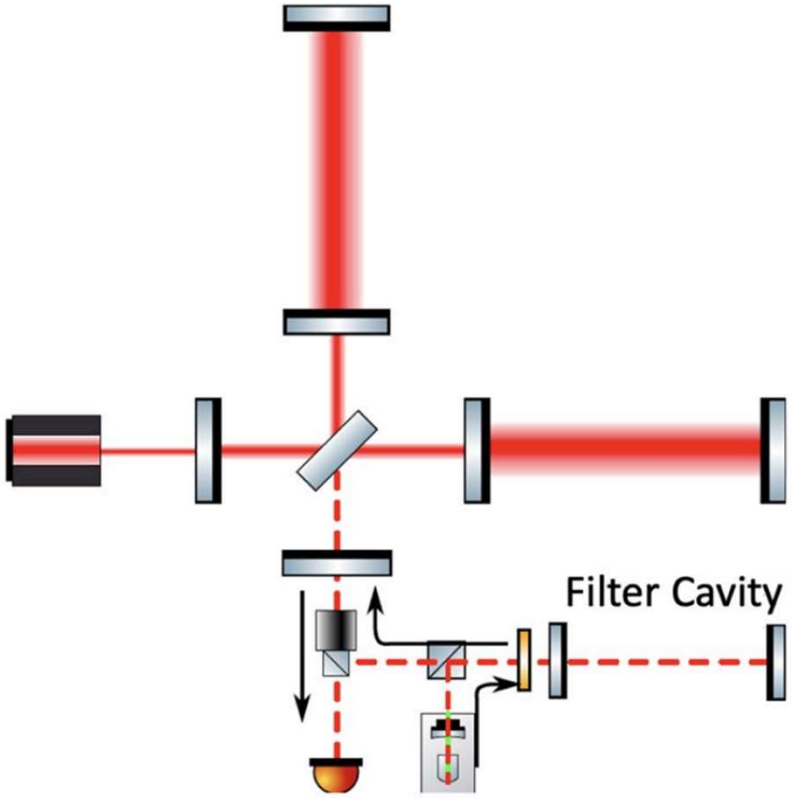

$$E^{(+)}(t) = \int_0^\infty E(\omega) e^{-i\omega t} \frac{d\omega}{2\pi}$$

$$E^{(+)}(t) = e^{-i\omega_0 t} \int_0^\infty \left(E(\Omega) e^{-i\Omega t} + E(-\Omega) e^{+i\Omega t} \right) \frac{d\Omega}{2\pi}$$

$$\omega = \omega_0 + \Omega$$

Laser frequency

GW signal frequency

Frequency dependent squeezing using filter cavity

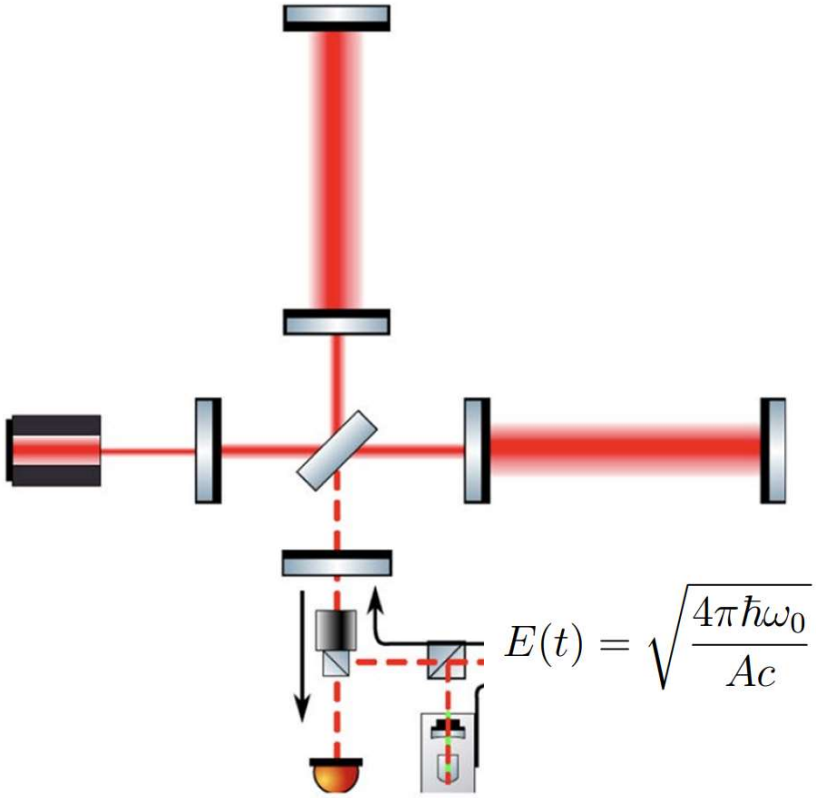

$$E(t) = \sqrt{\frac{4\pi\hbar\omega_0}{Ac}}\left[a_1(t)\cos(\omega_0 t) + a_2(t)\sin(\omega_0 t)\right]$$

$$\textbf{Amplitude Quadrature}: \; a_1(t) = \frac{a(t) + a^\dagger(t)}{\sqrt{2}}$$

$$\textbf{Phase Quadrature}: \; a_2(t) = \frac{a(t) - a^\dagger(t)}{i\sqrt{2}}$$

$$E(t) = \sqrt{\frac{4\pi\hbar\omega_0}{Ac}}\left[\cos(\omega_0 t)\int_0^\infty (a_1(\Omega)e^{-i\Omega t} + a_1^\dagger(\Omega)e^{+i\Omega t})\frac{d\Omega}{2\pi}\right.$$

$$\left. + \sin(\omega_0 t)\int_0^\infty (a_2(\Omega)e^{-i\Omega t} + a_2^\dagger(\Omega)e^{+i\Omega t})\frac{d\Omega}{2\pi}\right]$$

Squeezed light

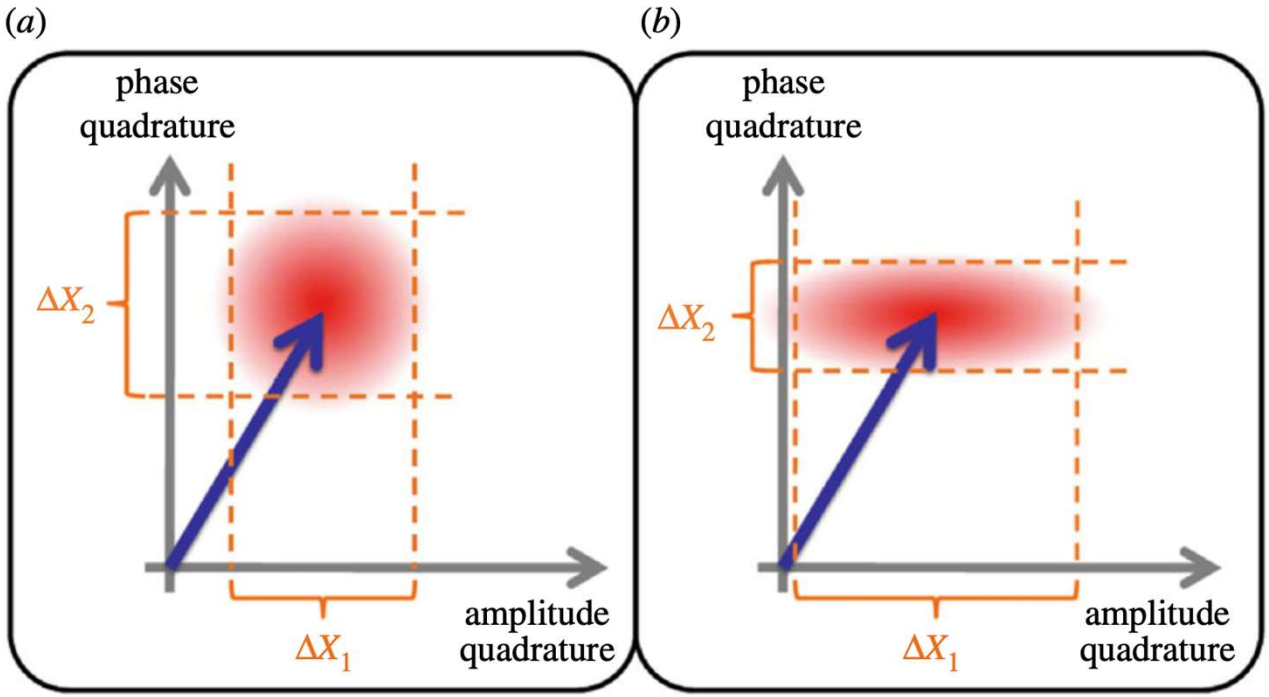

Heurs M. 2018 Gravitational wave detection u sing laser interferometry beyond the standard quantum limit.Phil. Trans. R. Soc. A 376: 20170 289.

Squeezed light

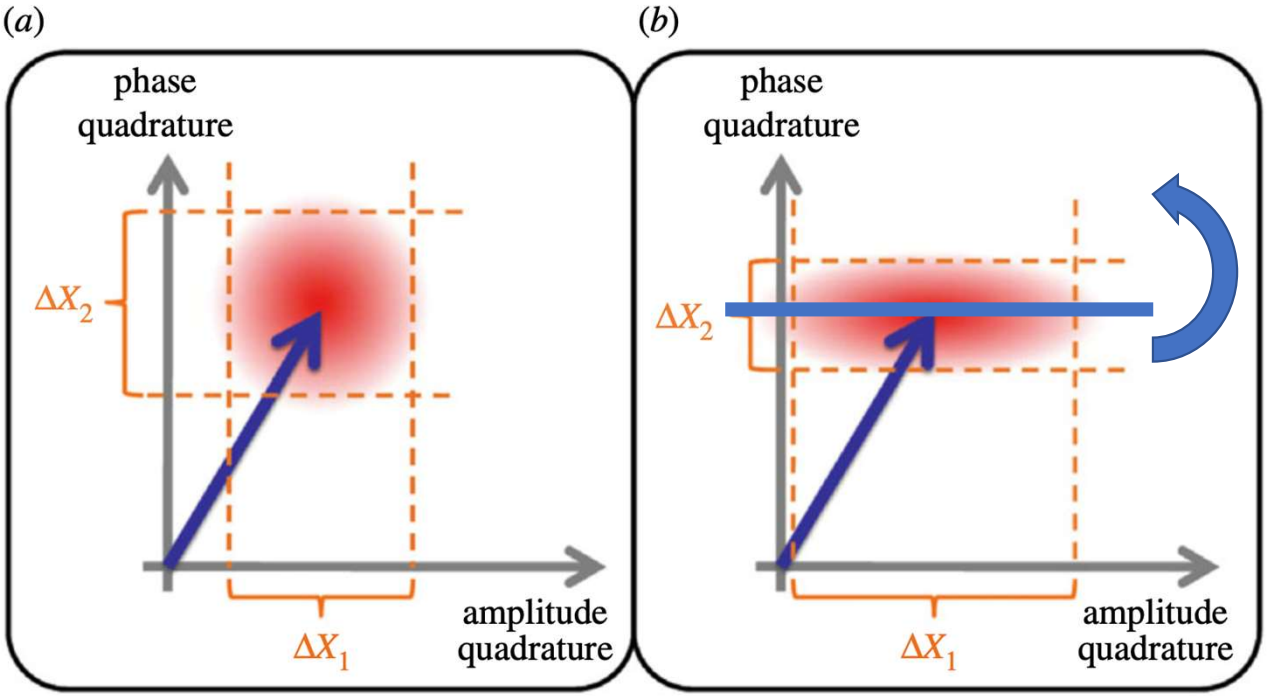

Squeeze angle rotation

Heurs M. 2018 Gravitational wave detection u sing laser interferometry beyond the standard quantum limit.Phil. Trans. R. Soc. A 376: 20170 289.

Squeeze angle rotation

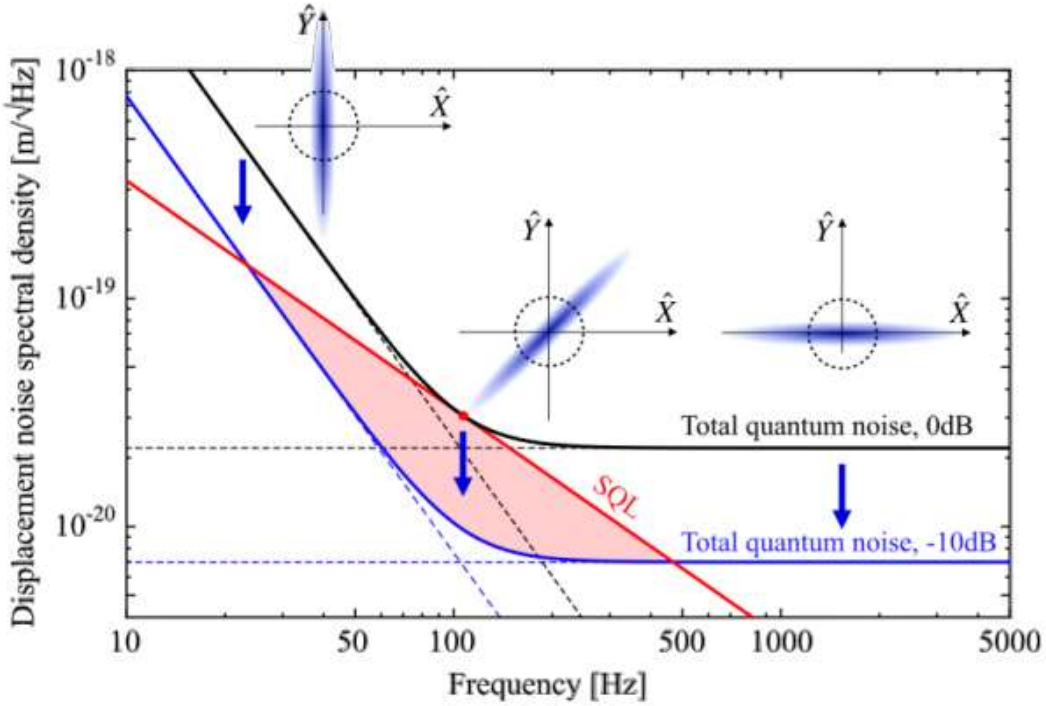

$$\alpha_p = \arctan\left(\frac{2\gamma_{\mathrm{fc}}\Delta\omega_{\mathrm{fc}}}{\gamma_{\mathrm{fc}}^2 - \Delta\omega_{\mathrm{fc}}^2 + \Omega^2}\right)$$

$$t_{\mathrm{st}} = \frac{1}{\gamma_{\mathrm{fc}}} = \frac{\sqrt{2}}{\Omega_{\mathrm{SQL}}} \simeq 3\,\mathrm{ms}$$

Frequency dependent squeezing using filter cavity

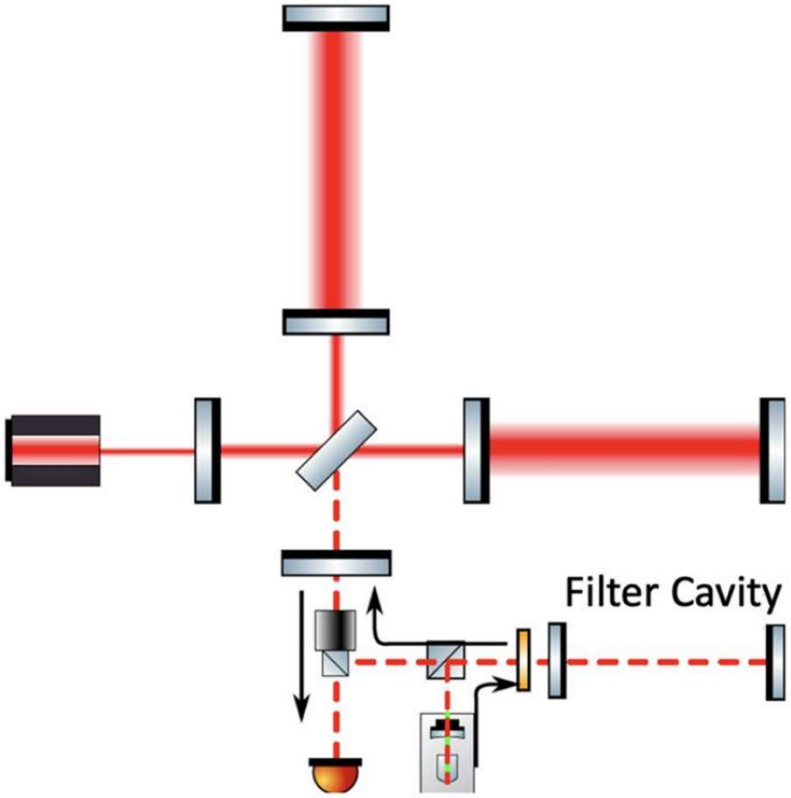

Frequency dependent squeezing - KAGRA

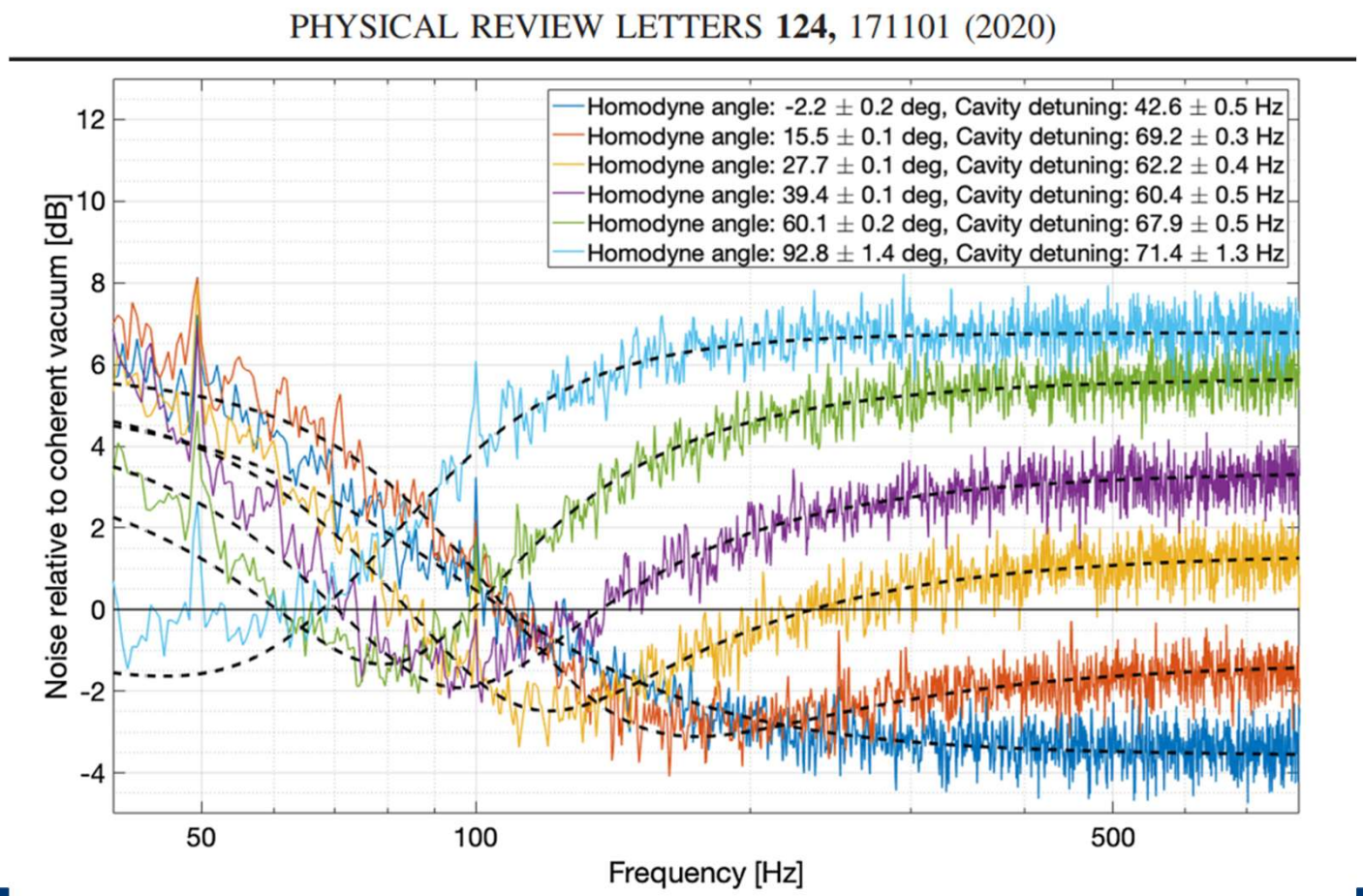

Quantum noise of gravitational wave detector

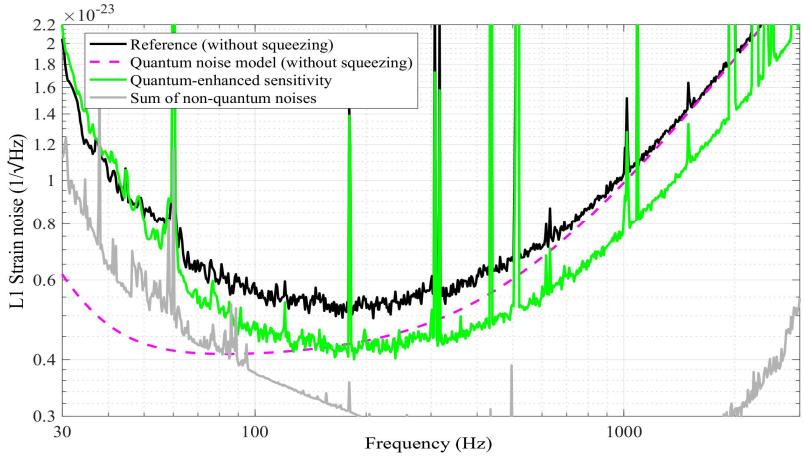

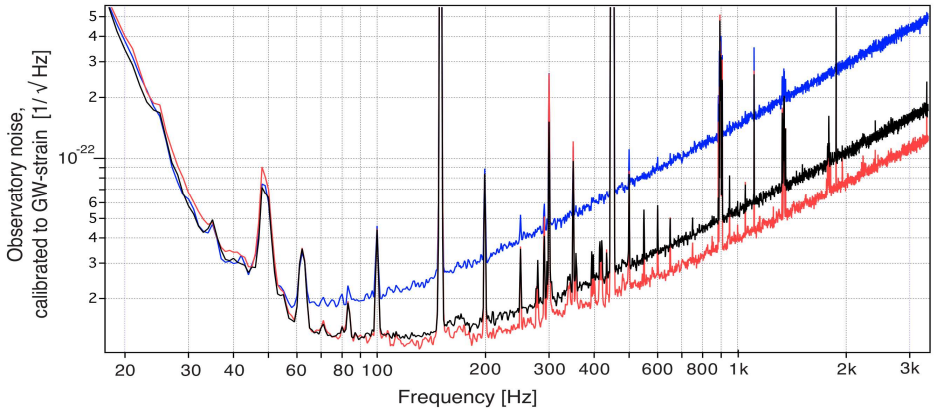

Quantum optics experiment implementation on the scale of kilometers

Summary

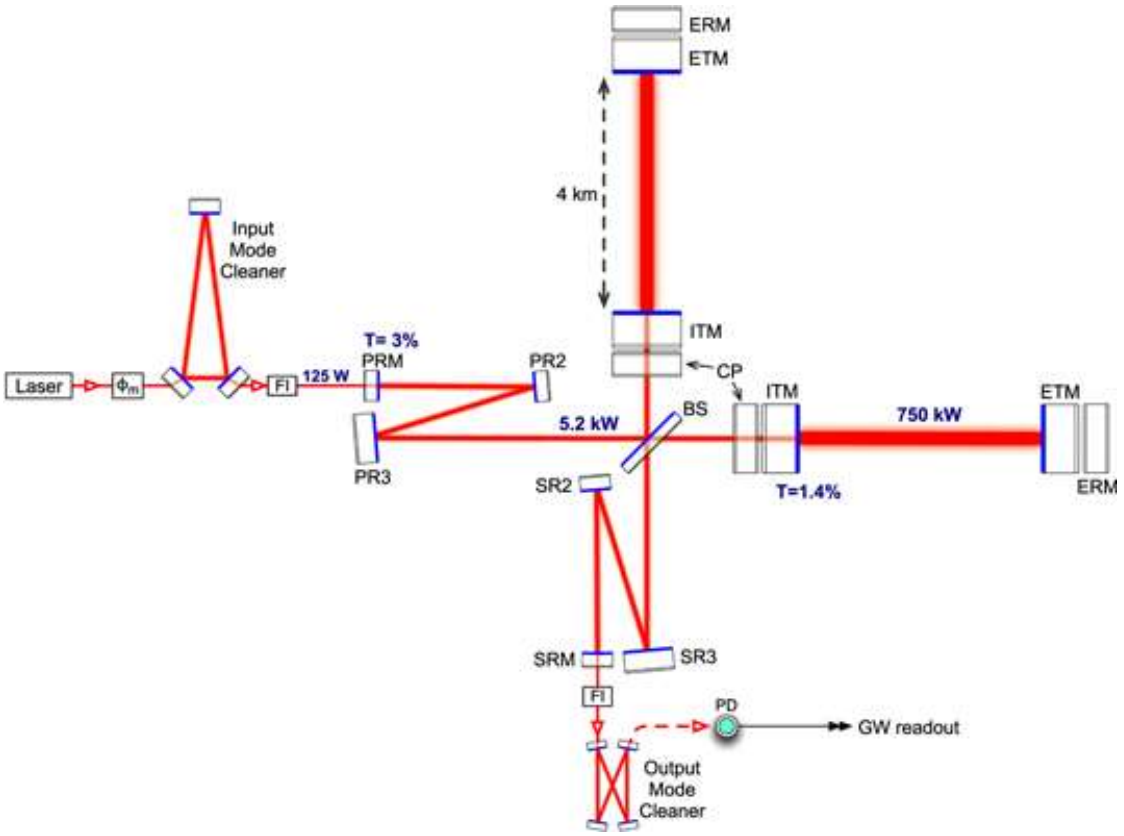

- **Stabilized laser**
- **Michelson Fabry-perot cavity**
- **Test mass**
- **Suspended system**
- **Dual recycling system**
- **Photon calibration**
- **FD squeezing**

Summary

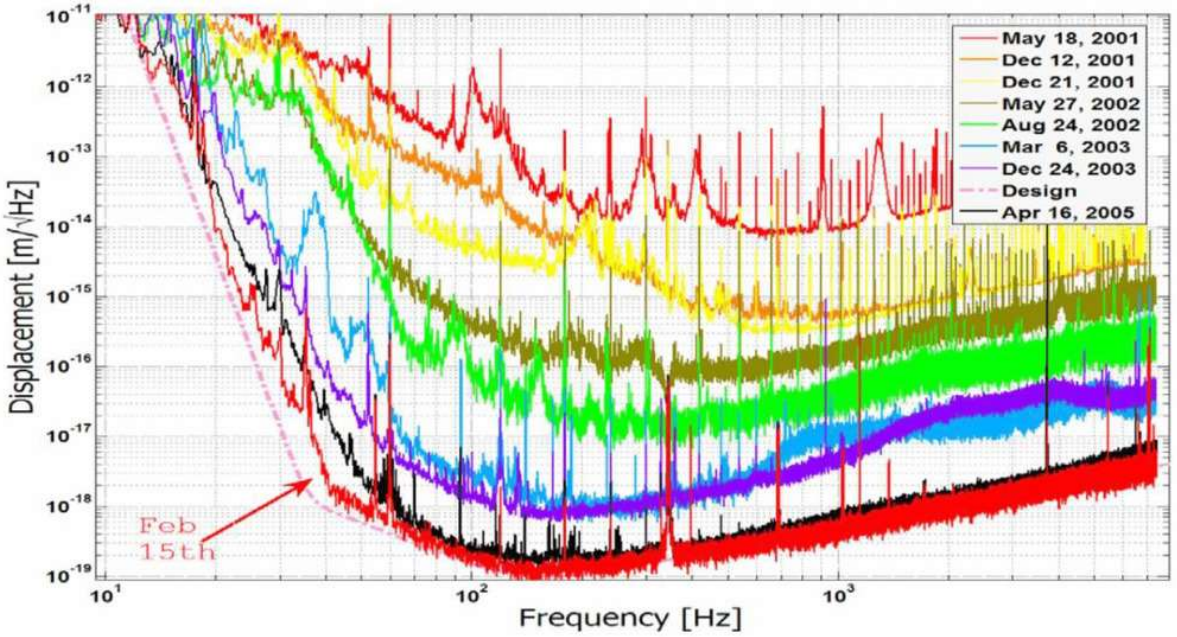
May 18, 2001
Dec 12, 2001
Dec 21, 2001
May 27, 2002
Aug 24, 2002
Mar 6, 2003
Dec 24, 2003
Design
Apr 16, 2005
Feb 15th
Displacement [m/√Hz]
Frequency [Hz]

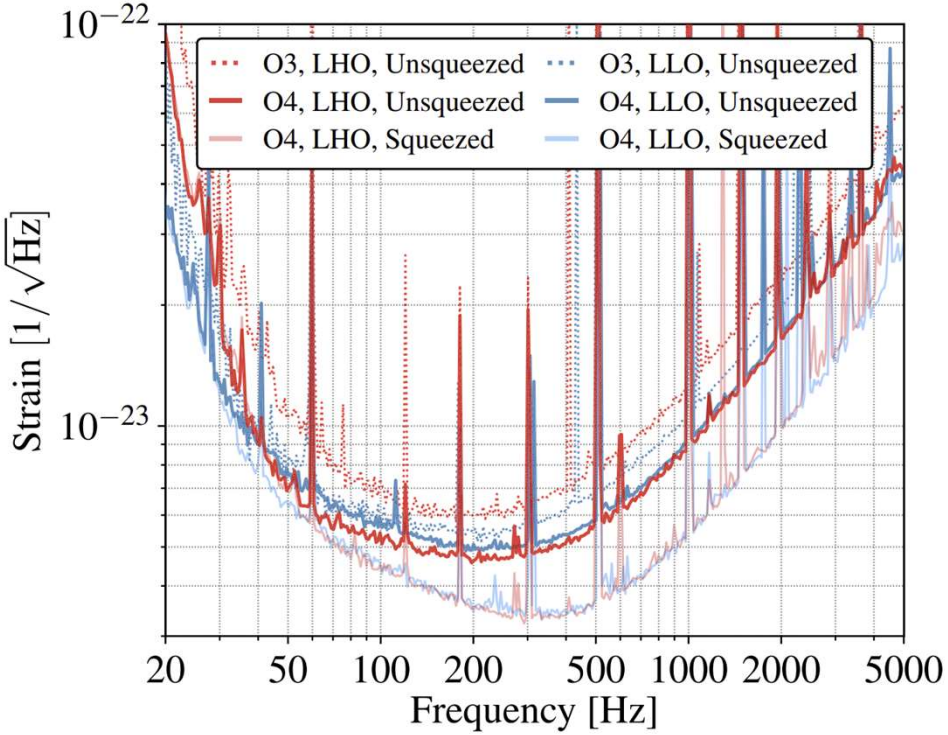
O3, LHO, Unsqueezed
O4, LHO, Unsqueezed
O4, LHO, Squeezed
O3, LLO, Unsqueezed
O4, LLO, Unsqueezed
O4, LLO, Squeezed
Strain [1/√Hz]
Frequency [Hz]